

How to Address Flame-Retardant Technology on Cotton Fabrics by Using Functional Inorganic Sol–Gel Precursors and Nanofillers: Flammability Insights, Research Advances,

*Original*

How to Address Flame-Retardant Technology on Cotton Fabrics by Using Functional Inorganic Sol–Gel Precursors and Nanofillers: Flammability Insights, Research Advances, and Sustainability Challenges / Trovato, V., Sfamini, S., Ben Debabis, R., Rando, G., Rosace, G., Malucelli, G., Rosaria Plutino, M.. - In: INORGANICS. - ISSN 2304-6740. - ELETTRONICO. - 11:7(2023), pp. 1-55. [10.3390/inorganics11070306]

*Availability:*

This version is available at: 11583/2980489 since: 2023-08-02T13:49:01Z

*Publisher:*

MDPI

*Published*

DOI:10.3390/inorganics11070306

*Terms of use:*







This article is made available under terms and conditions as specified in the corresponding bibliographic description in the repository

*Publisher copyright*

(Article begins on next page)

Review

# How to Address Flame-Retardant Technology on Cotton Fabrics by Using Functional Inorganic Sol–Gel Precursors and Nanofillers: Flammability Insights, Research Advances, and Sustainability Challenges

Valentina Trovato <sup>1,\*</sup>, Silvia Sfameni <sup>2</sup>, Rim Ben Debabis <sup>1</sup>, Giulia Rando <sup>3</sup>, Giuseppe Rosace <sup>1</sup>,  
Giulio Malucelli <sup>4,\*</sup> and Maria Rosaria Plutino <sup>2,\*</sup>

- <sup>1</sup> Department of Engineering and Applied Sciences, University of Bergamo, Viale Marconi 5, 24044 Dalmine, Italy; rim.bendebabis@unibg.it (R.B.D.); giuseppe.rosace@unibg.it (G.R.)
- <sup>2</sup> Institute for the Study of Nanostructured Materials (ISMN–CNR), Palermo, c/o Department of ChiBioFarAm, University of Messina, Viale F. Stagno d’Alcontres 31, Vill. S. Agata, 98166 Messina, Italy; silvia.sfameni@ismn.cnr.it
- <sup>3</sup> Department of ChiBioFarAm, University of Messina, Viale F. Stagno d’Alcontres 31, Vill. S. Agata, 98166 Messina, Italy; giulia.rando@unime.it
- <sup>4</sup> Department of Applied Science and Technology, Politecnico di Torino, Viale T. Michel 5, 15121 Alessandria, Italy
- \* Correspondence: valentina.trovato@unibg.it (V.T.); giulio.malucelli@polito.it (G.M.); mariarosaria.plutino@cnr.it (M.R.P.)



**Citation:** Trovato, V.; Sfameni, S.; Ben Debabis, R.; Rando, G.; Rosace, G.; Malucelli, G.; Plutino, M.R. How to Address Flame-Retardant Technology on Cotton Fabrics by Using Functional Inorganic Sol–Gel Precursors and Nanofillers: Flammability Insights, Research Advances, and Sustainability Challenges. *Inorganics* **2023**, *11*, 306. <https://doi.org/10.3390/inorganics11070306>

Academic Editors: Roberto Nisticò, Torben R. Jensen, Luciano Carlos, Hicham Idriss and Eleonora Aneggi

Received: 27 June 2023

Revised: 14 July 2023

Accepted: 16 July 2023

Published: 18 July 2023



**Copyright:** © 2023 by the authors. Licensee MDPI, Basel, Switzerland. This article is an open access article distributed under the terms and conditions of the Creative Commons Attribution (CC BY) license (<https://creativecommons.org/licenses/by/4.0/>).

**Abstract:** Over the past decade, inorganic fillers and sol–gel-based flame-retardant technologies for textile treatments have gained increasing research interest as useful alternatives to hazardous chemicals previously employed in textile coating and finishing. This review presents the current state of the art of inorganic flame-retardant technology for cotton fabrics to scientists and researchers. Combustion mechanism and flammability, as well as the thermal behavior of neat cotton samples, are first introduced. The main section is focused on assessing the effect of inorganic and sol–gel-based systems on the final flame-retardant properties of cotton fabrics, emphasizing their fire safety characteristics. When compared to organic flame-retardant solutions, inorganic functional fillers have been shown to be more environmentally friendly and pollution-free since they do not emit compounds that are hazardous to ecosystems and humans when burned. Finally, some perspectives and recent advanced research addressing the potential synergism derived from the use of inorganic flame retardants with other environmentally suitable molecules toward a sustainable flame-retardant technological approach are reviewed.

**Keywords:** inorganic flame retardants; sol–gel technology; nanoclays; functional nanofillers; functional coatings; cotton fabrics

## 1. Introduction

In the last decades, continuous improvements in people’s living standards, together with environmental problems and population growth, have generated a demand for advanced materials, thus resulting in ever-accelerating scientific progress and research. In this regard, a special place is covered by textiles, which are present in everyday human life, not only for conventional clothes and accessories, but also as decoration and comfort elements in homes, and public and private buildings, as components in transportation, and as structural elements for buildings. As a matter of fact, besides the conventional textiles sector, more complex fabric manufacturing is growing, aiming to a high level of product innovation and cutting-edge process technologies, continuously searching for specific textiles aesthetics and high-quality characteristics, as well as new functionalities

(i.e., resulting from hybrid material additives capable of providing protection, comfort, and performance to the final textile products). At this stage, it appears very clear that textile fabrics must be treated not only as artistic surfaces for fashion but as materials between the wearers and the surroundings for all intents and purposes, with their tunable intrinsic structures and performances.

Today, the so-called technical textiles, designed for their functional properties rather than their aesthetic features, have become a revolutionary product category, providing the foundation for an entirely new variety of applications [1]. They can be utilized for various industrial sectors, also thanks to the possibility of introducing many functionalizations during the finishing step, such as water-repellent, antibacterial, or flame-retardant properties, among others [1,2]. Keeping an eye on nature and human health protection, stringent environmental restrictions and greater interest in natural resource usage have recently led to an increasing trend toward the exploitation of natural fibers in technological applications as eco-friendly options to synthetic counterparts [3].

Among others, cotton fabric represents one of the most widely employed natural fibers in the textile industry. Indeed, the average global production of cotton fibers reached about 25 million tonnes during recent years, representing 28% of all fibers' global production [4]. Cotton fiber structure consists of a polysaccharide component of  $\beta$ -D-glucopyranose units linked together by  $\beta$ -1,4 bonds (Figure 1); non-reducing and reducing sugar units stabilize the end terminal of cellulose polymer chains [5]. Chemical modifications and fiber behavior are mainly attributable to the -OH groups on positions C-2, C-3, and C-6 of the D-glucopyranosyl units [5,6].

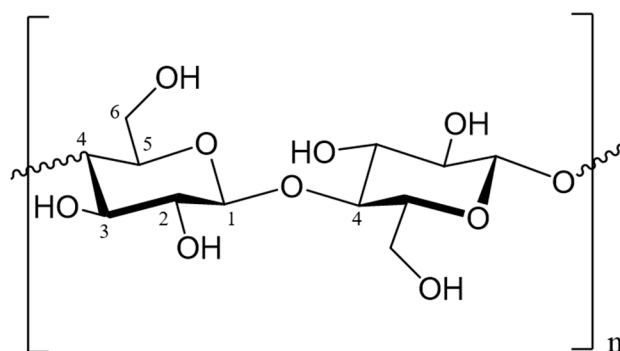


**Figure 1.** Cellulose structure with carbon atoms numbering. Numbers (1 and 4) were used in the text to explain the link between monomers (Cotton fiber structure consists of a polysaccharide component of  $\beta$ -D-glucopyranose units linked together by  $\beta$ -1,4 bonds).

Due to these superior characteristics (i.e., fast moisture absorption, mechanical properties, breathability, softness, comfort, biodegradability, and good thermal conductivity), cotton is used extensively in clothing, bedding, furniture, and wall hangings, as well as in apparel manufacturing, home furnishings, medical textiles, and other industrial products [7]. Moreover, cotton-based textiles have been used as protective clothing for workers and, more generally, as uniforms employed in workplaces where there is a chance of accidental contact with flames [8]. However, its disadvantage is represented by the easy ignition and aptitude to burn in the air (its limiting oxygen index, LOI, is around 18%) [9] as well as the quick flammability propensity, which have restricted its application in particular fields requiring textiles with enhanced flame retardancy [10]. As a significant component in a range of everyday textiles, most of the research efforts have been addressed to investigate the flammability of cotton fabrics [11].

Currently, the research on flame-retardant treatments for fabrics has become a necessary pathway, and many countries have created relevant testing standards and legislation to standardize the market [12]. As reported in the scientific literature [13], the estimated costs from fire losses are approximately 1% of the global gross domestic product. Only in the United States, home fires are the most frequent type of fire accidents [14]: the single most

significant cause of civilian deaths refers to home fires (about 24%), due to the presence of residential upholstered furniture, with a yearly estimated average of 8900 fires, 610 deaths, and 1120 injuries, resulting in \$566 million in direct damage [15]. Furthermore, the annual United Kingdom fire statistics demonstrate that most of the fire accidents that occur in houses involve upholstering furniture, bedding, and nightwear [16]. According to statistics from the International Association of Fire and Rescue Services [17], in the period 2016–2020, several fires involving textiles as a major fuel element have driven the research toward the development of new fire precautionary and preventative procedures.

The most common flame-retardant (hereafter, FR) finishes for cotton fabrics were developed from 1950 to 1980, and were based on halogen derivatives, phosphorous, and/or nitrogen [18]. In particular, during the combustion of halogen-containing flame-retardant fabrics, toxic gases, such as hydrogen halide, are produced, causing harm to human health and environmental pollution. Because of these concerns, halogenated finishes have been rigorously restricted in textile finishing [19].

In this regard, the development of flame-retardant textile finishing able to provide self-extinguishing properties and delay or inhibit the flame spread is relevant. Accordingly, the flame-retardant effect is attained when at least one or more factors among fuel, heat, and oxygen are reduced or eliminated, thus further enhancing the thermal stability of the polymer fabric and quenching the formed high-energy free radicals. Generally, flame-retardant mechanisms involve chemical, physical processes, or a combination of both. Mainly, the action mechanism of flame retardants can be traced back as follows [20]:

- a. Gas phase. FRs following this mechanism act by diluting the gas phase and/or by chemical quenching of active radicals. The former effect is based on releasing non-combustible gases (e.g.,  $H_2O$  and  $CO_2$ ) that can dilute the oxygen or the fuel concentrations by lowering them under the flammability limit. Metal hydroxides and carbonates are generally believed to follow this mode of action due to their endothermic thermal decomposition and production of non-combustible gases. On the other side, because of the occurrence of radical reactions during combustion, the flame retardants decompose in radical species able to quench the high-energy free radicals formed during cellulose combustion (e.g.,  $H\bullet$  and  $\bullet OH$ ) by decreasing the burning rate of the combustible materials and, finally, interrupting the exothermic reactions of the combustion. However, the mechanism in the gas phase may be slightly different, depending on the used chemicals [21];
- b. Condensed phase. The thermal cracking reaction process of cellulose can be modified by flame retardants. Indeed, many reactions (e.g., dehydration, condensation, cross-linking, and cyclization) take place at lower temperatures by producing coherent carbon layers on the fabric surface, thus lowering both the evolution of combustible gases and the decomposition rate of the fabric. For more in detail, the depolymerization of fiber materials is observable under the action of the flame retardant, as well as a decrease in the melting temperature that leads to a higher temperature difference between the melting and ignition point [22]. According to the chemical structure of the employed FR, an intumescent effect can also be observable. Moreover, a certain amount of heat is absorbed by interrupting the feedback of the heat to the fibers and, finally, the combustion process. Inorganic finishes containing phosphorus, boron, sol-gel precursors, nanoclay, and metal-based finishes, as well as carbon nanotubes and graphene, are believed to follow this mode of action.

However, combustion is a complex process, and the action of flame retardants may occur across both gas and condensed phases or in just one of the two. Indeed, synergistic flame-retardant actions can be obtained by combining different mechanisms that, conversely, are barely assignable to a single flame-retardant system [23].

As an alternative to most common FR treatments, whose flame-retardant mechanism mainly occurs in the gas phase, formulations acting in the condensed phase and containing nitrogen and phosphorus have been developed, promoting the formation of a char during thermal degradation, which provides an insulating layer to the underlying polymer. Indeed,

organophosphate flame retardants containing synergistically active nitrogen may be more effective than pure phosphate flame retardants. According to [24], in systems based on the P–N synergism, the phosphoric acid undergoes the nucleophilic attack of the nitrogen, resulting in the formation of P–N bonded polymers. This bond is more polar than the already present P–O bonds, and the improved electrophilicity of the phosphorus atom boosts its capacity to phosphorylate the C(6) primary hydroxyl group of cellulose [25]. This, in turn, prevents the intramolecular C(6)–C(1) rearrangement process that produces levoglucosan. At the same time, the char formation derived by the action of the same flame retardants is promoted and consolidated by the auto-cross-linking of cellulose. Although several research works on P–N synergy in cotton have been published, to the best of our knowledge, only qualitative observations of this phenomenon are often discussed. Lewin [26] and Horrocks [27] have shown that the actual synergy between two species (i.e., phosphorus and nitrogen) can only be determined by calculating synergy parameters, according to which the effects of these two species may be additive or even antagonistic.

In this scenario, among others, organophosphorus compounds, such as tetrakis (hydroxymethyl) phosphonium chloride (THPC), hydroxyl functional organophosphorus oligomer (HFPO), as well as N-alkyl-substituted phosphono-propionamide derivatives, have been largely used on the market, dramatically increasing the number of applications for cellulose-based flame-retardant textiles [8,28].

A common FR process for cotton fabrics exhibiting washing fastness is provided by Proban<sup>®</sup> (Rhodia, La Défense, France), consisting of tetrakis-hydroxymethyl-phosphonium chloride (THPC) cross-linked with gaseous ammonia. The durability of this FR is explained by its resistance on textiles even after 70 washing cycles performed at temperatures beyond 70 °C in contrast with some drawbacks such as the formaldehyde release and the stiffness of treated fabrics. On the other side, Pyrovatex<sup>®</sup> (Huntsman, Woodlands, TX, USA), based on dimethyl-N-dihydroxymethylcarbamoyl-ethylphosphonate, is another commercial FR with slightly lower durability than Proban<sup>®</sup> (Rhodia). This FR treatment is based on the acid-catalyzed N-methylol moiety chemical bonding of phosphorous-based compounds to cotton surfaces, but it has the problem of formaldehyde release both during the process and the use of the treated fabrics.

However, all these finishes need high loading of chemicals on the textile surface, requiring more synthetic substances in the treatments [29], which can alter the physical qualities and “hand” (i.e., soft touch) of the treated textiles. Moreover, according to recent research, some phosphorus-containing substances emit much smoke, may be toxic or potentially mutagenic, or pose other risks to the environment and human health [30]. Furthermore, as previously stated, most of them have an adverse environmental profile for producing free formaldehyde during application or use due to active hydroxymethyl units in their chemical structure [23].

The need to replace the above-mentioned fire-retardant finishes with eco-friendly, halogen- and formaldehyde-free formulations is an environmental progression according to the European directives and REACH regulation [31,32]. Moreover, internationally active private programs, such as Bluesign, Global Organic Textile Standard (GOTS), and Zero Discharge of Hazardous Chemicals (ZDHC), and major textile trading companies have defined guidelines limiting hazardous substances, which are usually even more restrictive than the government laws [33]. The design of alternative FRs to the conventional ones that are often banned due to their health and environmental concerns must fulfill several characteristics, including ease of application, maintenance of the main textile properties (e.g., comfort, appearance, aesthetics, tensile properties, and air permeability), durability, relatively low cost/performance value, no release of toxic substances (e.g., formaldehyde), no toxicity, and low environmental impact during application or use. Furthermore, innovative approaches focus not only on the selection of non-hazardous molecules but also on processes and methods exhibiting low environmental impact [16].

Recent advances in flame-retardant strategies have proposed the treatment of cotton textiles with insulating inorganic materials to mimic the formation of a char layer onto

cellulose-based fabrics due to the presence of finishes containing zinc sulfide or oxide [19], Lewis acids, and aluminum sulphate, among others. Compared with organic counterparts, inorganic flame retardants are relatively green and pollution-free because they do not generate harmful chemicals to ecosystems and humans when they are burnt [34]. At low temperatures, they work by reducing the decomposition temperature by dehydration, decarboxylation, gradual depolymerization, and recombination of the breakdown products to form carbonaceous char. This prevents reactions that occur at high temperatures through the breakdown of the macromolecule by intramolecular transglycosylation to anhydroglucose units and their subsequent degradation to lower molecular weight flammable volatiles.

Following this overview of FR conventional solutions, this review aims to discuss the recent developments in the inorganic flame retardation of cotton fabrics. According to Ling et al. [23], several classifications are available for flame retardants: among them, the one based on the chemical element is often exploited. Furthermore, taking into consideration other relevant aspects, such as sustainability and performance, the flame retardants discussed in this review have been classified as follows: inorganic FRs (including phosphorous- or boron-based), sol-gel-derived FRs, and inorganic FR nanoparticles (including nanoclays, carbon nanotubes, graphene, and metal-based structures). First of all, a special emphasis is placed on the flammability and thermal behavior of untreated cotton fabrics with the aim of providing a detailed overview of the finishing processes, their optimization, and the related mechanism to researchers interested in the study of the influence of sol-gel- and inorganic-based flame-retardant finishes and coatings on cellulose-based textiles. Then, the comprehensive properties of inorganic sol-gel precursors and fillers as flame-retardant coatings and finishes for cotton are presented. Finally, an outline of the mentioned flame-retardant methods and materials, together with future challenges toward sustainability, is provided.

## 2. Mechanism of Cotton Combustion

As a cellulose-based polymer, the combustion of cotton is an exothermic oxidation process that takes place upon heating, consuming flammable gases, liquids, and solid residues produced during the pyrolysis of the textile material, thus generating heat. The process is considered to involve mainly four stages: heating, pyrolysis, ignition, and flame spread. During the heating step, the temperature of the cotton is raised by external ignition to a level that depends on the intensity of the ignition source and the thermal properties of the textile. When cellulose is heated at temperatures not exceeding 150 °C, water desorption occurs.

Once the cellulosic material exceeds 250 °C, pyrolysis occurs as an endothermic process [35,36], resulting in the irreversible polymer decomposition by producing tar (of which levoglucosan is the main component), flammable gases (methane, ethane, and carbon monoxide), non-flammable gases (carbon dioxide and formaldehyde), other by-products (water, alcohols, organic acids, aldehydes, and ketones), and char. If the combustion process generates sufficient heat, the heat is further transferred to the textile substrate, further accelerating the degradation processes and leading to a “self-sustaining” combustion cycle (Figure 2). The thermal decomposition of cotton fabrics generates approximately 51% water and gases, 47% tar, and 2% char [37].

More specifically, the depolymerization of cellulose can be mainly divided into three stages as a function of the temperature range:

- a first stage (between 300 and 400 °C), corresponding to the pyrolysis that takes place through two competing decomposition reactions: dehydration and depolymerization [38]. The former produces anhydro-cellulose (dehydro-cellulose), which further decomposes at higher temperatures and produces various volatile products such as alcohols, alkanes, aldehydes, fuel gases, carbon monoxide, methane, ethylene, and non-flammable gases (carbon dioxide and water vapor), and an aliphatic char (char I). Otherwise, depolymerization by breaking of glycosidic linkages results in the for-

- mation of tar (condensed phase), which is mostly composed of levoglucosan and glycolaldehyde (hydrogen acetaldehyde);
- a second stage (between 400 and 600 °C), corresponding to the competitive conversion of aliphatic char to aromatic and char oxidation [38]. In this stage, tar is further decomposed into small volatile flammable molecules and aromatic char (char II, stable up to 800 °C), while volatile compounds from Stage 1 are also oxidized to produce similar oxidized char and aromatic molecules;
  - a third stage (between 600 and 800 °C), corresponding to the further char decomposition to acetylene, CO, and CO<sub>2</sub> (beyond 800 °C), as well as other cellulose pyrolytic products [39–42].

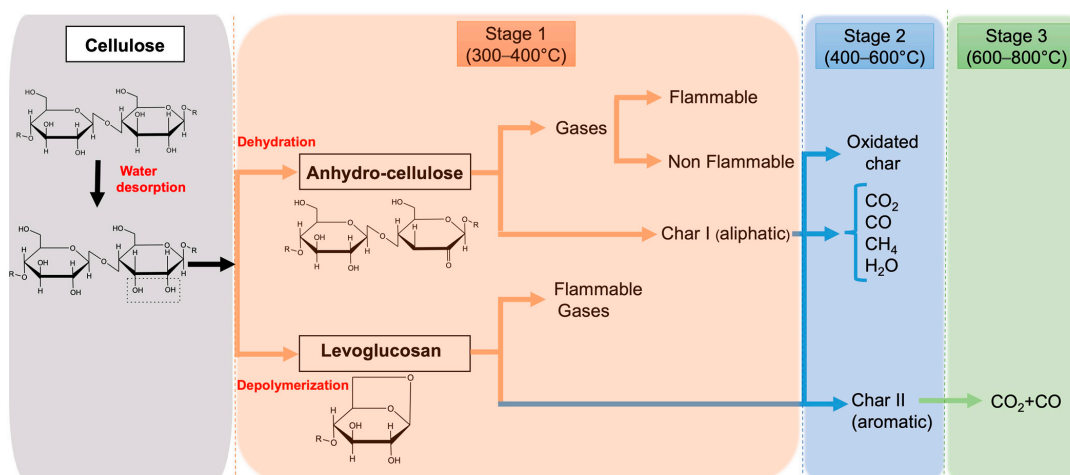


**Figure 2.** Schematic process of thermal degradation of cellulose.

The heating rate has been proven to influence the concentration of fuel products during the overall combustion steps: in particular, low heating rates promote dehydration and subsequent char formation, whereas high heating rates lead to depolymerization and fast volatilization by forming levoglucosan (whose yield can be reduced by dehydration, thus resulting in the formation of fewer volatile species), as well as higher gaseous flammable products. The formed char acts as an insulating layer on the surface of the cellulosic material, reducing the heat transfer, and as a diffusion barrier for combustible gases. Moreover, the level of material protection is strictly affected by its structure: a char, featuring an open channel structure, promotes the transfer of combustible gases to the flame, while a char with a closed structure hinders volatile species to reach the flame. Furthermore, the formation of char leads to condensed water that dilutes the flammable gases [17].

Generally, neat cellulose fibers lead to the formation of around 13% char, an amount that can be significantly enhanced by using FRs, thus reaching 30–60% [43]. Moreover, the presence of FRs on textile surfaces slows down the combustion due to the low heat involved, which is required to maintain pyrolysis. As a result of the highly flammable nature of cellulose-based materials, as a consequence of their chemical composition, a fire-hindering mechanism integrated into textiles is needed to decrease or eliminate possible fire dangers.

### 3. Flame Retardancy of Cotton Fabrics

Among the wide panorama of textile fibers, most of them are highly flammable, making exceptions only for protein fibers (e.g., wool and silk) and leather. Therefore, the term “combustible fibers” is intended to include readily and freely combustible fibers commonly found on the market, which are stored in relatively large quantities and pose a considerable fire hazard when stored. The leading causes of fires can be ascribed to faulty electrical equipment, friction between fibers, presence of foreign materials in the stored fibers (e.g., metals), fiber fermentation in the presence of high humidity that raises the temperature, possible spontaneous heating (oxidation reactions occur), as well as smoking [44].

Different fibers have varying flammability levels depending on their chemical composition and structure. Table 1 shows the thermal properties in terms of glass transition ( $T_g$ ), melting temperature ( $T_m$ ), degradation or pyrolysis temperature ( $T_d$  or  $T_p$ ), and ignition combustion ( $T_c$ ) values, as well as the limiting oxygen index (LOI), which are crucial parameters for evaluating the thermal stability and flame retardancy of some natural and synthetic fibers.

**Table 1.** Significant temperature values and LOI (%) of the most commonly used fibers.

Fiber	$T_g$ (°C)	$T_m$ (°C)	$T_d$ (°C)	$T_c$ (°C)	LOI (%)
Cotton	-	-	350	350	18.4
Viscose	-	-	350	420	18.9
Wool	-	-	245	600	25
Polyamide 6	50	215	431	450	20–21.5
Polyester	80–90	255	420–447	480	20–21.5

In general, for natural cellulosic fibers, the lower the  $T_c$  the hotter the flame, and the more flammable the fibers. As known, the primary component of mature cotton fibers is cellulose (from 88% to 96.5%). All the rest consists of non-cellulosic materials found in the outer layer and lumen.

These components include protein (1–1.9%), wax (0.4–1.2%), pectin (0.4–1.2%), and other substances [45]. Moreover, as evident from data reported in Table 1, cotton fabrics exhibit the lowest LOI value concerning other fibers, hence confirming high inherent flammability.

The expression “flame retardancy of textiles” concerns the possibility of making these materials less likely to ignite and, once they are ignited, to burn much less efficiently. Finishes used with this aim act to break the self-sustaining polymer combustion cycle and, thus, extinguish the flame or reduce the burning rate and flame propagation. Flame retardancy in cellulose-based textiles may be achieved in the followings ways and means, either by individual or combined mode (from a to f) as follows:

- (a) by using fire-retardant materials that thermally decompose through strongly endothermic reactions to not easily achieve the heat required for thermal decomposition (temperature of pyrolysis ( $T_p$ ) of the fiber should not be reached);
- (b) by applying a material that forms an insulating layer around a temperature below the fiber  $T_p$ ;
- (c) by using phosphorous-containing fire retardants that modify the pyrolysis reaction (‘condensed phase’ mechanism) according to two mechanisms: (i) production of phosphoric acid through thermal decomposition, and cross-link with hydroxyl-containing polymers altering the pyrolysis pattern and yielding less-flammable byproducts; (ii) blocking of the primary hydroxyl group in the C-6 position of the cellulose units, preventing the formation of flammable byproducts (levoglucosan), and catalyzing the dehydration and char formation [46];
- (d) by preventing combustion through scavenging the generated free radicals (e.g.,  $\text{Br}^\bullet/\text{Cl}^\bullet$  halogen-containing fire-retardant compounds), thus reducing the available heat (‘gas phase’ mechanism);
- (e) by enhancing the  $T_c$  (combustion temperature) [47];
- (f) by raising the initial decomposition temperature (i.e.,  $T_p$ ) for preventing/reducing the formation of flammable volatile species and increasing the formation of char and non-flammable gas.

For more in detail, the mechanism of FRs through the breaking the self-sustaining combustion cycle of cellulose is schematized in Figure 3. As a result, FRs should be able to (i) lower the heat, hence interrupting the combustion sustainability, (ii) modify the pyrolysis by lowering the formation of flammable volatile species and increasing the amount of char or intumescent coating (that acts as a barrier between the flame and the polymer), (iii) isolate the flame from oxygen, and (iv) decrease the heat flow back to the polymer to prevent further pyrolysis.

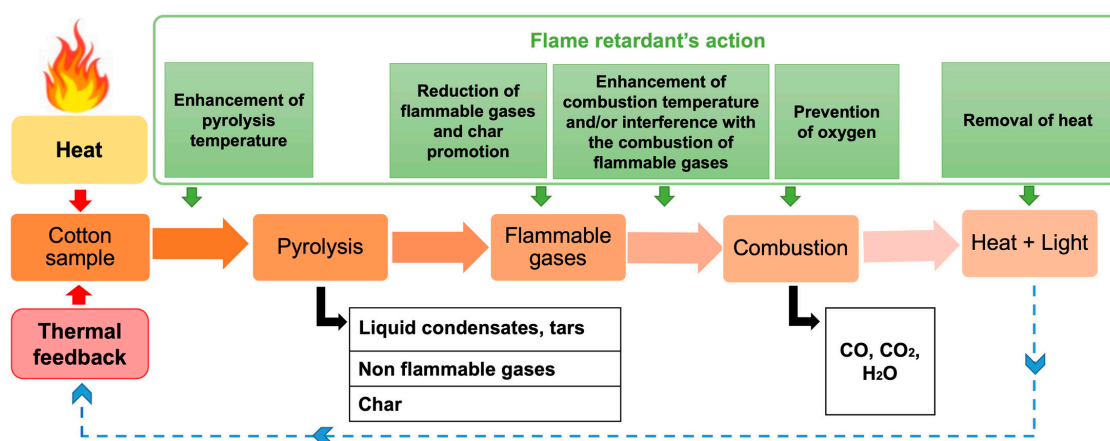


**Figure 3.** Combustion mechanism of cotton, together with the flame-retardant effect.

Therefore, all species that can acid-catalyze the dehydration and, subsequently, act as char formers in the condensed phase, are the best candidates for the flame retardation of cotton.

Thus, when textile fabrics are exposed to a heat source, a temperature increase occurs, and, if the temperature of the heat source (radiation or gas flame) is high enough and the net rate of heat transfer to the cellulosic substrate is high, only pyrolytic degradation of the fibrous matrix will occur.

The same reasoning applies to manufacturing flame-retardant fabric items, by employing a flame-retardant coating or laminate to any textile substrate to limit direct contact with free oxygen in the air, which actually helps any substance to burn. Such coatings or laminations of various agents, such as metal oxides, inorganic halides, organic compounds, and nanomaterials, are suitable for flame retardancy. Flame propagation rate, flame-retardant effectiveness, and combustion behavior depend on different materials and process parameters [2].

Although FRs can be classified by several methods, a simple method is based on their elemental compositions, according to which FRs are halogen-, phosphorous-, nitrogen-, and silicon-based, as well as metal hydroxides [23,48]. Furthermore, they can be classified as a function of their action mechanism, thus resulting in nano-FRs, co-effective FRs, or biological macromolecular FRs [23,49]. Another classification is based on the durability characteristics of the finishing applied to the fabrics, which represents another challenge. Persistent flame retardancy is, generally, obtained through chemical modification, which involves a chemical reaction of cellulose hydroxyl groups with reactive flame retardants. Accordingly, FRs can be classified as non-durable, semi-durable, and durable. Since non-durable FRs are easily removed by water, they are very often used for disposable goods (e.g., medical gowns) or, when used for work clothes, their application should be periodically performed.

Common examples of non-durable FRs are represented by water-soluble inorganic salts of phosphoric acid, zinc chloride, boric acid and borates, bases such as sodium hydroxide and potassium carbonate, as well as mono- or di-ammonium phosphates or water-soluble short-chain ammonium polyphosphate. Semidurable FRs are often used for textiles, which do not require frequent washings and can withstand a limited number of cleaning cycles, i.e., between 1–20. Some examples are provided by phosphates or borates of tin, aluminum, zinc, aluminates, stannates, and tungstates.

Moreover, metal oxides and hydroxides that are easily reducible can also catalytically alter cellulose's thermal decomposition path by combining water-insolubility with flame-retardant properties. Generally, FRs that withstand more than 50 laundry cycles are defined as durable and mainly represented by phosphorous- or halogen-based molecules (e.g., Tetrakis-(hydroxymethyl)phosphonium chloride).

Moreover, the difference between additive and reactive flame retardants is to be pointed out in the framework of FR classifications. The main difference is based on the

means of their incorporation into the textile polymer chain. Usually, additives are represented by mineral fillers, organic or hybrid molecules physically deposited or incorporated into the textile polymer.

On the other side, reactive FRs are involved in the chemical modification of polymers by coating, chemical grafting, or copolymerization. As already introduced, since many available fire-retardant additives (e.g., halogen-based) are considered environmentally unacceptable [50], during the second half of the last century, several efforts have been made to develop novel flame-retardant treatments for textiles, meeting fire safety regulations.

#### 4. Assessment of the Thermal Behavior and Flammability of Cotton Fabrics

With the development of innovative and performing flame-retardant chemical coatings and finishings, great attention has also been recently focused on the characterization techniques available to describe a realistic fire scenario. In this regard, to correctly interpret the results of flame-retardant treatments on cotton fabrics, it is essential to understand the flammability and thermal behavior of untreated (pristine) cotton.

However, the comprehensive characterization of the flammability properties of a polymeric material is not straightforward since the material behavior in a real fire scenario can be quite different from experimental conditions. Therefore, several analytical techniques and other prescriptive tests (small-, medium-, and large-scale) were developed over the years.

With the aim of providing fundamental knowledge for understanding and adequately comparing combustion data of untreated cotton with results obtained after flame-retardant treatments, the main techniques for characterizing flammability properties and thermal behavior of cotton samples are reported in this paragraph, indicating the measurable parameters and the most significant values reported in the literature for pure cotton, used as a reference for research in flame-retardant finishes.

Accordingly, common tests for determining the flame behavior of polymers such as the flammability tests (i.e., UL-94 and limiting oxygen index (LOI)), cone calorimetry, microscale combustion calorimetry (MCC), thermogravimetric analysis (TGA) and differential scanning calorimetry (DSC) are briefly described.

##### 4.1. Flammability Tests

With the aim of depicting realistic fire scenarios, it is crucial to test the flammability of a sample under fire-propagation conditions, in terms of flammability by vertical/horizontal flame-spread tests (according to ASTM D-6413-11, ASTM D1230-22, and ISO 3795 standards).

Following UL-94 procedure, similar to those of the standard for fabrics (ISO 6940 (2003). Textile fabrics—Burning behaviour—Determination of ease of ignition of vertically oriented specimens), a textile sample with dimensions 50 mm × 150 mm is tested in vertical configuration by applying a methane flame for 5 s at the bottom of the specimen. As an index of flame-propagation resistance and combustion behavior of the material, some parameters can be evaluated, such as the total burning time(s), kinetics after the flame applications (total burning rate, mm/s), the final residue (%), as well as the time for flaming combustion (after-flame) and flameless combustion (after-glow) [51]. In particular, the flaming combustion corresponds to cellulose pyrolysis (production of volatile species and combustible gases). Otherwise, the after-glow combustion is due to the interaction between oxygen and residual carbon. Moreover, flameless combustion requires higher temperatures than those for flaming combustion [23,52]. To test the flammability of textile fabrics, a modified version of ASTM D3801 is performed by taking into account the actual flame height used, according to which the test method can be classified as being between the UL-V0 (ASTM D3801) and UL-94 5 V (ASTM D5048) tests in severity [53]. Depending on the dripping behavior and the self-extinguishing time, according to these test methods, materials could be rated as V-0, V-1, or V-2. However, since the method was developed for plastic materials, the above ratings should be used carefully when applied to textile fabrics.

For the 45° configuration, a special apparatus is used, in which a strip of fabric is held in a frame. A standard flame is applied to the surface near the lower edge for 10 s. The time

is taken for the flame to penetrate the fabric and break the trigger thread and the physical reaction of the fabric at the ignition point is recorded. The data obtained from the 45° test in various laboratories show that the flame-spread rate is inversely proportional to the fabric weight per unit area for a given fabric [54]. This suggests that the rate of heat release from a given type of fabric, for example, cotton, is independent of the fabric weight. However, the total amount of heat released per unit area for any given fabric will be dependent on fabric weight, showing that the total heat transferred to a vertical surface from a burning fabric is proportional to the fabric weight [55].

The flammability performance index (FlaPI, %/s) is another parameter for the evaluation of flame-retardancy performance, and it is defined as the ratio of the final residue to the total burning time. Accordingly, better flame-retardancy performance is expected for higher FlaPI [56].

Using the horizontal configuration, according to which the flame is applied on the short side of the specimen, Rosace et al. [57] measured the time ( $t_1$  and  $t_2$ ) necessary for the flame to reach two horizontal lines drawn on the specimens (at 25 and 75 mm from the side on which the flame was applied, respectively). The findings confirmed that, immediately after ignition, on the untreated cotton a vigorous flame appears, the duration of which is about 23 s, followed by a prolonged after-glow (139 s); no residue was found at the end of the test.

In Table 2, and in the following ones in this section, data on the flammability properties of cotton fabrics when used as technical textiles (mass per unit area in the range of 110–300 g/m<sup>2</sup>) are reported.

The presence of an FR treatment on the cotton surfaces results in a significant variation in its flammability. Indeed, FR-treated fabrics highlight a noticeable reduction in the total burning time, as well as a high final residue as a consequence of the formation of narrow char. In this regard, in [58] the authors measured an enhanced total burning time of up to 35 s, a total burning rate decreased to 4.2 mm/s and a final residue increased up to 46% for cotton treated with a silica phase containing nano-alumina particles.

On the other side, LOI is widely used to evaluate the flame retardancy of materials and is defined as the minimum oxygen percentage required to maintain the flame state when the sample is burned in oxygen and nitrogen atmosphere [59], by an oxygen index apparatus according to the ASTM D2863-10 standard method. Although it is not relevant for precisely determining mutual differences in FR properties, this parameter is a valuable method for the rapid characterization of samples with respect to flame resistance.

**Table 2.** Flammability tests performed on untreated cotton fabrics.

Mass Per Unit Area (g/m <sup>2</sup> )	Configuration of Flammability Test	Total Burning Time (s)	Total Burning Rate (mm/s)	After-Flame Time (s)	After-Glow Time (s)	Residue (%)	FlaPI (%/s)	Ref.
145	horizontal	34	-	-	-	3.1	-	[51]
237	horizontal	149	0.67	-	-	0	-	[60]
331	horizontal	23	-	-	139	0	0	[57]
122	Vertical	-	-	15.8	20.7	-	-	[12]
129	Vertical	-	-	15	21	-	-	[61]
150	Vertical	-	-	15	26	0	-	[62]
184	Vertical	-	-	14.3	31.4	0	-	[63]
200	Vertical	45	2.2	-	27	<2	-	[64]
210	Vertical	38	-	-	-	14	0.37	[56]
220	Vertical	-	-	7	21	0	-	[65]
237	Vertical	35	7.50	-	-	-	-	[38]

LOI value is calculated as the maximum percentage of oxygen ([O<sub>2</sub>]) in an oxygen-nitrogen gas mixture ([O<sub>2</sub>] + [N<sub>2</sub>]), able to sustain burning a standard sample for a specific time, according to the following equation:

$$\text{LOI} = \frac{[\text{O}_2]}{[\text{O}_2] + [\text{N}_2]} \times 100 \text{ [\%]} \quad (1)$$

Untreated cotton fabrics show an LOI value in the range of 17–19.8% [62,66–69], exhibiting high flammability as materials with an LOI value below 21.0%. When LOI

is between 21.0 and 25.0%, cotton samples turn to be moderately flammable and show flame retardancy when LOI is beyond 25.0%. However, to consider as complete and safe fire-retardant materials, it is better to have values of LOI nearly 35–36% at least [46]. In general, heavier fabrics experienced slower flame-spread rates [70].

The differences in the results given in the publications can be attributable to the amount of non-cellulosic components and crystallinity of the untreated cotton samples, as well as their mass per unit area values and fabric structural properties. Indeed, due to less air presence and less oxygen among fibers, heavier-weight and structured materials ignite less easily and burn more slowly than lighter-weight fabrics. Thus, the burning rate decreases as the fabric weight increases. At the same time, increasing the fabric weight, the flame temperature increases, indicating that heavy fabrics provide more fuel, sustaining the burning process. This results in a slower burn of heavier fabrics than light fabrics due to the high flame temperature during burning [71]. When the cotton sample is heated, the thermal decomposition occurs in multiple stages with different transition temperatures, which can affect the final burnability.

However, flammability is not entirely reliable and, as already noted in the literature [72,73], can only measure the ability of materials to burn when directly exposed to a small flame. For this purpose, more sophisticated instruments, such as the conical oxygen consumption calorimeter, are considered very useful tools [74,75]. These flammability tests can give surprising results, as products marketed as being constructed of flame-retardant materials are ineffective in inhibiting or preventing the combustion of polymers under a given heat flux [76,77]. Indeed, LOI values and combustion data collected by cone calorimetry often do not match. Although high LOI values have been accepted as an indication of the flame resistance of a product, this criterion is not sufficient to guarantee a high level of safety and it has never been used as an official test criterion for textiles. Indeed, new standards for transport, automotive, furniture, and protective clothing are required, in addition to high LOI values, high performance of fabrics against radiation, and cone thermometry [78–80].

#### 4.2. Cone Calorimetry Test

Cone calorimetry is used for investigating the dynamic combustion behavior of polymeric materials in a forced-combustion scenario, providing information on time to ignition (TTI), peak of heat-release rate (PHRR) and total heat release (THR) as crucial parameters for assessing the flammability of polymers because they are reliable indicators of the size and fire-growth rate [81–83]. Moreover, reaction parameters, such as mass loss, smoke production, and generated gas composition (CO and CO<sub>2</sub> yields), are measured for the quantitative assessment of combustion phenomena. In addition, cone calorimetry allows assessing the flame-retardant behavior of polymer composites in the presence of different FRs, as well as the development of burning and pyrolysis models in gas and condensed phases, and the estimation of the potential hazards in fire scenarios [84]. The test is standardized in North America as ASTM E1354, “Standard Test Method for Heat and Visible Smoke Release Rates for Materials and Products Using an Oxygen Consumption Calorimeter”, and internationally as ISO 5660-1:2015, “Reaction-to-fire tests—Heat release, smoke production and mass loss rate—Part 1: Heat release rate (cone calorimeter method) and smoke production rate (dynamic measurement)”. The test is performed by applying an external irradiative heat flux on the textile surface able to generate a rapid increase in the surface temperature that, in a steady state before ignition, reaches a fixed value. In the cone calorimetry simulated fire scenario, the fabric surface temperature is higher than its decomposition temperature. Then, the increased temperature is responsible for the endothermic decomposition of the material and diffusion of reactive components toward the gas phase. Finally, pyrolysis and combustion processes are initiated within the cone calorimeter when it is reached the critical energy required for ignition [84].

Time to ignition (TTI) defines how quickly flaming combustion of material will occur when exposed to a heat source: accordingly, the shorter TTI, the easier the fabric ignition and

spread as a threat to the surrounding materials. Peak of heat-release rate for the tested sample occurred after ignition and just before the flame went out. PHRR is the point where the material is burning most intensely and is, therefore, also crucial for estimating the fire cascading effect.

Among several parameters, heat-release rate (HRR), which is based on the oxygen consumption in the gas phase, is the most relevant for describing material flammability and related fire hazard [84]. In the HRR curve of cellulose-based samples, four significant points of interest can be observed [38]. The first point is the initial peak of heat-release rate (PHRR) that occurs when the sample surface ignites, causing great heat production and increasing HRR (heat-release rate). The second point of interest is the great decrease in HRR soon after the first PHRR. This is due to char formation, which acts as a protective barrier, preventing the exchange of volatile gases and oxygen. The third point of interest is a second PHRR close to the end of the combustion that occurs as a response to sample burn-through, which means that the heat gradient reaches the rear side of the sample. The second PHRR is highly dependent on the boundary condition defined by the rear material, which determines the heat losses at the rear side of the specimen, and, consequently, the temperature of the sample. The pyrolysis rate and, therefore, the second PHRR, increase in relation to the specimen temperature. High moisture content further prolongs the period until the second PHRR occurs because more water must go through a phase transition, requiring a high amount of energy. The fourth point of interest is the final decrease in HRR due to fuel depletion, leading to the sample smoldering or the fire being extinguished. The heat-release rate decreases down to the flame out (FO).

Furthermore, through the HRR curve generated by cone calorimetry is possible to calculate the slope of the FIGRA (fire-growth rate) line, extending from the origin to the earliest, highest peak, providing an estimation of both the spread rate and the size of the fire, thus estimating the contribution to fire growth of materials. Accordingly, the higher the FIGRA, the greater the fire hazard, suggesting a very low PHRR value with a high time to ignition, thus representing a thermal acceleration parameter.

Moreover, since fire deaths are caused more by toxic fumes than burns [85], the analysis of smoke and toxic fumes is very useful for predicting the fire toxicity of polymeric materials. As reported by Horrocks and co-workers, the evaluation of CO and CO<sub>2</sub> species in conjunction with smoke is significant for two reasons: first of all, CO and CO<sub>2</sub> are the main constituents of fire gases and high CO concentrations can be lethal; second, the analysis of these species can provide helpful information on the mechanism of decomposition of such polymer, as cotton [86]. Low CO<sub>2</sub>/CO ratios suggest the inefficiency of combustion, inhibiting the conversion of CO to CO<sub>2</sub>.

Alongi et al. [38] investigated the combustion behavior of square cotton samples ( $50 \times 50 \times 0.5 \text{ mm}^3$ ) using cone calorimetry under a  $35 \text{ kW/m}^2$  irradiative heat flow in horizontal configuration. Such parameters as time to ignition (TTI, s), flame out time (FO, s), total heat release (THR,  $\text{kW/m}^2$ ), peak of heat-release rate (PHRR,  $\text{kW/m}^2$ ) were measured, as well as total smoke release (TSR,  $\text{m}^2/\text{m}^2$ ), peak of rate of smoke release (PRSR, 1/s), smoke factor (SF, calculated as  $\text{PHRR} \times \text{TSR}$ ,  $\text{MW/m}^2$ ), and CO, as well as CO<sub>2</sub> release (ppm and %, respectively). Time of production (s) of both CO and CO<sub>2</sub> gases generated during the oxidation of the char are also reported.

Some of these combustion data by cone calorimetry of pure cotton fabrics (under  $35 \text{ kW/m}^2$  heat flow), selected in a range of mass per unit area  $110\text{--}330 \text{ g/m}^2$ , reported in the literature are summarized in Table 3. According to [87], the areal density values of samples significantly affect some flammability parameters, such as TTI, PHRR, or FIGRA, after ignition.

**Table 3.** Combustion data by cone calorimetry of neat cotton samples, selected with an areal density in the range 110–330 g/m<sup>2</sup>.

Mass per Unit Area of the Sample (g/m <sup>2</sup> )	TTI (s)	THR (MJ/m <sup>2</sup> )	HRR		FIGRA (kW/m <sup>2</sup> s)	TSR (m <sup>2</sup> /m <sup>2</sup> )	CO <sub>2</sub> /CO Peak	Residue (%)	Ref
			Peak (kW/m <sup>2</sup> )	Time (s)					
110	-	2.35	179.2	15	11.94	-	71.5	2.6	[88]
115	6	2.84	196	20	10	-	77	7.5	[89]
118	7	2.68	181.55	25	7.26	-	77.05	0.93	[90]
122	2	6.3	232.1	35	6.6	-	22.1	4.3	[12]
129	7	2.8	181.5	22	8.3	5.3	88.7	0.9	[61]
145	48	2.1	147	-	-	-	-	2	[51]
150	8	1.2	97	23	4.2	-	-	3.4	[62]
200	22	2.0	83	-	-	4.3	-	0.01	[91]
220	4	4.6	269	7.7	34.9	-	-	0	[92]
237	18	4.6	143	58	-	26	0.024	4	[38]
280	45	19.2	223	55	4.05	-	-	0.6	[93]
290	18	3.8	131	-	-	24	-	<1	[94]
331	43	3.9	154.2	-	-	-	142.86	1	[57]

As observable from data reported in Table 3, the mass per unit area of cotton fabrics significantly affects the flame rate: the heavier the fabric, the slower the flame-spread rates. Moreover, no residue of cotton fabrics was observed at the end of the experiments. As reported in literature [95], cone calorimetry parameters are affected by the cotton grammage regardless of the heat flux set. According to data reported in Table 3, fabric with low mass per unit area provide high TTI and low THR, while just PHRR should be taken into consideration as an intrinsic characteristic of the material.

The presence of an inorganic FR coating on the cotton surface should affect the cone calorimetry parameters listed in Table 3. Generally, a delay is observed in TTI values, together with a decrease in THR and PHRR. Additionally, the coating has a significant impact on average TSR, which is a measure of how much smoke is produced during a full-scale fire. This is because the coating encourages the formation of char by preventing the generation of volatile species that can fuel thermal degradation, which results in a reduction in smoke production. Accordingly, Alongi et al. measured lower TSR peaks for Si and Si-ZnO treated cotton (11 m<sup>2</sup>/m<sup>2</sup> and 9 m<sup>2</sup>/m<sup>2</sup>, respectively) with respect to untreated cotton (24 m<sup>2</sup>/m<sup>2</sup>).

#### 4.3. Microscale Combustion Calorimetry (MCC)

The combustion behavior of a small amount of cotton samples can be monitored by microscale combustion calorimetry (MCC), also known as pyrolysis combustion flow calorimetry (PCFC), obtaining flammability parameters such as heat-release combustion (HRC), temperature at the maximum pyrolysis rate ( $T_{max}$ ), heat-release rate (HRR), peak of heat-release rate (PHRR), total heat release (THR) values and temperature at peak release (TPHRR) [96].

The PCFC measurement is performed using an MCC-2 micro-scale combustion calorimeter, according to ASTM D7309-2007. The sample (about 5 mg) is heated to a selected temperature using a linear heating rate of 1 °C/s in a stream of nitrogen, with a flow rate of 80 cm<sup>3</sup>/min. The thermal degradation products are mixed with a 20 cm<sup>3</sup>/min stream of oxygen. The HRR vs. temperature curve indicates that the untreated cotton starts to decompose and to form fuel gases at less than 300 °C and presents the peak of heat-release rate (PHRR = 235 W/g) at about 384 °C ( $T_{max}$ ), with an estimated value of about 12 kJ/g in THR. Moreover, Yang et al. [97] demonstrated that the MCC technique can be utilized as a trustworthy analytical methodology in determining the flammability of textile materials by providing good agreement between calculated and experimental LOI data.

Table 4 collects some significant MCC data of untreated cotton reported in the literature.

**Table 4.** MCC data of untreated cotton samples, selected with an areal density in the range 110–350 g/m<sup>2</sup>.

Mass per Unit Area (g/m <sup>2</sup> )	T <sub>PHRR</sub> (or T <sub>max</sub> ) (°C)	PHRR (or Q <sub>max</sub> ) (W/g)	HRC (or η <sub>c</sub> ) (J/g·K)	THR (kJ/g)	Ref.
119	381	285	-	12.8	[98]
121	379.2	343.5	341.1	14.9	[99]
156	371	183.0	181.0	8.8	[100]
180	377.92	241.8	520.7	15.2	[101]
184	-	224.3	235.6	14.1	[63]
240	383.9	253.7	250.3	12.0	[96]
258	390.0	269.4	270.0	12.0	[102]
347	314.1	62.5	61.0	-	[103]

Contrary to the parameters of cone calorimetry, it was found that  $T_{\text{initial}}$ , THR, and PHRR decreased with increasing the cotton mass per unit area [95]. These differences can be explained considering the nature of the cellulose that forms char in cotton fabrics. In particular, by thermogravimetry, heavy cotton fabrics (around 400 g/m<sup>2</sup>) lead to more char (35% and 23% in O<sub>2</sub> and N<sub>2</sub>, respectively) compared to cotton at half or quarter weight (25% and 17%), thus indicating that a lower number of volatile molecules are released from heavier than lighter cotton fabrics. Accordingly, the higher volatile species generated from the lightest cotton (100 g/m<sup>2</sup>) lead to more pyrolysis products that are further oxidized in PCFC, thus providing higher THR (11.7 kJ/g) than that of heavier cotton (8.8 kJ/g).

PHRR values assed with PCFC also differ from those obtained from cone calorimetry. Indeed, these values are a function of cotton weight and are directly related to the char formation characteristics.

In conclusion, PCFC provided the lowest THR and PHRR values for the largest cotton weights, which led to the maximum thermogravimetric char production [95].

On the other hand, the presence of FR coating on cotton surfaces accounts for a significant decrease in the main MCC parameters listed in Table 4 (THR, PHRR and  $T_{\text{max}}$ ) as well as an increase in the final residue.

#### 4.4. Pyrolysis Behavior of Cotton Fibers by Thermogravimetric Analysis

As already described, the generation of volatile fuel gas when a polymer or textile is heated may be roughly represented by the scission of the macromolecular chains, which results in a reduction of the molecular mass and the removal of monomers or oligomers, as well as the formation of non-saturated species.

The thermal stability of a sample is investigated by thermogravimetric analysis (TGA), which allows for measuring the changes in the sample weight, either as a function of time (isothermally) or with increasing temperature, in an atmosphere of air, nitrogen, helium, or other gases [104]. The thermogravimetric parameters are strictly related to the type of fibers and, for this reason, the thermal stability of natural-based fibers is measured by the decomposition of their constituents (i.e., cellulose, hemicellulose, lignin, and others) [105].

Generally, the oxidation resistance and the thermal stability of samples are investigated, respectively, under air and nitrogen atmosphere, in the temperature range of 30–700 °C, setting a heating rate of 10 °C/min. Similarly, the derivative thermogravimetric curve (DTG) shows the maximum rate of thermal decomposition, and fiber constituents are indicated by the appearance of peaks in each degradation range.

In nitrogen atmosphere, cotton samples follow a one-step thermal degradation, during which the maximum weight loss is observed [11]. According to literature [106,107], the pyrolysis of cotton in N<sub>2</sub> follows two alternative pathways involving the dehydration and polymerization of cellulose polymeric chain by forming stable aromatic char and volatile products. As demonstrated by Wang et al. [12], cotton samples rapidly degrade in the range of 331–391 °C, with a mass loss of about 85% due to flammable substances (e.g., L-glucose) produced by cellulose pyrolysis. As the temperature rises, the weight-loss rate is lowered, achieving a final residual weight of only 4% of the original sample, measured at 700 °C.

Since these two pathways concurrently occur, the two different weight losses as a function of temperature cannot be distinguished using thermogravimetric analysis.

Otherwise, the thermal degradation process of cotton textiles in air is more complicated, and proceeds according to three steps. The loss of bound water occurs in the first stage, resulting in a modest drop in the weight of cotton fabrics. During the first step of cellulose degradation in O<sub>2</sub> ( $T_{\max 1} \approx 300\text{--}400\text{ }^{\circ}\text{C}$ ), the two competitive dehydration and depolymerization pathways take place by providing the main and faster weight loss [51]. Further increasing the temperature, a second peak of maximum weight-loss rate appears ( $T_{\max 2} \approx 400\text{--}500\text{ }^{\circ}\text{C}$ ): it can be ascribed to the conversion of some aliphatic char in aromatic, and the simultaneous carbonization and char oxidation [108]. In particular, in the temperature range of 500–600 °C, the mass retention rate of treated cotton tends to be stable, aromatic carbon decomposes into ethylene, and a competitive relationship between aliphatic carbon and volatile substances produced by cellulose dehydration and depolymerization process is established [65]. As the temperature continues to rise, the thermal degradation rate decreases, thus resulting in a slight mass decrease, while further char decomposition leads to CO, CO<sub>2</sub>, H<sub>2</sub>O, and CH<sub>4</sub> [65]. Another relevant parameter concerning thermal degradation is related to the maximum degradation rate of a sample,  $T_{\text{deg}}$  [109].

According to this mechanism, in [38], two decomposition peaks at 340 and 470 °C were found for cotton. Moreover, Wang et al. [110] observed during the first degradation stage in O<sub>2</sub> that neat cotton fabrics start dehydration at 268 °C ( $T_{\text{onset}}$ : the initial decomposing temperature), thus reaching the maximum rate degradation temperature at 346 °C ( $T_{\max}$ ). At  $T_{\max}$ , almost 62.3% carbon layer can be measured, which is the result of the mass loss due to the volatiles produced from the cellulose decomposition, while a final residual weight of only 1.6% of the original sample was measured at 700 °C. It was demonstrated that materials having a high  $T_{\text{onset}}$  do not feed the combustion reaction and, as a result, possess better flame-retardant features [111]. In another work, Simkovic et al. [112] found for bleached cotton one endotherm at 259 °C, probably ascribed to the dehydration of hydroxyls and carboxyls introduced by bleaching. Moreover, the three exotherms observed at 327, 351, and 482 °C might be related to random oxidation on the surface, ignition temperature [113], and residual glowing [114], respectively. No residue was observed at 500 °C, thus indicating that the process is completed before this temperature.

Some thermal degradation parameters by TGA of neat cotton fabrics, selected in a range of mass per unit area 110–330 g/m<sup>2</sup>, reported in the literature are summarized in Table 5.

**Table 5.** TGA data of untreated cotton samples, selected with a mass per unit area between 110 and 300 g/m<sup>2</sup>.

Mass per Unit Area (g/m <sup>2</sup> )	Atm.	$T_{\text{onset}10\%}$ (°C)	$T_{50\%}$ (°C)	$T_{\max 1}$ (°C)	R@ $T_{\max 1}$ (%)	$T_{\max 2}$ (°C)	R@ $T_{\max 2}$ (%)	R > 600 °C (%)	Ref.
115	N <sub>2</sub>	331	372	368	-	-	-	5.9	[89]
	O <sub>2</sub>	327	378	352	-	-	-	1.1	
122	N <sub>2</sub>	338	-	374	40	-	-	4	[12]
	O <sub>2</sub>	327	-	353	42	-	-	1	
129	N <sub>2</sub>	358.4	-	376.1	31.5	-	-	4.7	[61]
	O <sub>2</sub>	345.6	-	349.2	43.1	489.5	4.5	0	
150	N <sub>2</sub>	311	-	346	23.3	-	-	0.9	[62]
	O <sub>2</sub>	297	-	327	49.7	-	-	0.6	
200	N <sub>2</sub>	-	-	366	42	-	-	13	[58]
	O <sub>2</sub>	-	-	341	52.5	482	6.0	<2.0	
220	N <sub>2</sub>	-	-	365.7	-	-	-	-	[92]
	O <sub>2</sub>	-	-	346.6	-	463.9	-	1.8	
237	N <sub>2</sub>	336	360	362	50.3	-	-	8.3	[60]
	O <sub>2</sub>	330	349	351	41.7	471	5.6	1.6	
290	N <sub>2</sub>	316	-	366	42.3	-	-	13.4	[94]
	O <sub>2</sub>	309	-	344	50.0	485	5	1.4	

In principle, a flame-retardant coating acts by strongly anticipating the cellulose decomposition, as observable from the temperature at which 10% weight loss occurs ( $T_{\text{onset } 10\%}$ ) and maximum weight-loss rate temperature  $T_{\text{max}}$  [115].

In another study, the main thermal oxidative degradation process of control cotton was found between 250 and 440 °C, with the  $T_{\text{max}}$  at 327.5 °C and a weight loss of 90.4%. Finally, cotton fabrics led to a carbon residue of only 1.2% at 600 °C, ascribed to the instability of the aliphatic carbon residue in the O<sub>2</sub> atmosphere undergoing further oxidation at high temperatures. Conversely, FR-treated cotton fabrics started decomposing at low temperatures since  $T_{5\%}$  and  $T_{10\%}$  were found at 73.1 and 122.4 °C, respectively. Moreover, treated samples led to a  $T_{\text{max}}$  of 265.5 °C and a carbon residue of 12.5% at 600 °C, which are lower and higher than those of control cotton, respectively [116]. The decomposition of FR generates phosphoric acid by promoting the formation of carbon residue, which can effectively protect the underlying cellulose polymer from the action of heat flow and O<sub>2</sub>, thus inhibiting the decomposition of treated cotton and highlighting its high thermal oxidation stability.

#### 4.5. Differential Scanning Calorimetry

The thermal behavior of untreated cotton is also studied by differential scanning calorimetry (DSC). In DSC, analyses are performed in a temperature range of 30–600 °C with a flow rate range of nitrogen of 20–50 mL/min; the heating rate is 10 °C/min. Generally, due to the low heat conduction properties of cotton, the sample is cut into small pieces (in the range of 2–20 mg) to achieve uniform heat transfer from one point to another [70].

A typical DSC curve of untreated cotton is characterized by two endothermic peaks, corresponding to the water evaporation (100 °C) [117] and to the heat absorbed by the thermal decomposition of cellulose (350 °C) [118]. It was demonstrated [70] that the thermal degradation of hemicellulose starts above 200 °C with the breakage of bonds at 250 °C and the formation of volatile species.

At high temperatures, cellulose decomposes into L-glucose that further originates CO, other small molecules and char able to absorb a great amount of heat [119]. As the thermal degradation process goes on and more volatile species are generated, more energy is produced, which favors the breaking of the more resistant cellulosic chains and the formation of further volatile molecules. The volatilization of these molecules can be observed through the corresponding endothermic peaks above 360 °C. Overall, the thermal reaction from 220 °C and up to 370 °C can be considered a continuous reaction involving the decomposition of hemicellulosic and cellulosic components and volatilization of the resulting degradation products. Since the main endothermic peak is at 360–370 °C, it can be stated that the predominant reaction over 300 °C is related to cellulosic degradation that leads to the formation of less char and more tar.

Furthermore, since the dehydration rate of untreated cotton to char is significantly small, the exothermic peak at around 400 °C is very low and not immediately noticeable in the thermogram [61].

However, for untreated cotton, the decomposition of hemicellulose and cellulose, as well as the volatilization of formed compounds, are complete at 370 °C.

For more in detail, Teli et al. studied the peak temperature and corresponding heat release of cellulose and its components. The authors found a dehydration peak temperature at 92.2 °C that corresponds to a heat release of 127.3 J/g. Furthermore, the peak of cellulose and hemicellulose combustions were measured at 339.1 and 368.1 °C corresponding to 189.96 and 9.9 J/g heat release, respectively [120].

In another study [121], both untreated and FR-treated cotton samples provided an endothermic peak related to the dehydration phenomenon in the range of 100–160 °C. Moreover, for untreated cotton samples,  $\Delta H$  of 155 J/g was measured. This value decreased to 125.48 and 113.08 J/g for FR-treated cotton samples resulting in higher intensity with respect to untreated cotton, thus highlighting the action of the FR applied. Moreover, the

exothermic peak occurred for treated cotton at 250 °C, due to the high temperature of the cross-linking reaction, while at 380 °C the formation of levoglucosan was observed [121].

#### 4.6. Study of Pyrolysis Products of Cellulose

The flammability of cellulose polymer is significantly affected by the pyrolysis; thus, the resulting products of FR and control fabric provide relevant information about the FR mechanism. In this regard, the pyrolysis and pyrolysis product of FR-cotton materials can be investigated by pyrolysis–gas chromatography–mass spectroscopy (PY–GC–MS) [122].

As reported in the literature [123–125], several flammable fragments are generated from the thermal decomposition of cellulose, such as levoglucosan, furfural, furans, ketones, and aldehydes. In this regard, the characterization of cotton fabrics by PY–GC–MS revealed more than 40 chromatographic peaks and more than 20 kinds of thermally decomposed products [122]. Similarly, in [125], fewer gas products as a consequence of a gas scavenging effect were detected for flame-retardant cotton fiber.

Accordingly, it was demonstrated that more peaks or more products are produced by the pyrolysis of the untreated cotton fibers than that of the flame-retardant cotton. Moreover, PY–GC–MS spectra of cotton fibers revealed a significant reduction in the numbers of peaks of the flame-retarded fiber, due to a reduction in the thermal degradation products. Indeed, the intensity of the peaks is strictly related to the amount of pyrolyzed products. Among the pyrolysis products, the incombustible ones (e.g., water and CO<sub>2</sub>) play a key role in reducing the material flammability, contrary to the combustible ones (e.g., alcohol, aldehyde, ketone, furan, benzene ring, ester, and ether), whose amount is significantly different when they are released from thermal decomposition of FR-cotton or control cotton.

Furthermore, the pyrolyzed pure cotton can be characterized by Fourier transform infrared spectroscopy (FTIR) to assess the chemical composition of char. Spectra of cotton fabric char residue revealed some absorption bands at 3400, 2900, 1740, 1700, 1600, and 1444 cm<sup>-1</sup>, assigned to OH, CH, CO stretching of aldehyde and unsaturated aldehyde, C–C stretching of alkenes, and aromatic C=C stretching vibration, respectively, as result of dehydration and loss of hydroxyl groups [126,127]. Moreover, another peak at 1032 cm<sup>-1</sup> was assigned to the C–O–C bond, thus revealing the formation of ether molecules in the char [127].

### 5. Inorganic Chemicals Currently Used as Flame Retardants for Cotton

The use of flame retardants for developing protective cotton-based clothing has attracted increasing interest in recent years, owing to the unique properties of obtained materials that find numerous applications in many technical fields. According to their chemical composition, the broad field of finishes can be divided into two main categories: inorganic and organic compounds. Typically, the former may also be of natural origin but generally do not contain any carbon atoms, while the latter specifically includes carbon atoms. The exception to this rule refers to carbon nanotubes and graphene, which are arbitrarily categorized as inorganic fillers despite only being made of carbon atoms. Although many papers have been published on this topic, to the best of our knowledge, a detailed review of the effectiveness of inorganic-based formulations applied to cotton fabrics has not been published yet.

In the following sections, the most widely used inorganic products to enhance flame-retardant properties of cotton fabrics will be summarized. For each example, selected materials and their application to cellulose-based samples will be illustrated, emphasizing the structure–property relationships that enhance thermal behavior and fire-resistant properties of textiles.

The use and performance of phosphorus-containing inorganic molecules and salts, as well as the use of clays with other layered minerals of interest, will be discussed. Furthermore, FR finishing treatments on cotton fabrics by inorganic sol–gel precursors, as well as the use of metallic nanoparticles, will also be discussed. At the same time, a section will be dedicated to the rise of carbon-based finishes, such as carbon nanotubes and

graphene, as promising candidates for developing new advanced materials with flame-retardant properties. A summary of the action mechanism and effect of each flame retardant discussed in the next paragraphs is reported in Table 6.

**Table 6.** Summary of the action mechanism and effect of the different flame retardants.

Inorganic Flame Retardant	Action Mechanism	Mode of Action	Effect
Red Phosphorous	Condensed Phase Gas Phase	- Char-forming agent - Reduce heat combustion	- Decrease the formation of combustible gases/mass loss - Production of H <sub>3</sub> PO <sub>4</sub> (dehydration agent) enhancing the char formation - Radical quenching
Boron-based FRs	Condensed Phase	- Char-forming agent	- Enhance thermal insulation - Inhibit pyrolysis - Prevent heat transfer to the textile - Reduce the generation of smoke and toxic gases
Sol-gel-based FRs	Condensed Phase	- Char-forming agent	- Block O <sub>2</sub> transfer - Block heat exchange - Block oxidative decompositions
Nanoclays	Condensed Phase	- Char-forming agent	- Slow the evolution of combustible gases - Block the entry of O <sub>2</sub> - Prevent heat transfer to the textile - Reduce polymer degradation

**Table 6.** *Cont.*

Inorganic Flame Retardant	Action Mechanism	Mode of Action	Effect
CNTs	Condensed Phase	- Char-forming agent	- Act as a heat barrier - Act as a thermal insulator - Prevent heat transfer to the textile - Reduce polymer degradation
Graphene	Condensed Phase	- Char-forming agent	- Retard the mass- and heat-transfer processes
Metal-based NPs	Condensed Phase Gas Phase	- Char-forming agent - Catalytic role in the redox reactions	- Promote the dehydration of cotton - Reduce heat release - Absorb active species (e.g., free radicals) - Reduce O <sub>2</sub> concentration through redox mechanisms

### 5.1. Inorganic Phosphorus-Based Flame Retardants

Over the past 50 years, phosphates, phosphonates, phosphoramides, and phosphonium salts, as phosphorus-based flame retardants, have been used in flame-retardant finishing for cellulosic fabrics [118]. Among these phosphorus compounds, red phosphorus is one of the ecologically and physically most harmless alternative fire retardants, although its use was deterred by problems of handling safety, stability, and color. It is one of the primary allotropes of phosphorus, which includes white phosphorus and black phosphorus, and is the most concentrated source of phosphorus-containing flame retardant. A red phosphorus emits highly toxic PH<sub>3</sub> gas when exposed to air for an extended period of time, much progress has been achieved in its encapsulation, thanks to the commercial availability of masterbatches in a wide range of polymer precursors [128]. Therefore, the most significant disadvantage for its widespread application as a flame retardant is the reddish-brown color of treated polymeric materials. Red phosphorus can act in both the

condensed and the gas phases [129]. In the former case, favored by the presence of water in the polymer, it acts as a char-forming agent, decreasing the formation of combustible gases and the mass loss. When red phosphorus burns, it produces phosphorus (V) oxide, which can absorb water vapor from the air, producing phosphoric acids that act as a dehydration agent, enhancing the formation of char. In the second case, in the gas phase, red phosphorus reduces the heat of combustion.

The flame-retardant effect of red phosphorus applied to a pure cotton fabric was confirmed by Mostashari et al. [130]. The optimum concentration of red phosphorus to impart flame retardancy onto cotton was around 4% (*w/w*). At this concentration, the comparative TG/DTG curves of the untreated and treated samples in air displayed the weight loss for the treated cotton around 290 °C, about 60 °C lower than that of the untreated fabric. At this temperature, the presence of red phosphorus promoted the thermal dehydration of the substrate and the formation of carbon residue.

Similarly, the combined effect between red phosphorus and calcium chloride on the flame-retardant behavior of cotton samples has also been studied [131]. According to the results of thermogravimetric analyses, a synergistic effect to promote the formation of non-volatile char residues and less flammable gases in the finished samples was observed. The authors proposed that the presence of phosphorous, with a mechanism similar to halogenated flame retardants but only in the condensed phase, could scavenge the free radicals produced during the thermal degradation of the polymer, delaying the non-oxidative pyrolysis of cotton samples. Furthermore, red phosphorous was found to show a synergistic effect in combination with zinc chloride due to their respective abilities to increase char formation and reduce the formation of combustible gases during the thermal decomposition of cotton [132]. After the deposition of 5.6% (*w/w*) anhydrous additives, vertical flame-spread tests on treated samples showed a flame-retardant effect, with a char length of 2 cm. Unfortunately, the authors admitted no uniformity in the observation during the burning process due to uneven fabric impregnation.

Furthermore, several inorganic phosphorus salts, such as urea phosphate, diammonium and ammonium phosphates, and ammonium sulfamate were studied to confer flame-retardant properties to cellulose-containing fabrics. When heated, these salts break down into acids, catalysing the dehydration and char-forming reactions that occur during the cellulose breakdown process.

A typical example of inorganic phosphate salt is ammonium polyphosphate (hereafter, APP), which is obtained by heating ammonium phosphate with urea. It is a branched or linear polymer compound with varying chain lengths (*n*). APP with short linear chains (where *n* is less than 100, crystal form I) is more sensitive to water and less thermally stable, while APP with long chains (*n* > 1000, crystal form II) has very low water solubility (<0.1 g/100 mL). APP is a stable and non-volatile compound. The long chains start to decompose at temperatures above 300 °C, producing polyphosphates and ammonia, while the short chains decompose at 150 °C. Therefore, it is important to change the crystal form of APP to match the polymer decomposition temperature. Incorporating APP into polymers containing oxygen and/or nitrogen atoms results in the charring of the polymer. The thermal decomposition of APP produces free acidic hydroxyl groups, which condense through thermal dehydration and produce highly cross-linked structures. Polyphosphoric acid reacts with polymers containing oxygen and nitrogen, catalyzing dehydration and charring formation. However, the effect of APP depends on its loading [133]. A simple treatment with an inorganic phosphorus aqueous solution also improves the flame resistance of cotton fabrics [134]. Cotton fabric treated with H<sub>3</sub>PO<sub>3</sub> was not burnable and the residue increased by almost 50% at 800 °C. After treatment, the fibers became brittle with some disconnection, but the cellulose crystal structure suffered little damage. Some of H<sub>3</sub>PO<sub>3</sub> reacts with the hydroxyl groups and is phosphorylated, which can promote dehydration and carbonization of cellulose and enhance its flame-retardant performance.

Recent findings by Lin et al. [135] confirmed the flame-retardancy properties of APP-coated cotton. Indeed, when exposed to heat, APP pyrolyzed earlier than cellulose to

generate polyphosphoric acid and some inert gases, such as  $\text{CO}_2$  and  $\text{H}_2\text{O}$ , boosting the pyrolysis of cellulose mostly toward the generation of intumescent char layers. Accordingly, the char residue of the APP-treated samples showed a significant rising trend, reaching 32.1 wt%. Moreover, due to the lower degradation temperature of APP, the temperature at 5 wt% mass loss ( $T_{5\%}$ ) of the treated samples decreased accordingly.

Additionally, Wang et al. [136] reported an interlayer-confined approach for intercalating two-dimensional zirconium phosphate (ZrP) within reduced graphene oxide (RGO) interlayers, yielding a hierarchical ZrP-RGO product. This latter was combined with APP particles to create an intumescent flame-retardant coating on cotton fabrics via automatic screen printing. The treated samples exhibited excellent self-extinguishing performance after the withdrawal of flame. Moreover, compared to untreated cotton, its PHRR and THR values were significantly reduced by 92.1% and 61.8%, respectively.

### 5.2. Boron-Based Flame Retardant

Boron-based inorganic flame retardants have been used for more than 200 years [137]. When undergoing endothermic decomposition, the boron-based flame retardant shows a mechanism in the condensed phase forming a protective layer that enhances the thermal insulation barrier of treated samples, thus inhibiting pyrolysis processes and preventing heat transfer to the textile. At the same time, this layer prevents the exchange of organic volatiles in a fire and reduces the generation of smoke and toxic gases [138]. However, since boron-based FRs easily hydrolyzed, their washing fastness performance has been challenging for application on cotton and other cellulose fibers [139]. Some authors reported the use of hydrated sodium metaborate (SMB), as an example of an inexpensive and non-toxic flame retardant for cellulose-based materials, also exploiting its ability to release water molecules during combustion, in addition to the glassy charring effect of boron-hydroxyl compounds [140]. First, Mostashari et al. [141] demonstrated that impregnating sodium borate decahydrate onto cotton fabric resulted in better flame retardancy. The comparative TG curves of untreated and treated cotton fabric, with the salt at its optimum loading, displayed a main mass loss for the treated fabric around 275–325 °C, corresponding to a characteristic range of cotton thermal degradation. TG curves showed that the pure salt does not break down into oxide at the decomposition range of the pyrolyzing material.

Due to the removal of its crystallization water, the mass loss occurs at around 100 °C, thus permitting the remaining products to act as a barrier to absorb and dissipate the heat from the combustion zone. Then, Tawiah et al. [142] treated cotton fabrics with hydrated sodium metaborate (SMB) crystallized in situ in the pore spaces and on the surface of the impregnated cotton fabric. TGA results showed that SMB treatment improved the thermal stability of cotton fabric and enhanced the char yield. The treated cotton also had an LOI value of 28.5% with an after-glow time below 1 s in the UL-94 test (V-0 rating). Considerable reductions in peak heat-release rate (PHRR ~91.8%), total heat release (THR ~47.2%), peak carbon monoxide, and carbon dioxide produced (PCOP ~28.6,  $\text{PCO}_2\text{P}$  ~85.5%) were observed. The post-burn residues examined by SEM and Raman spectroscopy demonstrated a maintained fabric structure with high graphite content. SMB-treated cotton fabrics showed negligible changes in tensile strength and elongation at break values.

Furthermore, Akarslan [143] investigated the application of boric acid (BA) to cotton fabrics for flame-retardant purposes. Different concentrations of boric acid nanoparticles were tested to optimize the flame-retardant effect. The results showed increased flame-spreading times of the coated fabrics with increasing boric acid content. Compared to neat cotton (2.5 s and 2.4 s in weft and warp direction, respectively), the best result was observed by adding 30 g/L of BA, increasing the flame-spreading time by about 40% in the two directions. Unfortunately, an inevitable decrease in tensile strength was demonstrated for the treated samples.

Moreover, Liu et al. [144] used boron nitride nanosheets modified with hexachlorocyclotriphosphazene to develop a flame-retardant finishing by impregnation-drying method for cotton. Compared to the untreated fabric, the combustion rate of the treated counterpart

decreased in vertical and horizontal flame-spread tests, and the limiting oxygen-index value increased to 24.1%, thus becoming less flammable than the reference.

On the other hand, zinc borate plays a leading role in delaying the thermal oxidation of the fabric. Indeed, over 300 °C, it loses crystal water diluting the oxygen in the air, significantly lowering the combustion surface temperature, and absorbing a lot of heat. High temperatures cause some of the zinc borate to break down into B<sub>2</sub>O<sub>3</sub> and hydrolyze to produce boric acid, which is then chemically and physically adsorbed onto the surface of the fabrics to form a coating.

Diboron trioxide inhibits the oxidation reaction of carbon compounds, reducing the production of free radicals and promoting the termination of chain reactions. In addition, when zinc borate is hydrolyzed, a tiny amount of boric acid will be created and utilized as an acid source to promote the creation of char layers, giving rise to synergistic effects with silica sol, and lowering the amount of smoke produced during combustion. Additionally, under the same conditions, roughly 38.0% of the zinc in zinc borate transforms into zinc oxide or zinc hydroxide, which dilutes the combustible gas and slows down its combustion rate. Microscale combustion calorimetry showed THR and PHRR values of zinc borate-treated fabrics decreased by 34% and 3.1% (9.2 kJ/g and 300.8 W/g) when compared to the pristine textile, respectively [66].

In another study, Durrani et al. [29] investigated the flame-retardant effect of nano-zinc borate (ZnB) on cotton fabrics. Compared to untreated cotton, the fabrics treated with 12 wt% of ZnB exhibited increased LOI values (+12%), accelerated char formation acceleration, decreased PHRR (21 vs. 90 kW/m<sup>2</sup> for treated and untreated cotton, respectively), and THE values (1.6 vs. 3.8 MJ/m<sup>2</sup> for treated and untreated cotton, respectively). Moreover, the TG curve of the synthesized zinc borate showed thermal stability up to 700 °C.

Further, cotton fabrics were treated with boric acid doped with TiO<sub>2</sub> obtained by titanium (IV) butoxide precursor [145], showing good flame resistance.

Compared to untreated cotton, as assessed by thermogravimetric analysis, the treated samples showed lower degradation temperature (250 °C), the formation of a thermally stable char at high temperatures, and a residue that was significantly more important than that of the reference. In particular, the best results in terms of thermal stability and flame retardancy were obtained for textiles finished with the sol doped with a 2.5 molar ratio of boric acid.

Moreover, the flammability behavior of the treated sample in vertical configuration, after 10 s of flame application, showed no full ignition after the flame was removed and a residue of more than 90%. The burned area was approximately 16 cm<sup>2</sup>, and a higher FPI value of 45.46% demonstrated increased flame resistance of cellulose-based samples, due to the protective char layer and heat absorption introduced by the finishing treatment.

However, although boron-containing compounds are cited in several scientific papers as less toxic and cheaper alternatives to traditional flame retardants [137,139,146], many of them do not meet GOTS (global organic textile standard) compliance [147]. In particular, in the FR formulations, GOTS has kept the limit for boric acid, diboron trioxide, disodium octaborate, disodium tetraborate anhydrous, and tetraboron disodium heptaoxide hydrate individually under 250 mg/kg, while the use of disodium octaborate is forbidden.

### 5.3. Flame-Retardant Finishing by Sol–Gel Technique

Over time, the meaning of the sol–gel technique has evolved differently in the definitions of authors [148–152]. However, it can be summarized as a two-step reaction of hydrolysis and condensation, involving inorganic salts, (semi-) metal alkoxides and organosilanes as the most common components to form inorganic or hybrid organic–inorganic products [153–156]. The nature of precursors, pH, temperature, and reaction time values can affect the hydrolysis and condensation rates and, thus, the nature of new materials developed that show high homogeneity at the molecular level, and excellent physical and chemical properties [157]. Due to its tunable properties, the sol–gel technique has been extensively studied for textile applications to develop functional coatings on both natural

and synthetic fabrics [158,159]. In textile finishing, colloidal solutions in aqueous media are usually used to impregnate fabrics at room temperature by padding. Then, the treated samples are cured at 130–160 °C to produce porous, fully inorganic, or hybrid organic–inorganic coatings with structures depending on the nature of precursors, water/precursor ratio, acidic or alkaline conditions of the medium, curing temperature, time of reaction, and presence of solvents [160]. In the literature, several properties developed by the sol–gel technique on textile materials are reported, such as water repellence [161,162], stimuli-responsiveness [163], dyeability enhancement [164], anti-wrinkle finishing [165], drug delivery [166], UV radiation protection [167], self-cleaning [168], stain-resistance [169,170], antimicrobial [171], and flame retardancy [172], also assessing the phosphorus–nitrogen synergism [25]. Due to the focus of this review, the thermal behavior and flammability of cotton textiles exclusively treated with sol–gel and fully inorganic precursors and dopants are described. The common inorganic precursors used are metal alkoxides, such as tetraethoxysilane (TEOS), tetramethoxysilane (TMOS), tetrabutylorthosilicate (TBOS), tetraethylortho-titanate, zirconate, and aluminium isopropylate [173–176].

The first example of inorganic sol–gel-based coating to enhance flame-retardant properties on cotton was reported by Cireli et al. in 2007 [177]. The authors used TEOS as a sol–gel precursor in combination with phosphoric acid, the latter used as the agent to dehydrate cellulose samples. The TGA showed that P-doped silica-based powder has a weight-loss percentage equal to 37%, while the mass-loss value for silica powder only was 23%. After exposing fabrics to a flame for 15 s, the phosphoric acid-containing sol–gel-based finishing provided the production of nonflammable cotton fabrics. Moreover, the flame-retardant property was not completely lost after 10 washing cycles. The proposed finishing introduced a new approach to avoid additional post-treatment to improve washing fastness on treated cotton samples.

After that, another research investigated the influence of different TEOS/H<sub>2</sub>O ratios to explore the effect of the presence of inorganic silica-containing films on the thermal and fire stability of cotton fabrics [178]. At a TEOS/H<sub>2</sub>O ratio of 3:1, these films decreased up to 35% the peak of the heat-release rate (PHRR), and increased the time to ignition by up to 28%, as assessed by cone calorimetry tests. This behavior was attributed to the presence of the silica-based coating able to form a protective layer on treated cotton samples, also influencing their thermal stability in both nitrogen and air atmospheres. In the latter, the presence of coatings was responsible for slightly anticipating the decomposition step in the range between 300 and 400 °C and for an increase of about 20% of the final residue at 700 °C. These findings showed that, compared with pure cotton, the presence of the silica coatings did not improve in a remarkable way LOI values, though it changed the burning kinetics of treated samples. Indeed, the reference textile burned very quickly with a sparkling flame, while treated samples exhibited a very slow propagation of an incandescent front.

In 2012, Alongi et al. [94] developed sol–gel-based finishing of cotton fabrics using tetramethylorthosilicate precursor in the presence of various smoke suppressants, such as zinc oxide (ZnO), zinc acetate dihydrate (ZnAc), and zinc borate (ZnB), or flame retardants, such as ammonium pentaborate octahydrate (APB), boron phosphate (BP), and ammonium polyphosphate (APP), or in the presence of barium sulphate (BaS), which possesses both characteristics. According to TG studies, carried out both in nitrogen and air, the silica phase and the smoke suppressants showed combined effects that resulted in a remarkable increase in the residues at the various temperatures examined. As assessed by cone calorimetry, the presence of zinc in the silica coatings reduced the release of CO and CO<sub>2</sub> significantly. In particular, the joint effect of ZnO and silica promoted the most significant decrease in CO and CO<sub>2</sub> yields. This finding was ascribed to ZnO complete solubility in the sol solution that allows for the formation of a homogeneous coating, unlike ZnB, which formed macro aggregates. At variance, the highest residues at the maximum weight loss were found for BP and APP (69.3 and 69.0%, respectively).

In 2013, Colleoni et al. [179] focused on the sol–gel synthesis of silica thin films derived from TEOS on cotton fabrics. For this purpose, a new multi-step process consisting of

one to six subsequent depositions was set to obtain samples with different numbers of silica layers, further testing the presence of dibutyltin diacetate (DBTA) as a condensation catalyst. Vertical flame-spread tests were carried out, also after several laundry cycles, to assess the washing fastness of the designed coatings. After removing the fire source, the untreated cotton burns quickly in a few seconds, leaving a very poor residue. In contrast, in 0.3 M TEOS six-layer finished fabrics, the flame spreads to the upper end of samples, then extinguishes, leaving slightly shrunken burned specimens, with 17% final residue. Again, the silica-containing coatings on cellulose-based fibers favored the char formation rather than the evolution of volatile species that could lead to further burning, regardless of the use of DBTA in the formulation. In addition, the authors highlighted the laundering durability of applied inorganic coatings that exhibit the same residue (about 13%) after combustion both after one and five laundry cycles.

However, it is interesting to consider one piece of evidence that emerges in the research reported in the literature: TEOS has low solubility in water, and it is highly reactive, which should be taken into account when used in sol-gel technology. The low solubility can be easily addressed by using such co-solvents as ethanol or other alcohol. Conversely, the high reactivity strongly affects the composition of the resulting coating [175]. In particular, the higher the hydrolysis/condensation rate, the lower is the conversion of TEOS on the fabric surface.

More recently, Zhang et al. used tetraethoxysilane precursor in combination with ammonium pentaborate in order to enhance the flame retardancy of cotton fabrics [180]. Thermogravimetric analyses of treated fabrics showed increased  $T_{10\%}$ ,  $T_{\max}$  values up to 288.3 °C and 357.6 °C, namely, 18.4 °C and 12.0 °C, higher than the untreated sample (269.9 °C and 345.6 °C). Finally, the treated sample weight loss in primary pyrolysis stage was 54.8%, lower than the reference (64.0%). Furthermore, the LOI value was almost unchanged with respect to the untreated fabric (i.e., 20.2% vs. 18.3%, respectively), while the residue at 700 °C was 31.3%. These results were attributed to the formation of an inorganic coating that acts as a physical barrier, blocking oxygen transfer, heat exchange, and oxidative decomposition, thus improving the overall thermal stability and flame retardancy. According to TG results, the silica coating evolved during pyrolysis, producing high-temperature-resistant Si-C compounds, which were further transformed into a char layer on cotton samples, resulting in high final char residue. In particular, compared with carbon layers formed by the thermal decomposition of other classes of FRs, the Si-based stable adiabatic char is denser, thicker, and stronger, thus resulting in a higher isolating effect toward heat and oxygen and further able to block the diffusion of flammable gases and inhibit the combustion [23].

Furthermore, TEOS was combined with zinc borate, investigating its flame-retardant properties on cotton fabrics [66]. It was confirmed that during the combustion the silica-containing film acts as a barrier forming a carbon layer on the fibers' surface due to the polycondensation of the silica network at high temperature, promoting a decrease in THR and PHRR values of treated samples by 32.1% and 37.1% (9.5 kJ/g and 195.4 W/g), respectively, when compared to reference sample, as assessed by microscale combustion calorimetry.

In addition to TEOS, other silane sol-gel precursors were studied, investigating the water molar ratios and the alkoxide chain length. To this aim, TEOS was replaced with tetramethylorthosilicate (TMOS), an analogous silane bearing four methoxy groups [181]. Cone calorimetry tests showed that the best flame-retardant performance was achieved by the sol-gel-treated cotton samples (performing the treatment at 80 °C for 15 h, and using a 1:1 molar ratio of TMOS: H<sub>2</sub>O, without HCl as condensation catalyst). Compared to the reference, TTI increased from 18 s to 28 s and PHRR decreased significantly (−20%), according to the formation of a silica coating on cotton fibers, which acts as a barrier to heat and oxygen diffusion on cellulose-based surfaces. The authors highlighted that the obtained results strictly depended on the degree of distribution and dispersion of silica on and within the fiber interstices. In fact, when the morphology of the coating is more homogeneous, flame-retardant performance is better, as observed from the correlation

between cone calorimeter tests and  $^{29}\text{Si}$  solid-state nuclear magnetic resonance results [181]. As confirmed by forced-combustion tests, the presence of the thermal barrier promoted by silica coatings effectively reduced the maximum heat-release rate (by about 15%) allowing for the formation of stable aromatic carbon [182]. Furthermore, the flammability and combustion behavior of textile samples were significantly affected by the presence of different alkoxide chain-length in the precursors [183]. To this aim, the flame retardancy of cotton fabrics separately treated with tetramethyl orthosilicate (TMOS), tetraethyl orthosilicate (TEOS), and tetrabutyl orthosilicate (TBOS), bearing four methoxy, ethoxy, and butoxy groups, respectively, was investigated and compared. Vertical flame-spread tests showed that even a low amount of silica was enough to slow down the burning rate. The final residue of untreated cotton was 10 wt%, while those of samples treated with TMOS, TEOS and TBOS were 48, 35, and 33 wt%, respectively: the shorter the chain length of the precursor, the lower the flammability of cotton. These findings were in agreement with the cone calorimetry results, carried out with an irradiating heat flux of  $35 \text{ kW/m}^2$ : the lowest PHRR and THR values were observed in the case of TMOS-treated cotton samples.

In another research, TMOS was combined with  $\alpha$ -Zirconium dihydrogen phosphate (hereafter, ZrP) in order to enhance synergically the flame retardancy of cotton fabrics. ZrP was added to the sol solution prepared in a hydroalcoholic solution (TMOS:H<sub>2</sub>O molar ratio = 1:1), in the presence of dibutyltin diacetate as condensation catalyst (0.9 wt%) [56]. The results collected in Table 7 highlight the enhanced FR properties of TMOS with respect to the untreated cotton and the synergistic effect of Si and P, that act, particularly, on the kinetics of the burning process and thermo-oxidative stability of the fabric. Instead of silica-based precursors, other oxidic phases that can improve the fire resistance of cotton through the sol-gel technique were investigated [176]. In particular, the fire performance of cotton fabrics treated with silica was compared with those with alumina, titania, and zirconia derived from aluminium isopropylate, tetraethylorthotitanate, and tetraethylorthozirconate, respectively. The results from vertical flame-spread tests showed a significant reduction of the burning rate and an enhancement of the final residue after combustion for the treated samples compared to the untreated cotton, regardless of the nature of the precursor. Generally, the findings confirm once again the role of sol-gel-based coatings as thermal insulators for protecting textiles from exposure to fire. The better performance of TEOS compared to the other metal-containing precursors in producing a flame-retardant coating on cotton samples was pointed out by cone calorimetry tests. Indeed, compared to the reference, the silica-containing finishing increased TTI by 56% and decreased PHRR by 20%, significantly better than those containing zirconia, titania, and alumina. The authors concluded that the thermal protection on cotton exerted by the sol-gel derived oxidic species can be referred to two main reasons: the thermal insulating effect of the ceramic layer and the presence of metal cations in the precursor. The results from TGA, and the forced-combustion and flammability tests are summarized in Table 7.

In the latter scenario, the thermo-oxidation of cotton is influenced by metal cations, also in combination with phosphorus-based flame retardants, which promote cellulose dehydration and, as a result, the development of significant amounts of char.

These sol-gel-based coatings developed from different inorganic precursors were responsible for an overall improvement of the thermal and fire stability of the treated cotton samples. Based on these findings, in further research, silicon and aluminum as two different ceramic film precursors were investigated to reach an optimal formulation for conferring flame retardancy to cotton fabrics, exploiting the respective characteristics [58]. In detail, tetramethylorthosilicate sol-gel precursors were exploited for depositing coatings consisting of silica added of micro- or nano-sized particles of alumina on cotton fabrics, thus investigating their thermal stability and flame retardancy by thermogravimetry, flammability and combustion tests. As a result, compared to untreated cotton, 1% and 0.5% of micro- and nano-sized alumina particles within the silica coating were able to decrease the total burning rate by at least 70%, increasing the final residue of treated samples by more than 40%.

**Table 7.** Forced-combustion, flammability, and thermal behavior of cotton fabrics treated by inorganic sol–gel precursors.

Weight per Unit Area (g/m <sup>2</sup> )	Precursor (Molar Ratio of Precursor:H <sub>2</sub> O)	Cone Calorimeter Tests			Thermal Behavior						Vertical Flame-Spread Tests			Ref.
		TTI (s)	THR (MJ/m <sup>2</sup> )	PHRR (kW/m <sup>2</sup> )	TGA in Air		TGA in Nitrogen		Total Burning Time (s)	Total Burning Rate (mm/s)	Residue (%)			
					T <sub>max1</sub> (°C)	T <sub>max2</sub> (°C)	Residue at T > 600 °C (%)	T <sub>max</sub> (°C)				Residue at >600 °C (%)		
-	TEOS1 (1:1)	16	2	39	338	507 *	24	361	37	-	-	-	[178]	
-	TEOS2 (2:1)	9	3	38	338	507 *	24	361	32	-	-	-	[178]	
-	TEOS3 (3:1)	18	3	37	338	507 *	18	361	32	-	-	-	[178]	
200	TMOS	30	1.8	82	338	496	20	-	-	70	1.43	48	[183]	
200	TEOS	30	2.3	85	331	485	10	-	-	57	1.75	35	[183]	
200	TBOS	28	2.2	90	338	495	12	-	-	57	1.75	33	[183]	
200	TEOS	28	2.0	70	346	507	10	-	-	25	11	30	[176]	
200	Tetraethylortho titanate	22	2.3	84	326	445	9	-	-	29	9	31	[176]	
200	Tetraethylortho zirconate	22	2.7	82	340	498	7	-	-	24	12	21	[176]	
200	Aluminium isopropylate	20	1.9	106	339	511	9	-	-	23	12	32	[176]	
200	TMOS	24	3.5	114	346	484	24.0	362	34	26	5.8	23	[58]	
200	TMOS + Micro-alumina	36	3.2	110	346	492	22.5	360	37	34	4.4	46	[58]	
200	TMOS + Nano-alumina	22	3.4	101	346	486	27.0	361	38	35	4.2	46	[58]	
210	TMOS	28	2.5	81	349	487	24	-	-	41	-	34	[56]	
210	TMOS (1:1) + ZrP	22	2.9	107	344	498	31	-	-	110	-	62	[56]	
290	TEOS	18	3.3	118	343	499	19.8	362	34.0	-	-	-	[94]	
290	TEOS + ZnO	18	3.6	124	346	492	26.0	356	38.7	-	-	-	[94]	
290	TEOS + ZnAc	18	3.6	135	345	498	18.5	356	30.7	-	-	-	[94]	
290	TEOS + ZnB	18	3.6	133	346	503	23.3	359	34.8	-	-	-	[94]	
290	TEOS + APB	22	3.4	116	341	501	26.0	349	35.5	-	-	-	[94]	
290	TEOS + BP	20	3.6	132	349	505	24.0	358	40.8	-	-	-	[94]	
290	TEOS + APP	20	3.6	130	347	498	24.1	358	41.8	-	-	-	[94]	
290	TEOS + BaS	22	3.3	118	346	505	24.0	361	37.0	-	-	-	[94]	

\* T<sub>max3</sub>.

#### 5.4. Flame-Retardant Finishing by Inorganic Nanoparticles

Nanotechnology has been largely investigated since it represents a tool for obtaining non-toxic and high-performing flame-retardant systems of great scientific and industrial interest [184–186]. These particles have a size of 1–100 nm at least in one dimension, and they can be embedded in the fibers or coated on fabric surfaces to impart flame-retardant properties and improve the mechanical strength or the thermal stability of treated textiles. When uniformly dispersed, a small amount of inorganic filler (typically less than 5 wt%) can slow down the diffusion of gas molecules through the polymer matrix and the burning rate of materials [187].

According to the literature [75,175,188], nanoparticles can be applied to textiles by layer-by-layer (LbL) technique or nanoparticle adsorption. During combustion, these coatings give rise to intumescent barriers, the primary action of which is to form expanded char structures on the surface of the burning fabrics, thus reducing both the heat transferred by the flame and released flammable volatiles [189,190]. This mimics the FR of conventional intumescent coatings, which are macroscopically bigger, as they reach hundreds of microns in thickness [191].

The most common inorganic nanoparticles used to confer flame retardancy to cotton fabrics are reviewed in the following paragraphs.

##### 5.4.1. Nanoclays

Nanoclay composites have attracted great attention from researchers and manufacturers due to their outstanding properties, such as excellent mechanical and thermal stability [192–195]. The term “clay” generally refers to a class of materials composed of layered silicates or clay minerals with trace amounts of metal oxides and organics [196].

Clay minerals are usually crystalline, hydrous aluminum phyllosilicates and may contain variable amounts of iron, magnesium, alkali metals, alkaline earth, and other cations. As low-cost inorganic materials, they are commonly used as catalysts, decolorizers, and adsorbents in different scientific fields. In contrast, for industrial uses, they are employed in oil drilling, as well as in ceramics and paper productions [197–199].

Nanoclays occur naturally, but they can also be synthesized. Individual nanolayers in nanoclays comprise  $\text{SiO}_4$  tetrahedra or  $[\text{AlO}_3(\text{OH})_3]_6$  octahedra [200–202]. In general, clay particles have lateral dimensions in centimeters size, in-plane dimensions in the micron size of individual clay layers, and the thickness of a single clay plate in nanometers size. These layered clays are characterized by strong intralaminar covalent bonds within the individual sheets that form the clay [6].

In nanoclays, the thickness of the layered silicate sheets is about 0.7 nm, whereas the thickness of the bilayer is about 1.0 nm. The nanometric size of dispersed clays and the extremely high surface area induces unique properties, such as high tensile strength, low gas permeability, and a low coefficient of thermal expansion, without changing the optical homogeneity of the material [203,204]. The interaction between nanoclays and polymer chains is generally difficult because layered silicates are hydrophilic [205]. Therefore, to improve the organophilicity of nanoclays, the interlayer spacing is typically modified by organic molecules, surfactants, or exchangeable ions, such as  $\text{Na}^+$ ,  $\text{K}^+$ ,  $\text{Mg}^{2+}$ , and  $\text{Ca}^{2+}$  [193,194].

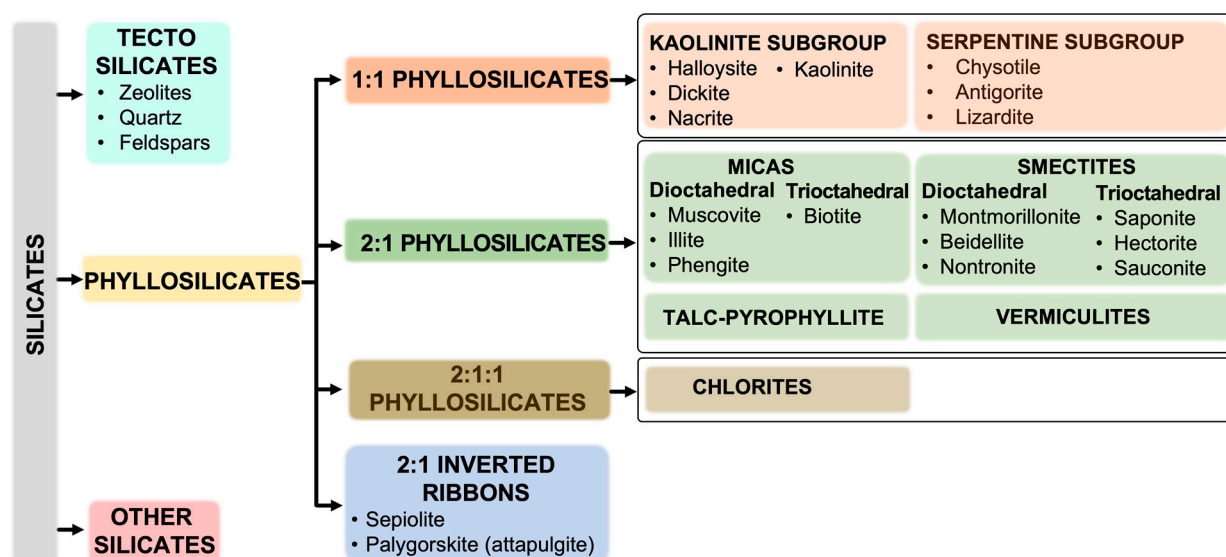
As shown in Table 8, clays can be classified according to the charge of their layers, exhibiting neutral lattice structures, low charge structures (negatively charged layers), and high charge structures (positively charged layers) [206,207].

**Table 8.** Classification of clays by layers' electrical charges.

	Type of Layers		
	Neutral	Negatively Charged	Positively Charged
Type of clay	Pyrophyllite, kaolinite, talc	Phyllosilicates: e.g., bentonites (main component: montmorillonite)	Hydrotalcite (HT): layered double hydroxides (HT-like family)
Main characteristic	Neutral clays (layers joined together by van der Waals interactions and/or hydrogen bonds)	Cationic clays (the negative layer charge is compensated by cations located in the interlayer space)	Anionic clays (the positive layer charge is compensated by anions located in the interlayer space)

Clays are also classified as phyllosilicates due to their layered structure, including tetrahedral silicon (Si) sheet(s) and octahedral aluminum (Al) sheet(s) [208]. Moreover, according to the literature [209], variable amounts of cations, such as  $\text{Fe}^{2+}$ ,  $\text{Mg}^{2+}$ , and other alkali metals, can be present in the space between layers or the lattice framework.

The layered silicates can be classified into three main groups: 1:1 (a), 2:1 (b), and 2:1:1 (c) (Figure 4).

**Figure 4.** Silicates classified according to their layered structure.

This classification is based on the number of building block sheets (silica tetrahedral and alumina octahedral) involved in their structure. Type (a) 1:1 consists of one tetrahedral silica sheet and one octahedral alumina sheet (including kaolinite, halloysite, and serpentine). On the other hand, the 2:1 type consists of an octahedral alumina sheet sandwiched between two silica tetrahedral sheets (examples include bentonite, hectorite, illite, laponite, micas, montmorillonite, saponite, sepiolite, talc, and vermiculite). Finally, type (c) clay minerals (2:1:1) are formed with a unique structure consisting of two layers of tetrahedral silica, an octahedral alumina layer, and an octahedral magnesium hydroxide (brucite) layer (e.g., chlorites) [210].

The clays display a hydrophilic nature in contrast to carbonaceous nanostructures. The most-used clays in flame retardancy are layered materials [211], usually modified through exchangeable ions, organic molecules, or surfactants [212]. The reason is that well-dispersed clay tiles in the polymer matrix form a barrier layer during the combustion process, slowing the evolution of combustible gases and blocking the entry of oxygen, thus preventing heat transfer and reducing degradation [213,214].

The following sections review the flame-retardant properties induced in cotton fabrics treated by nanoclays without organic components. The most significant results are collected in Figure 4.

### Montmorillonite

Montmorillonite (MMT) is a natural clay mineral that has been used in polymer nanocomposites for nearly three decades [215]. MMT nanoclay materials are a very soft phyllosilicate mineral belonging to the smectite family with an enlarged 2:1 crystal lattice [216]. The chemical structure of MMT is defined as  $M_x(Al_{4-x}Mg_x)Si_8O_{20}(OH)_4$ , where M is a univalent cation and x is an isomorphous substitution degree ranging from 0.5 to 1.3 [217]. It is a kind of smectite silicate, with a 2:1 layered structure about 1 nm thick and several microns in lateral dimensions, consisting of two tetrahedral silica layers (hereafter, T) separated by an octahedral alumina layer (hereafter, O), resulting in T:O:T structural unit [37,216]. MMT is the most significant species employed in creating commercial clay-polymer nanocomposites. It is important due to its swelling capabilities in water and other polar molecules. Idealized MMT has a negative charge of 0.67 units, so it behaves like a weak acid. MMT is usually characterized by a specific surface area of around 750–800 m<sup>2</sup>/g (theoretical value 834 m<sup>2</sup>/g) and a cation exchange capacity (CEC) of around 0.915 meq/g (corresponding to one ion per 1.36 nm<sup>2</sup> with anionic groups spaced about 1.2 nm) [218]. Moreover, the particle size of the commercially available MMT powder is around 8 μm, each containing approximately 3000 platelets with an aspect ratio of about 10–300. The toxicity profile of MMT appears to be safe and unlikely to pass the biological barriers, such as tissues and organs [218].

The required characteristics include a high aspect ratio, a large surface area, exceptional modulus, and nano-scale dispersion, dramatically encouraging improvements in mechanical, thermal, flammability, and barrier properties of polymers [219,220]. Figure 5 schematically illustrates the behavior of the polymer/MMT nanocomposites during combustion.

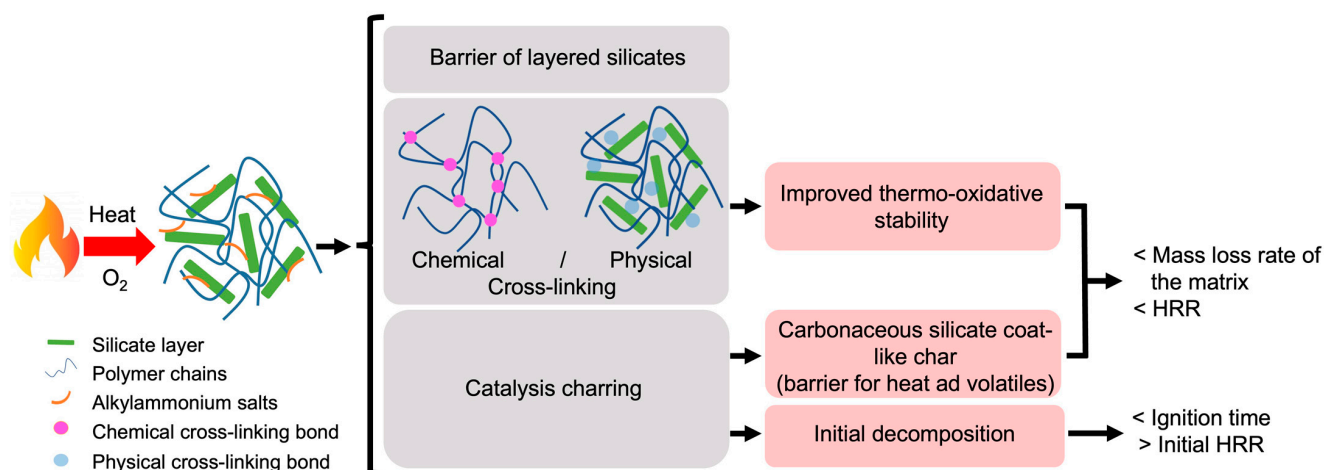


**Figure 5.** Schematic diagram of the flame-retardant mechanism of polymer/clay nanocomposites during combustion.

Due to the purpose of this review, only inorganic combinations were examined. In this regard, Alongi et al. studied a new concept of a fully inorganic intumescent flame-retardant nanocoating based on an inorganic expandable structure formed by montmorillonite (MMT) nanoparticles and ammonium polyphosphate (APP) using cotton as a model substrate [186]. A simple multi-step adsorption procedure was exploited to deposit APP/MMT coatings with the aim of improving the FR properties of cotton. Thermogravimetric analysis in nitrogen and air showed that the coating effectively promoted char formation from the cotton fibers and achieved self-extinction in horizontal flame-spread tests.

Furthermore, the results from the cone calorimetry tests, carried out under an irradiative heat flux of  $35 \text{ kW/m}^2$ , showed that the unmodified cotton ignites rapidly after 36 s, with an average PHRR of  $61 \text{ kW/m}^2$  and burns without leaving residue at the end. Using 2.5% APP/MMT lowers the TTI to 22 s, indicating early ignition, whereas with the addition of 5%, no ignition of the treated sample was observed. The analysis of the final residues showed the formation of a swollen inorganic coating that could significantly enhance char formation by providing a barrier function against volatile emissions and heat transfer.

Furthermore, Oliveira and co-workers investigated the combination of a polymeric formulation containing different ratios of sodium montmorillonite (Na-MMT) and ammonium polyphosphate for improving the thermal degradation resistance of cotton fabrics [221]. A polymer paste containing the additive was mixed up and applied to one side of the fabric using a direct coating method. The thermal stability and heat release of the treated samples improved as a function of the Na-MMT/APP ratio loaded onto the fabric. At  $800 \text{ }^\circ\text{C}$  the peak of heat-release rate (PHRR) decreased by around 51.6% and the carbonaceous residue increased.

In a further research effort, Furtana et al. assessed the possibility of using calcium-hypophosphite (CaHP) as flame retardant for cotton fabrics and evaluated its interaction with Na-MMT clay [222]. The TGA curves show that the Na-montmorillonite decomposes in two steps at  $94 \text{ }^\circ\text{C}$  (water evaporation) and  $638 \text{ }^\circ\text{C}$  (ascribed to dehydroxylation of the clay and the presence of CaHP), leaving 88% residue [223,224]. Indeed, at this temperature, the acidic compound phosphorylates the primary hydroxyl groups of cellulose through an esterification reaction that promotes the degradation of cellulose toward dehydration [225]. Accordingly, CaHP decomposes mainly in two steps corresponding to its decomposition into  $\text{Ca}_2(\text{HPO}_4)_2$  and  $\text{PH}_3$  at  $417 \text{ }^\circ\text{C}$ , and into calcium pyrophosphate and water at  $650 \text{ }^\circ\text{C}$ , thus yielding an inorganic residue of 87.4% [226]. When CaHP and clay were combined, no significant change in the  $T_{5\%}$  value was observed. However, when the amount of clay applied reached 10% mass of CaHP, a shoulder at about  $380 \text{ }^\circ\text{C}$  appeared [222].

Bronsted and Lewis acid sites present in the clay lattice are believed to provide a catalytic effect during the decomposition of CaHP [187]. The auxiliary effect of the nanoparticles was observed at different concentrations. For instance, when the coating CaHP:Clay was applied at the ratios of 1:99 and 10:90, the PHRR values increase from  $72 \text{ kW/m}^2$  to  $77 \text{ kW/m}^2$ , respectively, and THE (total heat evolved) values remaining almost unchanged. Conversely, when the CaHP:Clay was applied at the ratio of 5:95, a stronger reduction in the PHRR ( $57 \text{ kW/m}^2$ ) and THE ( $0.85 \text{ kW/m}^2$ ) with respect to the untreated cotton (PHRR of  $101 \text{ kW/m}^2$ , and THE of  $1.28 \text{ kW/m}^2$ ) was observed.

This finding demonstrated that when CaHP and nanoclay were used together, the fire performance of CaHP was further improved, with lower PHRR and THE values. Furthermore, the effect of clays at low concentrations was considered inadequate to form a continuous protective layer. At optimal concentration, the clay platelike structure acted as a barrier on the burning surface, reducing heat–mass transfer between the condensed and gas phases.

### Hydrotalcite

Hydrotalcite (HT) is a white hydrous mineral of rhombohedral structure, with a chemical formula given as  $\text{Mg}_6\text{Al}_2(\text{CO}_3)(\text{OH}_{16})_4(\text{H}_2\text{O})$ , showing low hardness (2.00) and low density ( $2.06 \text{ g/cm}^3$ ) [227]. HT is a naturally occurring, but rare, anionic mineral that is found on the earth's surface and is often associated with serpentine and calcite [228]. It gets its name from its similarity to talc and its high-water content. Indeed, hydrotalcite-type anionic clays and layered double hydroxides (LDH) containing exchangeable anions are materials that have attracted much attention in the last decade [228]. HT consists of stacked layers of brucite type built up of cationic octahedral units with common edges. Each octahedron consists of M(II) cations, some of which are replaced by M(III) cations. The M(III) cation is surrounded by six OH ions [227].

Alongi et al. [75] showed that a delay in TTI of the so-treated cotton fabrics might be caused by the high water content in the structure of hydrotalcite. These nanoparticles can partially protect the polymer from heat and oxygen since they form a ceramic layer during combustion and release large amounts of water upon heating. This way, the decomposition products released from the polymer are diluted, causing a significant delay in ignition.

The same research group investigated the influence of two impregnation times (namely, 30 and 60 min) on the thermal behavior of HT-treated cotton samples [229]. Comparing untreated cotton and the treated samples, it is possible to observe that the TTI increased from 14 s to 22 and 34 s and the PHRR decreased from 124 kW/m<sup>2</sup> to 87 and 94 kW/m<sup>2</sup>, respectively. As a result, the FPI value of HT-treated fabric was higher than that of untreated cotton.

Furthermore, additional effects on thermal stability and combustion behavior may result from the combination of HT lamellar nanoparticles characterized by layers arranged parallel to each other [230] with spherical SiO<sub>2</sub> nanoparticles [229]. At both immersion times, corresponding to 30 and 60 min, the combination of the two nanofillers improved the fire resistance of cotton and significantly increased TTI (30 s and 37 s vs. 14 s) and the corresponding FPI (0.32 and 0.43 vs. 0.11). This means that using a combination of SiO<sub>2</sub> and HT nanoparticles allows for achieving better fire resistance than that observed after performing treatments with single nanoparticles.

#### Vermiculite

Vermiculite (VMT) is a layered magnesia aluminosilicate clay mineral, with a 2:1 structure, composed of two Al for Si-substituted tetrahedral silicate sheets, which are separated by Al-Fe for Mg substituted octahedral sheet [231], corresponding to the chemical formula (Mg<sup>2+</sup>, Fe<sup>2+</sup>, Fe<sup>3+</sup>)<sub>3</sub>[(SiAl)<sub>4</sub>O<sub>10</sub>]OH<sub>2</sub>·4H<sub>2</sub>O [232].

When heated to a temperature higher than 200 °C, the VMT structure exfoliates as a result of water loss in the interlayer sheets and adaptation to the applied heat [233], inhibiting thermal transfer and imparting intumescent property to the treated materials [234]. Moreover, beyond 650 °C, vermiculite expands rapidly, showing excellent fire-retardant properties [235]. It is often used as packaging material in cardboard boxes when transporting chemical reagents [233].

Recent studies indicate that the concurrent use of VMT and nanoparticle structures (TiO<sub>2</sub>/VMT) in LBL-based fire-retardant coatings plays an important role [236–240]. In this regard, a system of vermiculite clay and TiO<sub>2</sub> nanoparticles (VMT/TiO<sub>2</sub>) in an aqueous solution was exploited for creating flame-retardant nanocomposite thin layers on cotton fabric as anionic species and cationized starch as cationic species [101]. The flame-retardant properties of LBL assemblies up to 15 BL were studied using thermogravimetric analysis, vertical flame-spread tests, and micro-combustion calorimetry. The after-burn surface and chemical analyses were performed to investigate the weave structure of the fabric. This is the first comprehensive investigation of the cationized starch (St)-VMT/TiO<sub>2</sub>-based LBL-deposited flame retardant.

The (St)-VMT-7 sample (i.e., coated with seven bilayers) showed the highest pyrolysis inhibition, as assessed by microscale combustion calorimetry (~30% pyrolysis inhibition) and thermogravimetric analysis (~21% inhibition). Furthermore, the use of MCC data profiles confirmed that the thermal properties of StVMT-7 were significantly improved compared to other samples (PHRR ~193 W/g, THR ~10 kJ/g, HRC ~390 J/gK, and a final LOI value of ~22.2%).

In addition, the after-glow time and flame spread were significantly reduced for (St)-VMT-7 but increased as the number of layers augmented. As a result of the lower intake of the VMT/TiO<sub>2</sub> components and the selective deposition process, it was demonstrated that layering the coatings with more than seven bi-layers might reduce their ability to provide thermal protection (Table 9).

**Table 9.** Combustion and pyrolysis parameters obtained from MMC analysis (0, 7, 10, and 15 refer to the number of deposited bi-layers).

Sample	THR (kJ/g)	T <sub>PHRR</sub> (°C)	PHRR (w/g)	FIGRA (PHRR/t <sub>max</sub> )	Hc (kJ g <sup>-1</sup> )	HRC (J/gK)	LOI (%)	Char Yield (%)
(St)-VMT-0	15.24	377.92	241.81	0.61	20.12	520.67	19.68	17.48
(St)-VMT-7	10.77	376.59	192.90	0.42	15.52	390.24	22.24	30.60
(St)-VMT-10	12.60	375.24	206.29	0.54	15.92	381.70	22.47	20.8
(St)-VMT-15	12.77	373.48	210.16	0.55	14.73	383.80	22.42	7.4

FIGRA: fire-growth rates, Hc: heat of combustion, HRC: values for each coated sample.

#### 5.4.2. Carbon Nanotubes

Carbon nanotubes (CNTs) are characterized by tubular structure consisting of one (single-wall carbon nanotubes, SWCNTs), or more (multi-wall carbon nanotubes, MWCNTs) graphene sheets usually characterized by nanometric diameter. Each carbon of graphene is fully bonded to three adjacent carbon atoms through sp<sup>2</sup> hybridization, forming a seamless shell [241].

Since their discovery in 1991, carbon nanotubes have had a great impact on most fields of science and engineering due to their distinctive physical and chemical properties [242]. There is currently great interest in using CNTs as nanoscale modifiers to improve mechanical and electronic properties of conventional polymeric materials as well as to add new functionalities to these materials [243]. Due to their exceptional mechanical and electrical properties, as well as excellent thermal conductivity, CNTs have found many exciting applications and they have been used as additives to various polymer-based nanocomposites [244]. Given the unique physical properties of carbon nanotubes, the functionalization of carbon nanotube fiber materials is of great importance for fundamental research and practical applications [245]. Moreover, CNTs have been researched as a potential flame retardant for cotton by developing a new generation of flame-retardant additives [245,246]. In polymer/CNT systems, the main mechanisms of flame retardation rely on the formation of char layers that serve as a heat barrier and thermal insulator, re-emitting the radiation back to the gas phase, which, in turn, delays the degradation of the polymer. Additionally, CNTs enhance the thermal conductivity of the polymer nanocomposites and increase the polymer melt viscosity increasing the amount of carbon nanotubes [247]. The wide use of carbon-based nanomaterials, such as graphene, carbon black, and carbon nanotubes, as fillers for various polymeric materials is due to their excellent mechanical, thermal, and barrier properties [248–251]. This is mainly ascribed to the formation of carbon layers by continuously and three-dimensionally bonded carbon nanofillers in the polymer matrix [252,253]. It was reported that because of the fibrous morphology of CNTs, their effect as a barrier requires a high concentration compared to nanoclays. The majority of studies has been focused on the application of CNTs embedded in a polymer matrix, while others have focused on the addition of other fillers, such as clay, graphite, or intumescent compositions, into CNT/polymer compounds [254]. In this regard, Goncalves et al. [255] oxidized and incorporated multiwalled carbon nanotubes (MWCNTs) onto cotton fibers using a dyeing-like methodology. The authors evaluated the hydrophobicity and flame retardancy of the novel functionalized textiles, as well as the washing resistance of the MWCNTs-based coating. The incorporation of MWCNTs heat treated under N<sub>2</sub> flow at 400 °C (i.e., MWCNTs featuring a strong acidic character) in the cotton substrate slightly reduced the burning rate from 243 mm min<sup>-1</sup> (untreated cotton) to 229 mm min<sup>-1</sup> (treated cotton).

In this context, it appears that functionalizing textiles with oxidized MWCNTs increases the flame-retardant properties. In a further study [256], carboxylated single-walled carbon nanotubes (CSWCNT) were immobilized on cotton fabrics using citric acid as cross-linker and sodium hypophosphite (SHP) as catalyst. As a dispersing agent, sodium dodecyl sulfonate was employed. The flammability of cotton fabric modified by CSWCNT, CA, and SHP was evaluated by measuring the percentage of char yield. The results were discussed in relation to the experimental parameters adopted for treating the cotton fabrics

(namely, different loading procedures of CSWCNTs, and the addition of citric acid and sodium hypophosphate).

The higher the concentration of the CSWCNT, the greater the flame retardancy observed on the treated samples. Indeed, considering the carbonization yield, compared to the untreated sample (1.72%), some treated samples increased significantly. Meanwhile, the cotton samples pretreated with CA and SHP achieved 6.12%, which can be a measure to evaluate the self-extinguish ability of the fabric. Recently, Xu et al. [257] investigated the potential of a novel carbonaceous nanomaterials-single-walled carbon nanohorns (SWCNHs) coating for improving the flame retardancy of cotton. The unique combination of SWCNHs and ammonium polyphosphate (APP) in a single halogen-free nanocoating showed a synergistic effect that conferred significant fire resistance to cotton fabric. By analyzing the impact of different SWCNHs concentrations on fabric flame retardancy, it was found that the optimum SWCNHs concentration was 0.15%, which provided cotton with self-extinction.

Furthermore, its LOI value reached 27.5% and the damage length was reduced to 6.5 cm (from 30 cm for cotton), preserving its original morphology apart from a partial carbonization. As assessed by cone calorimetry tests, APP/SWCNHs (0.15%)-treated cotton samples show a remarkable decrease in PHRR and THR, by 92.22% and 58.44%, respectively. The char residues of cotton, cotton-SWCNHs, and cotton-APP/SWCNHs (0.15) following vertical flammability tests were studied by FTIR and XPS spectroscopy in order to investigate the flame-retardant mechanism. The char layers of cotton-APP/SWCNHs (0.15) revealed the formation of complex cross-link structures spanned by C-C, C-O/C-O, C-N, and C-O-P bands [257]. Analyzing the gas products and char residues suggested the flame-retardant mechanism of APP/SWCNHs on cotton fabrics. Table 10 summarizes different examples of combustion and flammability tests for clay-based treated cotton, also previously described in montmorillonite and hydrotalcite sub-paragraphs.

The unique combination of SWCNHs and APP resulted in a thicker film and a more protective layer, showing a synergistic flame-retardant effect that promoted the creation of a char layer, reducing heat and oxygen diffusion. Indeed, the char layer containing carbon-nitrogen heterocycles acted as a barrier, preventing the release of volatile combustibles, such as hydrocarbons, ethers, and carbonyls.

#### 5.4.3. Graphene

The unique graphene lamellar structure provides interesting flame-retardant properties to treated materials. Indeed, it forms protective char layers, which act as an efficient shield toward the polymer degradation, retarding the mass- and heat-transfer process. Recently, Liu et al. [258] fabricated phosphorus-(PGO) and nitrogen-(NGO) containing graphene, with which they finished cotton samples. The LOI values of PGO-treated cotton fabrics increased from 18.7% to 21.7%, exhibiting some smoke suppression and flame-retardant effects. Cotton fabrics treated with NGO showed a 20.4% LOI value, with significant smoke-suppression performance.

#### 5.4.4. Metal-Based Nanoparticles

Metal-based nanoparticles have been used in textiles to improve flame resistance as they can act as heat and mass transfer barriers, altering the degradation pathways of polymers, limiting the mobility of polymer chains, and absorbing active species, such as free radicals [259]. In addition, they can enhance heat transfer within the material, slow the migration of air bubbles, and reduce heat release and local oxygen concentration through redox mechanisms [259–261].

Accordingly, in nanocomposites containing metal-based nanoparticles, improvements in many flame-retardancy parameters are evident. The following section presents more details on metal-based nanoparticles without organic components used as flame retardants in cotton fabrics.

**Table 10.** Combustion tests, flammability, and thermal behavior of cotton treated with clay additives.

Weight per Unit Area (g/m <sup>2</sup> )	Additive	Cone Calorimeter Tests			Thermal Behavior						Vertical Flame-Spread Tests		Ref.
		TTI (s)	THR (MJ/m <sup>2</sup> )	PHRR (kW/m <sup>2</sup> )	TGA in Air		Residue at T > 600 °C (%)	TGA in Nitrogen		Residue >600 °C (%)	Burning Rate (mm/s)	Residue (%)	
					T <sub>onset n%</sub> (°C)	T <sub>max</sub> (°C)		T <sub>n%</sub> (°C)	T <sub>max</sub> (°C)				
100	2.5%APP/MMT	22	0.38	38	263 <sup>n1</sup>	508	4	266 <sup>n1</sup>	301	31.0	1.6	78	[186]
100	5%APP/MMT	NA *	NA *	NA *	280 <sup>n1</sup>	607	5	276 <sup>n1</sup>	310	34.0	1.3	85	[186]
-	CaHP/1 MMT	15	0.9	72	-	-	-	276 <sup>n1</sup>	344	28.0	-	-	[222]
-	CaHP/5 MMT	13	0.85	57	-	-	-	277 <sup>n1</sup>	343	26.6	-	-	[222]
-	CaHP/10 MMT	12	0.88	77	-	-	-	278 <sup>n1</sup>	341	30.0	-	-	[222]
170	SWCNHs	8	9.17	248.95	309 <sup>n2</sup>	547	0.85	313 <sup>n2</sup>	647	1.4	-	-	[257]
170	APP/SWCNHs (0.1)	-	3.59	26.17	266 <sup>n2</sup>	533	16.11	267 <sup>n2</sup>	599	29.3	-	-	[257]
170	APP/SWCNHs (0.15)	-	3.35	22.14	264 <sup>n2</sup>	542	18.51	264 <sup>n2</sup>	598	30.2	-	-	[257]
170	APP/SWCNHs (0.2)	-	3.52	26.66	264 <sup>n2</sup>	549	15.36	268 <sup>n2</sup>	608	28.4	-	-	[257]
214	SiO <sub>2</sub> + HT (30 + 30 min)	30	-	93	-	-	-	-	-	-	-	-	[229]
214	SiO <sub>2</sub> + HT (60 + 60 min)	37	-	86	-	-	-	-	-	-	-	-	[229]
214	HT (30 min)	34	-	87	300	478	23	-	-	-	-	-	[229]
214	HT (60 min)	22	-	94	302	480	23	-	-	-	-	-	[229]

\* Parameters related to combustion are not available, as samples did not ignite during the test. n1: T<sub>5%</sub> (°C), n2: T<sub>10%</sub> (°C).

## Metal Oxides

Instead of nanotechnology, a new approach to nanomaterials has attracted researchers and worldwide textile finishers [262,263]. Due to cost considerations, nanometal oxide-coated woven fabrics play an important role in developing functional properties that are more desirable than metal nanoparticles [264]. Various metal oxide nanoparticles can produce fire-resistant nanoscale networks, surrounded by char structures and surface defensive materials in the fibers. Metal oxides (for example,  $\text{TiO}_2$ ,  $\text{MgO}$ ,  $\text{SiO}_2$ ,  $\text{CuO}$ ,  $\text{ZrO}_2$ , and  $\text{ZnO}$ ) have been used in a variety of ways to functionalize textile fabrics such as cotton [176,265]. The inclusion of nanoparticles in such fabric materials improves functional properties such as UV protection, antibacterial activity, flame retardancy, thermal stability, and physicochemical properties [266–269]. Nanoparticles can be easily incorporated into fabrics using a sol–gel technique followed by the pad-dry-cure method [270].

The optimum conditions for achieving high flame retardancy have been determined, and numerous mechanisms have been proposed [259]. The degradation pathway of the polymer can be changed, the mobility of the polymer chains is restricted, and active species, such as free radicals, can be absorbed by metal-based nanoparticles in addition to their barrier effect toward heat and mass transfer. Additionally, they may enhance the heat transfer within the material, which delays bubble migration and lowers the heat release and the concentration of local oxygen because of the oxidation-reduction mechanisms of the oxides [260,261]. The enhancement of significant flame-retardant parameters is evident in nanocomposites containing metallic nanoparticles. Some reports on the application of metal nanoparticles with only inorganic combinations are presented below. Silica spherical nanoparticles ( $\text{SiO}_2$ ) have been widely used to improve the flame retardation of cotton. For instance, Alongi et al. [229] impregnated cotton fabrics in nanometric silica suspensions at different times to enhance the thermal stability and flame retardancy of the cotton. Cone calorimetry test shows that the silica accounted for effectively decreasing the PHRR of cotton ( $124 \text{ kW/m}^2$  for the untreated cotton vs.  $95$  and  $99 \text{ kW/m}^2$  for the silica-treated cotton).

Titania (anatase crystalline form) is another globular form of metal oxide widely used as a flame retardant for cotton. In this regard, nano-sized titanium dioxide ( $\text{TiO}_2$ ) particles were successfully synthesized and deposited on cellulose fibers using the sol–gel process by Moafi et al. [271]. The authors investigated the effect of these nanoparticles as flame retardants and as a semiconductor photocatalyst for self-cleaning, in order to create a flame-retardant cellulose photoreactive fabric. Vertical flame-spread tests showed that the effective amount of titanium dioxide as a flame retardant for cellulosic fabrics is about 4.8%, expressed in g per 100 g of dry fabric. In addition, this added value is an effective amount for providing flame retardancy to cellulose fabrics. It should be noted from the TGA curve that the untreated fibers lost about 70% of their mass at  $350 \text{ }^\circ\text{C}$ . However, the treated sample lost only 50% of its mass at the same temperature. Therefore, it can be concluded that the application of titanium dioxide as a flame-retardant delays the formation of volatile products when the polymer undergoes pyrolysis. As assessed by TG analyses carried out in nitrogen atmosphere, the lower decomposition temperature of  $\text{TiO}_2$ -treated cotton with respect to the untreated fabric is due to catalytic dehydration of the fabric exerted by these nanoparticles. However,  $\text{TiO}_2$  in the remaining residue appears to act as dust or a wall for heat absorption and dissipation in the combustion zone, as stated in Jolles' wall effect theory [272], according to which no flame propagation can occur in the presence of a sufficient concentration of dust in the air. Recently, Shen et al. [273] investigated a new biomineralization technique to produce thin and homogenous  $\text{TiO}_2$  coatings on the surface of cotton. The fire behavior of the  $\text{TiO}_2$ -treated fibers was thoroughly evaluated using various methods ranging from micro-scale to macro-scale. Based on the surface morphology and chemical composition analysis, a uniform  $\text{TiO}_2$  coating was successfully created. The results from TGA and PCFC (pyrolysis combustion flow calorimetry) tests show that this  $\text{TiO}_2$  coating acts as a protective barrier in the condensed phase, directly slowing down the decomposition of cotton fibers and the release of flammable volatile pyrolysis products, protecting the char from thermal decomposition at low temperatures and reducing the intensity of combustion in the gas phase. Conversely, as assessed by cone calorimetry tests, the deposited protective coatings

showed a limited protective effect on the underlying cotton fibers exposed to the irradiative heat flux. However, due to incomplete combustion and the flame-retardant mechanisms occurring in the condensed phase, the combustion propensity of the cotton fabric was significantly reduced by the TiO<sub>2</sub> coating. After one, three, and seven treatment cycles, the PHRR for TiO<sub>2</sub>-coated cotton decreased by 5.5%, 27.1%, and 32.6%, respectively. It also showed the potential to slow down the rate of fire spread and the propensity of fire development. It can be concluded that under these experimental conditions, the flame-retardant performance is limited because a uniform TiO<sub>2</sub> coating cannot be formed on the cotton fiber surface after a single treatment cycle. Once a uniform TiO<sub>2</sub> coating is formed by biomineralization, the flammability of the cotton fabric is significantly reduced: after seven treatment cycles at a mass loading of 14.6 wt%, the LOI reaches 21.0% (LOI of pure cotton = 18.4%).

Additionally, in [274], the authors successfully prepared photoactive flame-retarded fibers by synthesizing nano-sized ZnO on cellulose fabric through a sol-gel technique performed at low temperatures. From the experimental results of vertical flame-spread tests, it can be concluded that the effective amount of zinc oxide added as a flame retardant to cellulosic fabrics, expressed in grams per 100 g of dry fabric, is about 15.24%. Furthermore, the flame-retardant outcomes of the ZnO coating are consistent with the Wall effect theory and the coating theory [272]. Moreover, Prilla et al. [275] investigated the effects of copper (II) oxide nanoparticles (CuO-NPs) on the flame-retardant properties of cotton fabrics. CuO-NPs were prepared from Copper (II) chloride through a standard procedure carried out under alkaline conditions. The resulting powder was annealed separately at 200 °C and 600 °C to obtain two products with different sizes, increasing, consequently, the functionality and adhesiveness of CuO-NPs. Indeed, the higher the temperature, the smaller the size of copper (II) oxide nanoparticles. Consequently, the smaller the size, the higher their attachment to the surface of the cotton samples. Tetraethyl orthosilicate was used to immobilize CuO-NPs on textile fabrics by the pad-dry curing method. These experimental findings showed that the smallest CuO-NPs, as obtained at the highest temperature, increased the thermal stability of cotton fabrics. Moreover, compared to the untreated sample, an increase in the burning time of the treated fabrics was observed (27 s or 54 s, depending on the sample sizes).

Most researchers have investigated the synergistic effect of the blending of metal oxides to improve the flame-retardant attributes of nanocomposites and textiles. To this aim, Alongi et al. [94] studied the effect of the combination of ZnO and silica in cotton fabrics. Indeed, in the presence of zinc-based smoke retardants, the release of smoke, and CO<sub>2</sub> emissions were significantly reduced compared to fabrics treated with silica-coated fabrics alone. In particular, the combined effect of ZnO and silica led to the largest decrease in TSR and CO<sub>2</sub> emissions (by 62% and 35%, respectively). The recent scientific literature [276] also reports that SiO<sub>2</sub> and ZnO nanoparticles can provide fire resistance to cotton fabrics by the sol-gel method. The flame spread and ignition times of the untreated samples were much shorter than those of the treated samples. The cotton fabric samples (COT) treated with SiO<sub>2</sub> and ZnO nanosols showed flame resistance. The overall burn time as well as the ignition time were significantly improved. In addition, samples COT-1 (0.25% SiO<sub>2</sub>, 0.25% ZnO), COT-2 (0.5% SiO<sub>2</sub>, 0.25% ZnO), and COT-3 (0.25% SiO<sub>2</sub>, 0.5% ZnO) effectively withstood the application of a flame and took, respectively, 17, 21, and 14 s to burn completely, unlike untreated cotton that showed a total burning time of just 8 s. The TGA curves showed that the presence of SiO<sub>2</sub> and ZnO in the nanosols causes thermal degradation of the COT samples. Silica and zinc oxide (acting as a physical barrier) protected the cotton from heat and oxygen, and promoted the formation of carbonaceous residues. As a result, silica degraded more efficiently than the silica/zinc combination; COT-2 provided the highest thermal stability to the cellulosic substrate. It can be concluded that the SiO<sub>2</sub> nanoparticles had a greater effect on the thermal properties of cotton fabrics than ZnO and the combination of the two metal oxides shows better fire resistance than when used separately. Furthermore, Dhineshabu and co-workers [277] investigated the influence of ZrO<sub>2</sub>/SiO<sub>2</sub> coating on the flammability of cotton fabrics. The finishes were prepared by the sol-gel technique and coated by the pad-dry method. Before and after washing, the burning performance of coated fabrics

was in the order:  $\text{ZrO}_2/\text{SiO}_2$  (19.5 s) >  $\text{SiO}_2$  (11.3 s). According to this finding, the fire resistance of the  $\text{ZrO}_2/\text{SiO}_2$ -coated fabric was better than that of the  $\text{SiO}_2$ -coated fabric.

Furthermore Wang et al. [19] used seeding and secondary growth to generate ZnO and ZnS microparticles on cotton fabric. A dip coating approach was used to deposit a seed layer of ZnO, ZnS, or both, on cotton. After that, the seeded cotton fabric was immersed in a secondary growth solution to promote and direct crystal growth in a certain crystallographic direction, resulting in rod-like shaped particles. ZnO and ZnO/ZnS combinations on cotton fabric reduced HRR and TSR by 41% and 68%, respectively. Despite a considerable decrease in HRR, the coating did not achieve self-extinction, as evidenced by small changes in after-flame and after-glow time. In addition, the authors found that burning ZnO or ZnS-coated fabric produced higher CO and  $\text{SO}_2$  amounts, both harmful to human health. It should also be stated that the attachment of ZnO and ZnS microparticles to the cotton surface was solely physical (i.e., physisorption), resulting in weakly bound particles. After repeated uses, the surface-finished cotton fabric may lose its flame-retardant efficiency.

Pursuing this research, Alongi et al. [58] also show the importance of combining alumina and silica regardless of the size of the employed  $\text{Al}_2\text{O}_3$  particles by comparing pure silica, alumina, and alumina-doped silica coatings on cotton, and alumina-doped silica coatings on cotton. In particular, the best results in terms of decreased combustion rate and increased final residue (about 46%) were achieved by the concurrent presence of both ceramic particles, compared with the coating containing only alumina (about 32% final residue) or silica (about 23%). In another study [91], silica bilayer-based coatings were deposited on cotton fibers by layer-by-layer assembly using three different deposition methods (dipping, vertical, and horizontal spray). SEM observations showed that only horizontal spraying achieved a very homogeneous deposition of silica coating compared to vertical spraying or dipping. As a result, the horizontal spray proved to provide the best flame-retardant properties, with a significant increase in total burning time and final residue as evaluated in flammability tests. In addition, cone calorimetry measurements showed that fabrics treated with the horizontal spray had a 40% increase in time to ignition (TTI), a 30% decrease in heat-release rate (PHRR) and a significant 20% decrease in total smoke release (TSR).

Another possibility to exploit the benefit of the combination of metal oxides has been demonstrated by Rajendran et al. [278]. In this investigation, various metal oxide nanoparticles (namely,  $\text{ZrO}_2$ , MgO, and  $\text{TiO}_2$ ) were prepared by hot air spray pyrolysis. The composite mixture of nanoparticles and sol (TEOS) was prepared by the sol-gel method and used to impregnate cotton fabrics. The addition of metal oxide nanoparticles significantly improved the thermal stability and flame resistance of the uncoated cotton fabric. Indeed, as far as the thermal stability is considered, the metal oxide composites obtained from the combination of silica hydrosol and metal oxide applied onto textile samples (hereafter, Zr-, Ti-, and Mg-based finishes) led to a significant decrease in initial decomposition temperature ( $T_{\text{onset } 5\%}$ : 293, 284, and 299 °C, respectively) compared to the silica-coated fabric and the uncoated cotton fabric (319 °C and 315 °C, respectively). In addition, the synergistic effect of silica and metal oxide also led to a remarkable increase in the final residue at ( $T_{\text{max}}$ ) 400 °C (52% for the Zr-based finish, 45% for the Mg-based finish and 44% for the Ti-based finish) with respect to silica-coated fabric 40%) and uncoated cotton fabric 38%. Therefore, according to these results, Zr-based sol-coated fabrics provide a larger amount of char than Si-based sol, Ti-based sol, and Mg-based sol-coated fabrics. Further, the flame-spread tests revealed that the char length of Zr-based sol-coated fabrics was less than 45% of those of untreated cotton and Ti-based sol, Mg-based sol, and Si-based sol-coated fabrics; besides, metal oxalate salts have been frequently utilized as precursors in producing high-purity oxides [261,279–286]. They decompose with the loss of carbon oxides at temperatures similar to many polymers (e.g., 200–400 °C) [261,280,282–286] and are water-insoluble [279].

Recently, they have received attention in this field [261,287], making them an interesting starting point for an investigation into potential new flame-retardant compounds either alone or as synergists. To this aim, Holdsworth et al. [288] reported the synthesis of six divalent metal oxalates, evaluating their potential flame-retardant properties on cotton fabrics, in combination with phosphorus- and bromine-containing flame retardants. In the presence of oxalates alone,

none of the metal oxalates promoted the disappearance of the cotton substrate; only manganese ( $\text{MnO}_x$ ) and iron ( $\text{FeO}_x$ ) oxalates reduced the burning rate at 2.49 and 2.46 mm/s, compared to pure cotton (2.66 mm/s), while stannous oxalate ( $\text{SnO}_x$ ) increased the burning rate to 3.04 mm/s. In contrast, in the presence of ammonium bromide (AB), all oxalates decreased the burning rate compared to untreated cotton, especially with calcium oxalate ( $\text{CaO}_x$ ) and iron ( $\text{FeO}_x$ ), which showed the lowest value (1.59 and 2.08 mm/s, respectively).

The effects of the application of AB or diammonium phosphate (DAP) alone on cotton samples were also found to be very different at relatively low concentrations (about 2.5 wt%).

Due to highly varied loadings achieved after impregnation compared to the pure cotton, only two oxalates ( $\text{CaO}_x$  and  $\text{MnO}_x$ ) were evaluated with DAP: they showed a reduction in the burning rate (2.18 and 2.78 mm/s, respectively) compared to untreated cotton (3.02 mm/s). However, adding ammonium bromide decreased the burning rate for all oxalates. Although all combinations of flame retardants and oxalates were char-forming, oxalates alone did not promote the char formation, and samples containing  $\text{SnO}_x$  were observed to produce a qualitatively higher degree of smoke than other oxalates (Table 11). According to Horrocks et al. [27], the synergistic properties of flame retardants can be compared by calculating the synergistic effectiveness ( $E_S$ ). In particular,  $E_S > 1$  indicates a synergistic effect, while  $E_S < 0$  is ascribed to antagonistic systems.

**Table 11.** Burning rates (mm/s) of cotton fabrics treated with different metal oxalates alone or in combination with ammonium bromide (AB) or diammonium phosphate (DAP) and calculated  $E_S$  of AB/metal oxalate systems.

Cotton Samples	Unfinished Sample	Metal Oxalates	Metal Oxalate + AB	Metal Oxalate + DAP	$E_S$ (AB/Metal Oxalates)
Cotton	2.66	-	2.50	3.02	-
COT_FeO <sub>x</sub>	-	2.46	2.08	-	0.801
COT_MnO <sub>x</sub>	-	2.49	2.22	2.78	0.741
COT_CuO <sub>x</sub>	-	2.73	2.56	-	0.360
COT_ZnO <sub>x</sub>	-	2.83	2.15	-	0.774
COT_CaO <sub>x</sub>	-	2.90	1.59	2.18	0.907
COT_SnO <sub>x</sub>	-	3.04	2.41	-	0.600

Moreover,  $E_S$  values equal to 1 are referred to as additive systems, while values below 1 to less-than-additive systems. Following this classification,  $E_S$  calculated values for ammonium bromide combined with different oxalates (Table 11) highlight their less-than-additive effect ( $E_S < 1$ ).

### Metal Hydroxides

Metal hydroxides have the advantages of good thermal stability, non-toxicity, low emission of smoke during processing and burning, and low cost, among others. For their use as flame retardants, metal hydroxides must ensure their endothermic decomposition and water release at temperatures higher than the polymer processing temperature range and around the polymer decomposition temperature. Among the metal hydroxides, magnesium di-hydroxide ( $\text{Mg}(\text{OH})_2$ ) and aluminum tri-hydroxide  $\text{Al}(\text{OH})_3$  are the most common FR fillers [40]. They have a high specific heat capacity, which allows for absorbing a significant amount of heat prior to decomposition; besides the crystallized water produced during decomposition can also absorb heat when evaporating, at the same time diluting the concentration of combustible gases. The metal oxides formed by thermal decomposition have a high melting point, and they cover the surface of cotton fibers to form an effective physical barrier, promoting the dehydration of cotton fibers into char, while separating the cotton fiber from the outside and preventing the spread of flame. The produced metal oxides also act as catalysts in the redox and cross-linking reactions of cotton fibers, which can promote the conversion of carbon monoxide (CO) to carbon dioxide ( $\text{CO}_2$ ) and reduce the generation of hazardous CO [289]. Aluminum hydroxide is only employed in polymers with low processing temperatures, such as polypropylene (PP) [290] and linear low-density polyethylene (LDPE) [291], due to the fact that it breaks down at about 200 °C. Magnesium hydroxide thermally decomposes at about

300 °C, making it suitable for usage in polymers that require higher processing temperatures. However, due to the low flame-retardant activity of inorganic hydroxides and the large amount added, they exert various effects on the physical performance of substrates, such as cotton fabrics, and are often used in combination with other FRs [23]. Ji et al. [289] investigated a novel and simple method for the preparation of flame-retarded cotton fabrics by using magnesium hydroxide ( $\text{Mg}(\text{OH})_2$ ) nanoparticles. A pad-dry-cure method was used to deposit  $\text{Mg}(\text{OH})_2$  nanoparticles on the surface of cotton fabrics. Thermogravimetric analysis in  $\text{N}_2$  atmosphere revealed an increased final residue at 800 °C for the treated fabrics (28%) with respect to the untreated counterparts (13.3%). These results clearly show that the addition of this metal hydroxide effectively suppresses cracking and dramatically reduces the weight loss of the fabric. The reasons for the high thermal stability of  $\text{Mg}(\text{OH})_2$ -coated cotton fabrics can be ascribed to the decomposition of magnesium hydroxide crystals into magnesium oxide ( $\text{MgO}$ ) and water vapor. In addition, the precipitation of  $\text{MgO}$  acts as an insulator and prevents the transfer of heat. Vertical flame-spread tests revealed that the pristine cotton fabric ignited immediately and burned completely without any residue. Conversely, the cotton fabric treated with  $\text{Mg}(\text{OH})_2$  can self-ignite after 48 s, followed by glowing for 52 s, indicating that it has excellent flame-retardant properties.

#### Metal (Oxide/Hydroxide)

Bohemite nanoparticles ( $\text{AlOOH}$ ) are aluminum oxide-hydroxides; they can be thought of as a two-dimensional nanomaterial and a mineral with a lamellar structure with  $\{010\}$  (side pinacoid) on the particles [292]. Theoretically, these nanoparticles are inherently flame retardant, as they are hydroxide of aluminum oxide:  $\gamma\text{-AlO}(\text{OH})$ , dehydrates in the range of 100–300 °C to release water and then transforms into the crystalline  $\gamma\text{-Al}_2\text{O}_3$  phase at about 420 °C [293]. This allows the volatile products generated from the polymer under irradiation to be diluted during the initial decomposition step, leading to ignition after a long time compared to unfilled polymer materials. In addition, the ceramic barrier due to the presence of freshly generated alumina inhibits further combustion. Bohemite nanoparticles are thought to behave like efficient flame retardants because of the cooling and dilution effects caused by the endothermic decomposition associated with the release of water [294]. The most important and also previously described experimental results, related to metallic nanoparticle-based flame-retardant cotton finishings, are summarized in Table 12.

Aiming to develop a new environmentally friendly flame retardant, a comparison of the performance of halogen-free finishing agents using sulfonate-modified bohemite nanoparticles (OS1) was reported [295]. The thermal stability and flame retardancy of the finished fabrics were compared with those of untreated cotton using thermogravimetric analysis (TGA) and cone calorimetry. Moreover, nanoparticles were found to exert a protective role in the thermal oxidation of cotton, modifying its degradation profile. Nanoparticles increased the thermal stability of cotton in air, facilitated the char formation, increased the final residue at high temperatures, and decreased the overall thermal oxidation rate.

The main outcome in the use of Bohemite nanoparticles is the development of a carbonaceous surface char that serves as a physical barrier to heat and oxygen transfer from the flaming zone to the polymer and vice versa. As revealed by cone calorimetry tests, compared to untreated cotton, the treated fabric showed increased TTI (22 s vs. 14 s, respectively) and decreased PHRR (57 vs. 50  $\text{kW}/\text{m}^2$  g, respectively, Table 12).

#### Zinc Carbonate

In comparison to nanoparticles, needle-like zinc carbonate has a high surface area and aspect ratio, allowing it to provide flame retardancy at low loadings. For the first time, Sharma et al. [296] synthesized and integrated zinc carbonate ( $\text{ZnCO}_3$ ) into cotton fabrics. The treated cotton fabrics had self-extinguishing properties with a specific char length of 40 mm and a LOI value as high as 30%. As assessed by thermogravimetric analyses, the treated fabrics showed a significant mass-loss peak at low temperatures and an increased residue at high temperatures (500 °C) compared to untreated cotton.

**Table 12.** Results from forced-combustion, flammability, and thermogravimetric analyses for cotton treated with metal-based nanoparticle additives.

Weight per Unit Area (g/m <sup>2</sup> )	Additive	Cone Calorimetry Tests			Thermal Behavior						Vertical Flame-Spread Tests		Ref.
		TTI (s)	FPI (sm <sup>2</sup> /kW)	PHRR (kW/m <sup>2</sup> )	TGA in Air			TGA in Nitrogen			Time to Ignite (s)	Flame-Spread Time (s)	
					T <sub>onset5%</sub> (°C)	T <sub>max</sub> (°C)	Residue (%)	T <sub>onset5%</sub> (°C)	T <sub>max</sub> (°C)	Residue (%)			
98	TiO <sub>2</sub> (1 cycle)	23	-	171	-	-	-	304	346	2.3	-	-	[273]
98	TiO <sub>2</sub> (3 cycles)	20	-	132	-	-	-	292	339	8.0	-	-	[273]
98	TiO <sub>2</sub> (7 cycles)	19	-	122	-	-	-	271	336	14.4	-	-	[273]
117	MgO	-	-	-	276	343	18.9 at 800 °C	324	422	28.0 at 800 °C	-	-	[289]
200	SiO <sub>2</sub> (by dipping)	20	-	75	-	-	-	-	-	-	22	-	[91]
200	SiO <sub>2</sub> (by vertical spray)	20	-	73	-	-	-	-	-	-	30	-	[91]
200	SiO <sub>2</sub> (by horizontal spray)	28	-	66	-	-	-	-	-	-	30	-	[91]
139	SiO <sub>2</sub>	-	-	-	224	541	40 at 400 °C	-	-	-	-	13.6	[278]
139	ZrO <sub>2</sub>	-	-	-	235	537	52 at 400 °C	-	-	-	-	19.4	[278]
139	MgO	-	-	-	222	562	45 at 400 °C	-	-	-	-	18.4	[278]
139	TiO <sub>2</sub>	-	-	-	239	549	44 at 400 °C	-	-	-	-	18.9	[278]
155	0.25% SiO <sub>2</sub> + 0.25% ZnO	-	-	-	-	-	-	330 <sup>b</sup>	410 <sup>b</sup>	8.9 <sup>b</sup> , at 600 °C	4 <sup>b</sup>	17 <sup>b</sup>	[276]
		-	-	-	-	-	-	333 <sup>a</sup>	413 <sup>a</sup>	7.6 <sup>a</sup> , at 600 °C	3 <sup>a</sup>	15 <sup>a</sup>	
155	0.5% SiO <sub>2</sub> + 0.25% ZnO	-	-	-	-	-	-	350 <sup>b</sup>	428 <sup>b</sup>	8.5 <sup>b</sup> , at 600 °C	5 <sup>b</sup>	21 <sup>b</sup>	[276]
		-	-	-	-	-	-	341 <sup>a</sup>	418 <sup>a</sup>	7.9 <sup>a</sup> , at 600 °C	4 <sup>a</sup>	19 <sup>a</sup>	
155	0.25% SiO <sub>2</sub> + 0.5% ZnO	-	-	-	-	-	-	340 <sup>b</sup>	420 <sup>b</sup>	8.6 <sup>b</sup> , at 600 °C	5 <sup>b</sup>	14 <sup>b</sup>	[276]
		-	-	-	-	-	-	336 <sup>a</sup>	415 <sup>a</sup>	7.8 <sup>a</sup> , at 600 °C	4 <sup>a</sup>	13 <sup>a</sup>	
210	OS1	22	0.44	50	278	239	1 at 800 °C	-	-	-	-	-	[295]
214	SiO <sub>2</sub> (30 min)	17	0.17	99	296	500	25 at 400 °C	-	-	-	-	-	[229]
214	SiO <sub>2</sub> (60 min)	20	0.21	95	299	479	25 at 400 °C	-	-	-	-	-	[229]
-	TiO <sub>2</sub>	-	-	-	-	-	-	314	-	26.36	-	296	[297]
400	ZnO microparticles	13.0	-	-	340	-	-	350	-	-	-	-	[19]
400	ZnO + ZnS microparticles	14.7	-	-	290	-	-	-	-	-	-	-	[19]

<sup>a</sup> Nanosol-treated sample after washing. <sup>b</sup> Nanosol-treated sample before washing.

## 6. Conclusions and Future Challenges

The unique properties of cotton, such as biocompatibility, breathability, hydrophilicity, softness, and comfortability, rendered this renewable resource to be largely used in daily life and different application fields. However, this cellulosic material is characterized by a limiting oxygen index (LOI) of about 18%, thus resulting in a high propensity to burn as demonstrated by the elevated proportion of fire accidents caused by cotton textiles with respect to other fibers. This drawback has limited the range of applications of cotton and required the need to improve its flame resistance. To this aim, several attempts were performed using flame-retardant finishes that have been identified as hazardous materials, and whose use was recently banned or restricted. In this regard, recent health and environmental awareness has prompted scientific research to develop environmentally friendly flame retardants without toxic components or byproducts, able to replace the hazardous conventional flame-retardant molecules.

Replacing flame retardants requires a variety of approaches, from fire chemistry to physics, and that must be non-toxic and environmentally friendly, i.e., sustainable. Over the last two decades, nanotechnology has attracted the interest of both academic and industrial researchers since the use of nano-sized coatings can improve the fire resistance of cotton. The surface modification of cellulose structures was performed through several implemented green approaches involving inorganic molecules (e.g., silanization, esterification, oxidation, polymer grafting, LbL, and sol-gel) for improving flame retardancy and thermal resistance of cotton.

Due to the increasing demand for technological innovation in the field of composite materials with improved flame retardancy, this review aimed to provide an overview of the inorganic coatings prepared by the use of sol-gel, LbL, and nanoparticle absorption as an effective strategy toward the development of sustainable and environmentally friendly flame-retardant treatments.

To better understand the relevance and the efficacy of the proposed technologies to impart flame retardancy to cotton fabrics, a throughout overview of the flammability and thermal behavior of neat cotton as a function of its weight per unit area was first proposed. Then, the most relevant scientific research conducted in the field of inorganic flame-retardant finishes for cotton fabrics was described.

According to the literature, the efficacy of inorganic- and sol-gel-based coatings on textile surfaces is ascribed to the protection action exerted by these inorganic coatings, which limits the heat- and mass-transfer phenomena involved during a fire occasion. In the wide panorama of inorganic molecules employed to impart flame retardancy to cotton fabrics, the most relevant study on the use and performance of phosphorous, boron-based chemicals, sol-gel precursors and inorganic nanoparticles (e.g., nanoclays, carbon nanotubes, and metal-based nanoparticles) were detailed, describing their physical barrier effect as well as fire-resistance mechanism and optimization conditions. The performance of each reported research was defined by experimental findings from the most relevant characterization techniques employed for assessing flame retardancy, such as vertical or horizontal flame-spread tests, cone calorimetry, and thermogravimetric analyses among others. Moreover, some studies reported the chemical analysis of the formed char residue after combustion performed by FTIR as an interesting tool for investigating the combustion behavior of the developed flame-retardant finishes and the fire-retardant mechanisms behind.

For a better understanding, Table 13 provides a summary of the most recent and relevant findings concerning the use of inorganic molecules for improving sustainable flame retardancy for cotton fabrics.

**Table 13.** Relevant inorganic finishings and their performances in providing flame retardancy to cotton fabrics.

Classification	Textile Finishing Process	Inorganic Chemicals	Main Outcomes	Ref.
Inorganic Phosphorus	Impregnation	Red phosphorus	- Lowering of the temperature of weight loss	[130]
		Red phosphorus + CaCl <sub>2</sub>	- Synergistic effect that promotes the formation of non-volatile char residue and less flammable gases - Delay of the non-oxidative pyrolysis of cotton	[131]
		Red phosphorus + ZnCl <sub>2</sub>	- Synergistic ability to increase char formation and combustible gas during thermal decomposition of cotton	[132]
		APP + TEOS	- TGA, char formation increased by 40% compared to untreated cotton - Damage length decreased as assessed by vertical flame-spread tests	[135]
		APP + zirconium phosphate + graphene oxide	- Self-extinction following the withdrawal of the flame	[136]
Boron-based FRs	Impregnation	Hydrate sodium metaborate (SMB)	- Improved thermal stability - Enhanced char yield - Increased LOI (28.5%) - After-glow time < 1 s (UL-94) - Considerable reduction of PHRR (~92%), THR (~43%), CO peak, CO <sub>2</sub> peak	[142]
		Zinc borate	- Transformed in ZnO or ZnOH that dilutes the combustible gases and slow down the combustion rate - Decrease in THR (~34%) and PHRR (~3%)	[66]
		Boric acid + TiO <sub>2</sub>	- Lower degradation onset - Formation of a thermally stable char at high temperatures - Residue > 90% (vertical flame-spread test) - Increased FPI (~46%)	[145]
		Nano-zinc borate (ZnB)	- Improvement in LOI value - Enhanced char formation - Reduced PHRR and THE values	[29]
		Boron nitride (BN) BN nanosheets BN modified with hexachlorocyclotriphosphazene	- The modified BN exhibited the highest flame retardancy with a LOI value of 24.1%	[144]
		Boric acid (BA)	- Reduction in the flame-spread rate - Decreased tensile strength	[143]
		Sodium borate decahydrate	- Reduction in the flame-spread rate	[141]
		TEOS Zinc oxide (ZnO) Zinc acetate dihydrate (ZnAc) Zinc borate (ZnB) Ammonium pentaborate octahydrate (APB) Boron phosphate (BP) Ammonium polyphosphate (APP) Barium sulphate (BaS)	- Maximum residues are obtained in the presence of APP and ZnO (30%) compared to sample coated with silica alone (20%) - The release of CO and CO <sub>2</sub> has been significantly reduced with respect to the fabric treated with the silica coating alone due to the presence of ZnO	[94]

Table 13. Cont.

Classification	Textile Finishing Process	Inorganic Chemicals	Main Outcomes	Ref.
Sol-gel	Impregnation	TEOS	<ul style="list-style-type: none"> <li>- Significant decrease in PHRR</li> <li>- Increased TTI</li> <li>- Anticipation of the decomposition temperature</li> <li>- Increase in the final residue (~20%)</li> <li>- Laundering durability</li> <li>- Promoting char formation (regardless of the use of DBTA)</li> </ul>	[178,179]
		TEOS Tetraethylortho titanate Tetraethylortho zirconate Aluminium isopropylate	Regardless of the nature of the precursor: <ul style="list-style-type: none"> <li>- Significant reduction of the burning rate</li> <li>- Enhancement of the final residue after combustion (vertical flame-spread test)</li> <li>- Best performance observed for TEOS:</li> <li>- Increased TTI (~56%)</li> <li>- Decreased PHRR (~20%)</li> </ul>	[176]
		TEOS + zinc borate	<ul style="list-style-type: none"> <li>- Decrease in THR and PHRR (microscale combustion calorimetry)</li> </ul>	[66]
		TEOS + H <sub>3</sub> PO <sub>4</sub>	<ul style="list-style-type: none"> <li>- Synergistic effect of phosphoric acid and silica coating: cotton does not burn (vertical flame-spread test)</li> </ul>	[177]
		TMOS	<ul style="list-style-type: none"> <li>- Increased TTI</li> <li>- Significant decrease in PHRR (~20%)</li> </ul>	[181]
		TMOS TEOS TBOS	<ul style="list-style-type: none"> <li>- The shorter the chain length of the precursor the lower the flammability of cotton</li> <li>- Increased final residue (TMOS = 48%, TEOS = 35%, TBOS = 33%)</li> <li>- TMOS showed the lowest PHRR and THR values (cone calorimetry)</li> </ul>	[183]
		TMOS + Al <sub>2</sub> O <sub>3</sub> (micro and nano)	<ul style="list-style-type: none"> <li>- Decreased total burning rate (~70%)</li> <li>- Increased final residue (&gt;40%)</li> </ul>	[58]
Nanoclay	Impregnation	Montmorillonite (MMT) + (ammonium polyphosphate) APP	<ul style="list-style-type: none"> <li>- Promotion of char formation</li> <li>- Self-extinction on the horizontal flame-spread test</li> <li>- Lowering of TTI</li> <li>- Swollen inorganic coating</li> <li>- Thermal stability and heat release improved as a function of MMT/APP ratio</li> <li>- Reduction in PHRR (~51.6%)</li> <li>- Increase in char formation</li> </ul>	[186,221]
		Calcium-hypophosphite (CaHP) + MMT clay	<ul style="list-style-type: none"> <li>- Strong reduction in PHRR (~50%) and THE (~44%)</li> </ul>	[222]
		Hydrotalcite (HT) + SiO <sub>2</sub>	<ul style="list-style-type: none"> <li>- Increase in TTI (almost doubled)</li> <li>- Decreased PHRR (~30%)</li> <li>- Increased FPI</li> <li>- Better performance when combined with SiO<sub>2</sub></li> </ul>	[229]
	LbL	Vermiculite + TiO <sub>2</sub>	Optimal conditions: seven layers <ul style="list-style-type: none"> <li>- Improved thermal properties</li> <li>- Reduction of after-glow time and flame spread</li> </ul>	[101]
Carbon nanotubes	Impregnation	MWCNTs	<ul style="list-style-type: none"> <li>- Reduction of the burning rate</li> </ul>	[255]
		SWCNTs + APP	<ul style="list-style-type: none"> <li>- Synergistic flame-retardant effect</li> <li>- Increased LOI (27.5%)</li> <li>- Significant reduction of PHRR and THR</li> </ul>	[257]

Table 13. Cont.

Classification	Textile Finishing Process	Inorganic Chemicals	Main Outcomes	Ref.
Graphene	Impregnation	Phosphorus-(PGO) Nitrogen-(NGO)	- The LOI values of PGO-treated cotton fabrics increased from 18.7% to 21.7% - The LOI values of NGO-treated cotton was 20.4%, with significant smoke-suppression performance	[258]
		LbL	Alumina-coated silica	- TTI increased by 40% - PHRR and TSR decreased by 30% and 20%, respectively
Metal-based nanoparticles	Impregnation	SiO <sub>2</sub> nanoparticles	- Reduction of PHRR	[229]
		TiO <sub>2</sub> nanoparticles	- Effective FR concentration of 4.8% (g per 100 g of fabric) - Delay in the formation of volatile pyrolysis products - Lowering decomposition temperature (TGA in N <sub>2</sub> )	[271]
		TiO <sub>2</sub> nanoparticles	- TGA and PCFC shows that TiO <sub>2</sub> coating provide a strong effect acting as the protective barrier in the condensed phase - Reduction of PHRR by 5.5%, 27.1%, and 32.6%, respectively, for the cotton coated with TiO <sub>2</sub> with one, three, and seven cycles of treatment - After seven processing cycles at a mass loading of 14.6 wt%, the LOI reaches 21.0% (LOI of pristine cotton = 18.4%)	[273]
		ZnO/SiO <sub>2</sub> nanoparticles	- The combined effect of ZnO/SiO <sub>2</sub> provided the largest reduction in TSR and CO <sub>2</sub> emissions - ZnO significantly decreased the release of smoke and CO <sub>2</sub> emissions than SiO <sub>2</sub>	[94]
		ZnO/SiO <sub>2</sub> nanoparticles	- The combined effect of ZnO/SiO <sub>2</sub> led to flame spread and ignition time much shorter than those of untreated cotton and better fire resistance than when used separately - SiO <sub>2</sub> showed greater effect on thermal properties of cotton than ZnO alone	[276]
		ZrO <sub>2</sub> /SiO <sub>2</sub>	- Flammability of ZrO <sub>2</sub> /SiO <sub>2</sub> is better than SiO <sub>2</sub> providing the highest burning times	[277]
		ZnO and ZnS microparticles	- Reduction in HRR and TSR by ~41% and ~68%	[19]
		Al <sub>2</sub> O <sub>3</sub> and SiO <sub>2</sub>	- Best reduction of combustible rate and increase in the final residue (46%) than coating containing only Al <sub>2</sub> O <sub>3</sub> (32%) or SiO <sub>2</sub> (23%)	[58]
		ZrO <sub>2</sub> , MgO, TiO <sub>2</sub> combined with TEOS sol	- Each metal oxide combined with silica sol significantly decrease initial decomposition temperature compared to silica sol - Zr-based sol provided: <ul style="list-style-type: none"> <li>the large amount of char than Si-based sol, Ti-based sol, and Mg-based sol</li> <li>char below 45% with respect to untreated cotton and Ti-based sol-, Mg-based sol-, and Si-based sol-coated fabrics</li> </ul>	[278]
		Mg(OH) <sub>2</sub>	- Increased char yields (TGA in N <sub>2</sub> ) - Increased ignition and glowing times	[289]
		Metal oxalates Ammonium bromide (AB) Diammonium phosphate (DAB)	- When applied alone only two metal oxalates (MnOx and FeOx) reduced the burning rate of cotton at 4.9 and 2.46 mm/s - When the metal oxalates combined with ammonium bromide, CaOx, and FeOx oxalates show an apparent possible additional effect in lowering the burning rate at 1.59 and 2.08 mm/s, respectively	[288]
		Sulfonate modified boehmite nanoparticles	- Increased thermal stability of cotton (TGA in air) - Enhanced char-forming character - Increased final residue at high temperature - Decreased overall thermal oxidation rate - Increased TTI - Decreased PHRR	[295]
		Zinc carbonate	- Cotton fabrics achieved self-extinction and a LOI value of 30%	[296]

As a result of the differences in the mutual interface contacts and multi-functional combined benefits, good synergistic effects may be obtained between inorganic, intumescent, and nanoparticle flame retardants. However, further investigations on the synergistic effect of interfacial compatibility between flame retardants, as well as methods for improving the interface compatibility between matrix and filler are important to better enhance the flame retardancy of materials. Indeed, most of the reported techniques are still in the stage of laboratory research and significant improvements in cost, process, and method are needed to ensure their continuous automatic production and commercialization. Furthermore, besides higher performance, an ideal flame retardant should ensure easy application, low cost, and environmentally friendliness. Indeed, although researchers are putting great efforts in the design of halogen-free, synergistic, multifunctional, and nanotechnology-based flame retardants, the topic has not yet been fully explored. Indeed, although many of the flame retardants described in this review present high performance and low environmental impact, the academic community is still working on solving some challenging issues. Indeed, designing new FRs requires large investments both for toxicity evaluation and production on at least a pre-industrial scale to maximize yields and reduce costs. In particular, the possibility of adopting green technology approaches at a pre-industrial scale is still a challenge, and whether it can be successfully tried will depend on the cost-effectiveness of the designed FR systems. A further challenge in implementing sustainable FRs concerns their durability to several washing cycles, often not at the level of conventional FRs yet, currently limiting their applications.

In conclusion, future efforts from both the academic and industrial communities should be focused on continuous implementation of even greener technologies for replacing hazardous conventional flame retardants, as well as on the design of more economical and environmentally friendly approaches for the surface modification of textiles, thus making possible the application of these methods also at the industrial scale.

**Author Contributions:** Conceptualization, V.T., S.S., R.B.D., G.R. (Giulia Rando), G.R. (Giuseppe Rosace), G.M. and M.R.P.; resources, G.R. (Giuseppe Rosace), G.M. and M.R.P.; data curation, V.T., S.S., R.B.D., G.R. (Giulia Rando), G.R. (Giuseppe Rosace), G.M. and M.R.P.; writing original draft preparation, V.T., S.S., R.B.D., G.R. (Giulia Rando), G.R. (Giuseppe Rosace), G.M. and M.R.P.; writing—review and editing, V.T., S.S., R.B.D., G.R. (Giulia Rando), G.R. (Giuseppe Rosace), G.M. and M.R.P.; supervision, V.T., G.R. (Giuseppe Rosace), G.M. and M.R.P. All authors have read and agreed to the published version of the manuscript.

**Funding:** This research received no external funding.

**Data Availability Statement:** Not applicable.

**Acknowledgments:** This review was carried out within the MICS (Made in Italy—Circular and Sustainable) Extended Partnership and received funding from the European Union Next-Generation EU (PIANO NAZIONALE DI RIPRESA E RESILIENZA (PNRR)—MISSIONE 4 COMPONENTE 2, INVESTIMENTO 1.3—D.D. 1551.11-10-2022, PE00000004). This manuscript reflects only the authors' views and opinions; neither the European Union nor the European Commission can be considered responsible for them. All authors wish to thank S. Romeo, G. Napoli, and F. Giordano for informatic and technical assistance.

**Conflicts of Interest:** The authors declare no conflict of interest.

## References

1. Aldalbahi, A.; El-Naggar, M.; El-Newehy, M.; Rahaman, M.; Hatshan, M.; Khattab, T. Effects of Technical Textiles and Synthetic Nanofibers on Environmental Pollution. *Polymers* **2021**, *13*, 155. [[CrossRef](#)] [[PubMed](#)]
2. Pandit, P.; Singha, K.; Kumar, V.; Maity, S. Advanced flame-retardant agents for protective textiles and clothing. In *Advances in Functional and Protective Textiles*; Elsevier: Amsterdam, The Netherlands, 2020; pp. 397–414.
3. Sreenivasan, V.S.; Somasundaram, S.; Ravindran, D.; Manikandan, V.; Narayanasamy, R. Microstructural, physico-chemical and mechanical characterisation of *Sansevieria cylindrica* fibres—An exploratory investigation. *Mater. Des.* **2011**, *32*, 453–461. [[CrossRef](#)]

4. Pavlović, Ž.; Vrljićak, Z. Comparing double jersey knitted fabrics made of Tencel and modal yarns, spun by different spinning methods. *J. Eng. Fiber. Fabr.* **2020**, *15*, 155892502091985. [[CrossRef](#)]
5. Azman Mohammad Taib, M.N.; Hamidon, T.S.; Garba, Z.N.; Trache, D.; Uyama, H.; Hussin, M.H. Recent progress in cellulose-based composites towards flame retardancy applications. *Polymer* **2022**, *244*, 124677. [[CrossRef](#)]
6. Chakrabarty, A.; Teramoto, Y. Recent Advances in Nanocellulose Composites with Polymers: A Guide for Choosing Partners and How to Incorporate Them. *Polymers* **2018**, *10*, 517. [[CrossRef](#)]
7. Liu, Y.; Pan, Y.-T.; Wang, X.; Acuña, P.; Zhu, P.; Wagenknecht, U.; Heinrich, G.; Zhang, X.-Q.; Wang, R.; Wang, D.-Y. Effect of phosphorus-containing inorganic–organic hybrid coating on the flammability of cotton fabrics: Synthesis, characterization and flammability. *Chem. Eng. J.* **2016**, *294*, 167–175. [[CrossRef](#)]
8. Islam, M.S.; van de Ven, T.G.M. Cotton-based flame-retardant textiles: A review. *BioResources* **2021**, *16*, 4354–4381. [[CrossRef](#)]
9. Siriviriyanun, A.; O’Rear, E.A.; Yanumet, N. Self-extinguishing cotton fabric with minimal phosphorus deposition. *Cellulose* **2008**, *15*, 731–737. [[CrossRef](#)]
10. Lewin, M. *Handbook of Fiber Chemistry*; Wake, P.J., Ed.; CRC Press: Boca Raton, FL, USA, 2006; ISBN 9780824725655.
11. Alongi, J.; Colleoni, C.; Rosace, G.; Malucelli, G. Thermal and fire stability of cotton fabrics coated with hybrid phosphorus-doped silica films. *J. Therm. Anal. Calorim.* **2012**, *110*, 1207–1216. [[CrossRef](#)]
12. Wang, S.; Sun, L.; Li, Y.; Wang, H.; Liu, J.; Zhu, P.; Dong, C. Properties of flame-retardant cotton fabrics: Combustion behavior, thermal stability and mechanism of Si/P/N synergistic effect. *Ind. Crops Prod.* **2021**, *173*, 114157. [[CrossRef](#)]
13. Zammarano, M.; Cazzetta, V.; Nazaré, S.; Shields, J.R.; Kim, Y.S.; Hoffman, K.M.; Maffezzoli, A.; Davis, R.D. Smoldering and Flame Resistant Textiles via Conformal Barrier Formation. *Adv. Mater. Interfaces* **2016**, *3*, 1600617. [[CrossRef](#)] [[PubMed](#)]
14. Roberts, B.C.; Webber, M.E.; Ezekoye, O.A. Why and How the Sustainable Building Community Should Embrace Fire Safety. *Curr. Sustain. Energy Rep.* **2016**, *3*, 121–137. [[CrossRef](#)]
15. Hall, J.R. Estimating Fires When a Product is the Primary Fuel But Not the First Fuel, With an Application to Upholstered Furniture. *Fire Technol.* **2015**, *51*, 381–391. [[CrossRef](#)]
16. Salmeia, K.; Gaan, S.; Malucelli, G. Recent Advances for Flame Retardancy of Textiles Based on Phosphorus Chemistry. *Polymers* **2016**, *8*, 319. [[CrossRef](#)] [[PubMed](#)]
17. Available online: [www.ctif.org](http://www.ctif.org) (accessed on 25 May 2023).
18. Horrocks, A.R. Flame retardant challenges for textiles and fibres: New chemistry versus innovatory solutions. *Polym. Degrad. Stab.* **2011**, *96*, 377–392. [[CrossRef](#)]
19. Wang, Y.-W.; Shen, R.; Wang, Q.; Vasquez, Y. ZnO Microstructures as Flame-Retardant Coatings on Cotton Fabrics. *ACS Omega* **2018**, *3*, 6330–6338. [[CrossRef](#)]
20. Morgan, A.B.; Gilman, J.W. An overview of flame retardancy of polymeric materials: Application, technology, and future directions. *Fire Mater.* **2013**, *37*, 259–279. [[CrossRef](#)]
21. Salmeia, K.; Fage, J.; Liang, S.; Gaan, S. An Overview of Mode of Action and Analytical Methods for Evaluation of Gas Phase Activities of Flame Retardants. *Polymers* **2015**, *7*, 504–526. [[CrossRef](#)]
22. Shen, J.; Liang, J.; Lin, X.; Lin, H.; Yu, J.; Wang, S. The Flame-Retardant Mechanisms and Preparation of Polymer Composites and Their Potential Application in Construction Engineering. *Polymers* **2021**, *14*, 82. [[CrossRef](#)]
23. Ling, C.; Guo, L.; Wang, Z. A review on the state of flame-retardant cotton fabric: Mechanisms and applications. *Ind. Crops Prod.* **2023**, *194*, 116264. [[CrossRef](#)]
24. Hendrix, J.E.; Drake, G.L.; Barker, R.H. Pyrolysis and combustion of cellulose. III. Mechanistic basis for the synergism involving organic phosphates and nitrogenous bases. *J. Appl. Polym. Sci.* **1972**, *16*, 257–274. [[CrossRef](#)]
25. Alongi, J.; Colleoni, C.; Rosace, G.; Malucelli, G. Phosphorus- and nitrogen-doped silica coatings for enhancing the flame retardancy of cotton: Synergisms or additive effects? *Polym. Degrad. Stab.* **2013**, *98*, 579–589. [[CrossRef](#)]
26. Lewin, M. Synergism and catalysis in flame retardancy of polymers. *Polym. Adv. Technol.* **2001**, *12*, 215–222. [[CrossRef](#)]
27. Horrocks, A.R.; Smart, G.; Nazaré, S.; Kandola, B.; Price, D. Quantification of Zinc Hydroxystannate\*\* and Stannate\*\* Synergies in Halogen-containing Flame-retardant Polymeric Formulations. *J. Fire Sci.* **2010**, *28*, 217–248. [[CrossRef](#)]
28. Glogar, M.; Pušić, T.; Lovreškov, V.; Kaurin, T. Reactive Printing and Wash Fastness of Inherent Flame Retardant Fabrics for Dual Use. *Materials* **2022**, *15*, 4791. [[CrossRef](#)] [[PubMed](#)]
29. Durrani, H.; Sharma, V.; Bamboria, D.; Shukla, A.; Basak, S.; Ali, W. Exploration of flame retardant efficacy of cellulosic fabric using in-situ synthesized zinc borate particles. *Cellulose* **2020**, *27*, 9061–9073. [[CrossRef](#)]
30. van der Veen, I.; de Boer, J. Phosphorus flame retardants: Properties, production, environmental occurrence, toxicity and analysis. *Chemosphere* **2012**, *88*, 1119–1153. [[CrossRef](#)] [[PubMed](#)]
31. De Smet, D.; Weydts, D.; Vanneste, M. Environmentally friendly fabric finishes. In *Sustainable Apparel*; Elsevier: Amsterdam, The Netherlands, 2015; pp. 3–33.
32. Chivas, C.; Guillaume, E.; Sainrat, A.; Barbosa, V. Assessment of risks and benefits in the use of flame retardants in upholstered furniture in continental Europe. *Fire Saf. J.* **2009**, *44*, 801–807. [[CrossRef](#)]
33. Höhn, W. Textile Industry Effluent. In *Sustainable Textile and Fashion Value Chains*; Springer International Publishing: Cham, Switzerland, 2021; pp. 123–149.
34. Wang, X.; Hu, W.; Hu, Y. Polydopamine-Bridged Synthesis of Ternary h-BN@PDA@TiO<sub>2</sub> as Nanoenhancers for Thermal Conductivity and Flame Retardant of Polyvinyl Alcohol. *Front. Chem.* **2020**, *8*, 587474. [[CrossRef](#)]

35. Price, D. *Fire Retardant Materials*; Elsevier Science & Technology: Amsterdam, The Netherlands, 2001; ISBN 9781855734197.
36. Horrocks, A.R.; Price, D. *Fire Retardant Materials*, 1st ed.; Woodhead Publishing Limited: Cambridge, UK, 2001; ISBN 1855734192.
37. Little, R.W. Fundamentals of Flame Retardancy. *Text. Res. J.* **1951**, *21*, 901–908. [[CrossRef](#)]
38. Alongi, J.; Colleoni, C.; Malucelli, G.; Rosace, G. Hybrid phosphorus-doped silica architectures derived from a multistep sol–gel process for improving thermal stability and flame retardancy of cotton fabrics. *Polym. Degrad. Stab.* **2012**, *97*, 1334–1344. [[CrossRef](#)]
39. Horrocks, A.R. An Introduction to the Burning Behaviour of Cellulosic Fibres. *J. Soc. Dye Colour.* **1983**, *99*, 191–197. [[CrossRef](#)]
40. Laoutid, F.; Bonnaud, L.; Alexandre, M.; Lopez-Cuesta, J.-M.; Dubois, P. New prospects in flame retardant polymer materials: From fundamentals to nanocomposites. *Mater. Sci. Eng. R Rep.* **2009**, *63*, 100–125. [[CrossRef](#)]
41. Shafizadeh, F.; Fu, Y.L. Pyrolysis of cellulose. *Carbohydr. Res.* **1973**, *29*, 113–122. [[CrossRef](#)]
42. Visakh, P.M.; Arao, Y. (Eds.) *Flame Retardants*; Engineering Materials; Springer International Publishing: Cham, Switzerland, 2015; ISBN 978-3-319-03466-9.
43. Kaur, B.; Gur, I.S.; Bhatnagar, H.L. Thermal degradation studies of cellulose phosphates and cellulose thiophosphates. *Die Angew. Makromol. Chem.* **1987**, *147*, 157–183. [[CrossRef](#)]
44. Merritt, M.J. *Textile Fibres, Their Physical, Microscopic, and Chemical Properties*, 6th ed.; John Wiley & Sons, Inc.: New York, NY, USA, 1954.
45. Cabrales, L.; Abidi, N. Kinetics of Cellulose Deposition in Developing Cotton Fibers Studied by Thermogravimetric Analysis. *Fibers* **2019**, *7*, 78. [[CrossRef](#)]
46. Xu, F.; Zhong, L.; Xu, Y.; Zhang, C.; Wang, P.; Zhang, F.; Zhang, G. Synthesis of three novel amino acids-based flame retardants with multiple reactive groups for cotton fabrics. *Cellulose* **2019**, *26*, 7537–7552. [[CrossRef](#)]
47. Pal, A.; Samanta, A.K.; Bagchi, A.; Samanta, P.; Kar, T.R. A Review on Fire Protective Functional Finishing of Natural Fibre Based Textiles: Present Perspective. *Curr. Trends. Fashion. Technol. Text. Eng.* **2020**, *7*, 19–30. [[CrossRef](#)]
48. Chang, S.; Slopek, R.P.; Condon, B.; Grunlan, J.C. Surface Coating for Flame-Retardant Behavior of Cotton Fabric Using a Continuous Layer-by-Layer Process. *Ind. Eng. Chem. Res.* **2014**, *53*, 3805–3812. [[CrossRef](#)]
49. Lu, H.; Song, L.; Hu, Y. A review on flame retardant technology in China. Part II: Flame retardant polymeric nanocomposites and coatings. *Polym. Adv. Technol.* **2011**, *22*, 379–394. [[CrossRef](#)]
50. Lomakin, S.M.; Zaikov, G.E.; Artsis, M.I. Advances in Nylon 6,6 Flame Retardancy. *Int. J. Polym. Mater.* **1996**, *32*, 173–202. [[CrossRef](#)]
51. Faheem, S.; Baheti, V.; Tunak, M.; Wiener, J.; Militky, J. Flame resistance behavior of cotton fabrics coated with bilayer assemblies of ammonium polyphosphate and casein. *Cellulose* **2019**, *26*, 3557–3574. [[CrossRef](#)]
52. Emsley, A.M.; Stevens, G.C. Kinetics and mechanisms of the low-temperature degradation of cellulose. *Cellulose* **1994**, *1*, 26–56. [[CrossRef](#)]
53. *UL-94*; Standard for Tests for Flammability of Plastic Materials for Parts in Devices and Appliances. UL Solutions: Northbrook, IL, USA, 1996.
54. Birky, M.M.; Yeh, K.-N. Calorimetric study of flammable fabrics. I. Instrumentation and measurements. *J. Appl. Polym. Sci.* **1973**, *17*, 239–253. [[CrossRef](#)]
55. Webster, C.T.; Wraight, H.G.H.; Thomas, P.H. 3—Heat-Transfer from Burning Fabrics. *J. Text. Inst. Trans.* **1962**, *53*, T29–T37. [[CrossRef](#)]
56. Alongi, J.; Ciobanu, M.; Malucelli, G. Novel flame retardant finishing systems for cotton fabrics based on phosphorus-containing compounds and silica derived from sol–gel processes. *Carbohydr. Polym.* **2011**, *85*, 599–608. [[CrossRef](#)]
57. Rosace, G.; Castellano, A.; Trovato, V.; Iacono, G.; Malucelli, G. Thermal and flame retardant behaviour of cotton fabrics treated with a novel nitrogen-containing carboxyl-functionalized organophosphorus system. *Carbohydr. Polym.* **2018**, *196*, 348–358. [[CrossRef](#)]
58. Alongi, J.; Malucelli, G. Thermal stability, flame retardancy and abrasion resistance of cotton and cotton–linen blends treated by sol–gel silica coatings containing alumina micro- or nano-particles. *Polym. Degrad. Stab.* **2013**, *98*, 1428–1438. [[CrossRef](#)]
59. Chang, S.; Condon, B.; Graves, E.; Uchimiya, M.; Fortier, C.; Easson, M.; Wakelyn, P. Flame retardant properties of triazine phosphonates derivative with cotton fabric. *Fibers Polym.* **2011**, *12*, 334–339. [[CrossRef](#)]
60. Rosace, G.; Colleoni, C.; Trovato, V.; Iacono, G.; Malucelli, G. Vinylphosphonic acid/methacrylamide system as a durable intumescent flame retardant for cotton fabric. *Cellulose* **2017**, *24*, 3095–3108. [[CrossRef](#)]
61. Liao, Y.; Chen, Y.; Wan, C.; Zhang, G.; Zhang, F. An eco-friendly N P flame retardant for durable flame-retardant treatment of cotton fabric. *Int. J. Biol. Macromol.* **2021**, *187*, 251–261. [[CrossRef](#)]
62. Vishwakarma, A.; Singh, M.; Weclawski, B.; Reddy, V.J.; Kandola, B.K.; Manik, G.; Dasari, A.; Chattopadhyay, S. Construction of hydrophobic fire retardant coating on cotton fabric using a layer-by-layer spray coating method. *Int. J. Biol. Macromol.* **2022**, *223*, 1653–1666. [[CrossRef](#)]
63. Hu, M.-Y.; Xiong, K.-K.; Li, J.-R.; Jing, X.-B.; Zhao, P.-H. Novel P/N/Si/S-containing Mononickel Complex as a Metal-based Intumescent Flame Retardant for Cotton Fabrics. *Fibers Polym.* **2019**, *20*, 1794–1802. [[CrossRef](#)]
64. Manfredi, A.; Carosio, F.; Ferruti, P.; Alongi, J.; Ranucci, E. Disulfide-containing polyamidoamines with remarkable flame retardant activity for cotton fabrics. *Polym. Degrad. Stab.* **2018**, *156*, 1–13. [[CrossRef](#)]
65. Li, P.; Wang, B.; Xu, Y.-J.; Jiang, Z.; Dong, C.; Liu, Y.; Zhu, P. Ecofriendly Flame-Retardant Cotton Fabrics: Preparation, Flame Retardancy, Thermal Degradation Properties, and Mechanism. *ACS Sustain. Chem. Eng.* **2019**, *7*, 19246–19256. [[CrossRef](#)]

66. Li, D.; Wang, Z.; Zhu, Y.; You, F.; Zhou, S.; Li, G.; Zhang, X.; Zhou, C. Synergistically improved flame retardancy of the cotton fabric finished by silica-coupling agent-zinc borate hybrid sol. *J. Ind. Text.* **2022**, *51*, 8297S–8322S. [\[CrossRef\]](#)
67. Cheng, X.; Shi, L.; Fan, Z.; Yu, Y.; Liu, R. Bio-based coating of phytic acid, chitosan, and biochar for flame-retardant cotton fabrics. *Polym. Degrad. Stab.* **2022**, *199*, 109898. [\[CrossRef\]](#)
68. Gaan, S.; Sun, G. Effect of phosphorus flame retardants on thermo-oxidative decomposition of cotton. *Polym. Degrad. Stab.* **2007**, *92*, 968–974. [\[CrossRef\]](#)
69. Camlibel, N.O.; Avinc, O.; Arik, B.; Yavas, A.; Yakin, I. The effects of huntite–hydromagnesite inclusion in acrylate-based polymer paste coating process on some textile functional performance properties of cotton fabric. *Cellulose* **2019**, *26*, 1367–1381. [\[CrossRef\]](#)
70. Parmar, M.S.; Chakraborty, M. Thermal and Burning Behavior of Naturally Colored Cotton. *Text. Res. J.* **2001**, *71*, 1099–1102. [\[CrossRef\]](#)
71. Alaybeyoglu, E.; Duran, K.; Körlü, A. Flammability Behaviours of Knitted Fabrics Containing PLA, Cotton, Lyocell, Chitosan Fibers. *Mugla J. Sci. Technol.* **2022**, *8*, 1–8. [\[CrossRef\]](#)
72. Babrauskas, V. Upholstered Furniture Heat Release Rates: Measurements and Estimation. *J. Fire Sci.* **1983**, *1*, 9–32. [\[CrossRef\]](#)
73. Babrauskas, V.; Baroudi, D.; Myllymäki, J.; Kokkala, M. The Cone Calorimeter Used for Predictions of the Full-scale Burning Behaviour of Upholstered Furniture. *Fire Mater.* **1997**, *21*, 95–105. [\[CrossRef\]](#)
74. Hirschler, M.M. Polyurethane foam and fire safety. *Polym. Adv. Technol.* **2008**, *19*, 521–529. [\[CrossRef\]](#)
75. Alongi, J.; Tata, J.; Carosio, F.; Rosace, G.; Frache, A.; Camino, G. A Comparative Analysis of Nanoparticle Adsorption as Fire-Protection Approach for Fabrics. *Polymers* **2014**, *7*, 47–68. [\[CrossRef\]](#)
76. Tata, J.; Alongi, J.; Carosio, F.; Frache, A. Optimization of the procedure to burn textile fabrics by cone calorimeter: Part I. Combustion behavior of polyester. *Fire Mater.* **2011**, *35*, 397–409. [\[CrossRef\]](#)
77. Tata, J.; Alongi, J.; Frache, A. Optimization of the procedure to burn textile fabrics by cone calorimeter: Part II. Results on nanoparticle-finished polyester. *Fire Mater.* **2012**, *36*, 527–536. [\[CrossRef\]](#)
78. ISO 5659; Plastics—Smoke Generation—Part 1: Guidance on Optical-Density Testing 1996 + Part 2: Determination of Optical Density by a Single-Chamber Test 2002. International Organization for Standardization: Geneva, Switzerland, 2017.
79. ISO 5660; Fire Test, Reaction to Fire—Part 1: Rate of Heat Release (Cone Calorimeter Method) + Part 2: Smoke Production Rate (Dynamic Measurement) + Part 3: Guidance on Measurement 2002 and 2003. International Organization for Standardization: Geneva, Switzerland, 2015.
80. ISO 9239; Reaction to Fire Tests for Floorings—Part 1: Determination of the Burning Behaviour Using a Radiant Heat Source + Part 2: Determination of Flame Spread at a Heat Flux Level of 25 kW/m<sup>2</sup> 2002. International Organization for Standardization: Geneva, Switzerland, 2010.
81. Nazaré, S.; Kandola, B.; Horrocks, A.R. Use of cone calorimetry to quantify the burning hazard of apparel fabrics. *Fire Mater.* **2002**, *26*, 191–199. [\[CrossRef\]](#)
82. Babrauskas, V.; Peacock, R.D. Heat release rate: The single most important variable in fire hazard. *Fire Saf. J.* **1992**, *18*, 255–272. [\[CrossRef\]](#)
83. Zhang, J.; Wang, X.; Zhang, F.; Richard Horrocks, A. Estimation of heat release rate for polymer–filler composites by cone calorimetry. *Polym. Test.* **2004**, *23*, 225–230. [\[CrossRef\]](#)
84. Quan, Y.; Zhang, Z.; Tanchak, R.N.; Wang, Q. A review on cone calorimeter for assessment of flame-retarded polymer composites. *J. Therm. Anal. Calorim.* **2022**, *147*, 10209–10234. [\[CrossRef\]](#)
85. Gann, R.G.; Babrauskas, V.; Peacock, R.D.; Hall, J.R. Fire conditions for smoke toxicity measurement. *Fire Mater.* **1994**, *18*, 193–199. [\[CrossRef\]](#)
86. Nazaré, S.; Kandola, B.K.; Horrocks, A.R. Smoke, CO, and CO<sub>2</sub> Measurements and Evaluation using Different Fire Testing Techniques for Flame Retardant Unsaturated Polyester Resin Formulations. *J. Fire Sci.* **2008**, *26*, 215–242. [\[CrossRef\]](#)
87. Hernandez, N.; Sonnier, R.; Giraud, S. Influence of grammage on heat release rate of polypropylene fabrics. *J. Fire Sci.* **2018**, *36*, 30–46. [\[CrossRef\]](#)
88. Gou, T.; Wu, X.; Zhao, Q.; Chang, S.; Wang, P. Novel phosphorus/nitrogen-rich oligomer with numerous reactive groups for durable flame-retardant cotton fabric. *Cellulose* **2021**, *28*, 7405–7419. [\[CrossRef\]](#)
89. Li, S.; Zhong, L.; Huang, S.; Wang, D.; Zhang, F.; Zhang, G. A novel flame retardant with reactive ammonium phosphate groups and polymerizing ability for preparing durable flame retardant and stiff cotton fabric. *Polym. Degrad. Stab.* **2019**, *164*, 145–156. [\[CrossRef\]](#)
90. Wan, C.; Liu, S.; Chen, Y.; Zhang, F. Facile, one-pot, formaldehyde-free synthesis of reactive N P flame retardant for a biomolecule of cotton. *Int. J. Biol. Macromol.* **2020**, *163*, 1659–1668. [\[CrossRef\]](#) [\[PubMed\]](#)
91. Alongi, J.; Carosio, F.; Frache, A.; Malucelli, G. Layer by Layer coatings assembled through dipping, vertical or horizontal spray for cotton flame retardancy. *Carbohydr. Polym.* **2013**, *92*, 114–119. [\[CrossRef\]](#)
92. Guo, W.; Wang, X.; Huang, J.; Zhou, Y.; Cai, W.; Wang, J.; Song, L.; Hu, Y. Construction of durable flame-retardant and robust superhydrophobic coatings on cotton fabrics for water-oil separation application. *Chem. Eng. J.* **2020**, *398*, 125661. [\[CrossRef\]](#)
93. Li, Z.-F.; Zhang, C.-J.; Cui, L.; Zhu, P.; Yan, C.; Liu, Y. Fire retardant and thermal degradation properties of cotton fabrics based on APTES and sodium phytate through layer-by-layer assembly. *J. Anal. Appl. Pyrolysis* **2017**, *123*, 216–223. [\[CrossRef\]](#)
94. Alongi, J.; Malucelli, G. Cotton fabrics treated with novel oxidic phases acting as effective smoke suppressants. *Carbohydr. Polym.* **2012**, *90*, 251–260. [\[CrossRef\]](#)

95. Alongi, J.; Cuttica, F.; Carosio, F.; Bourbigot, S. How much the fabric grammage may affect cotton combustion? *Cellulose* **2015**, *22*, 3477–3489. [[CrossRef](#)]
96. Grancaric, A.M.; Colleoni, C.; Guido, E.; Botteri, L.; Rosace, G. Thermal behaviour and flame retardancy of monoethanolamine-doped sol-gel coatings of cotton fabric. *Prog. Org. Coat.* **2017**, *103*, 174–181. [[CrossRef](#)]
97. Yang, C.Q.; He, Q.; Lyon, R.E.; Hu, Y. Investigation of the flammability of different textile fabrics using micro-scale combustion calorimetry. *Polym. Degrad. Stab.* **2010**, *95*, 108–115. [[CrossRef](#)]
98. Laufer, G.; Carosio, F.; Martinez, R.; Camino, G.; Grunlan, J.C. Growth and fire resistance of colloidal silica-polyelectrolyte thin film assemblies. *J. Colloid Interface Sci.* **2011**, *356*, 69–77. [[CrossRef](#)]
99. Ma, Z.; Zhang, Z.; Zhao, F.; Wang, Y. A multifunctional coating for cotton fabrics integrating superior performance of flame-retardant and self-cleaning. *Adv. Compos. Hybrid Mater.* **2022**, *5*, 2817–2833. [[CrossRef](#)]
100. Xing, W.; Jie, G.; Song, L.; Hu, S.; Lv, X.; Wang, X.; Hu, Y. Flame retardancy and thermal degradation of cotton textiles based on UV-curable flame retardant coatings. *Thermochim. Acta* **2011**, *513*, 75–82. [[CrossRef](#)]
101. Ur Rehman, Z.; Huh, S.-H.; Ullah, Z.; Pan, Y.-T.; Churchill, D.G.; Koo, B.H. LBL generated fire retardant nanocomposites on cotton fabric using cationized starch-clay-nanoparticles matrix. *Carbohydr. Polym.* **2021**, *274*, 118626. [[CrossRef](#)]
102. Chang, S.; Condon, B.; Nam, S. Development of Flame-Resistant Cotton Fabrics with Casein Using Pad-dry-cure and Supercritical Fluids Methods. *Int. J. Mater. Sci. Appl.* **2020**, *9*, 53. [[CrossRef](#)]
103. Kaurin, T.; Pušić, T.; Dekanić, T.; Flinčec Grgac, S. Impact of Washing Parameters on Thermal Characteristics and Appearance of Proban®—Flame Retardant Material. *Materials* **2022**, *15*, 5373. [[CrossRef](#)]
104. Krishnasamy, S.; Thiagamani, S.M.K.; Muthu Kumar, C.; Nagarajan, R.; Shahroze, R.M.; Siengchin, S.; Ismail, S.O.; Devi, I. Recent advances in thermal properties of hybrid cellulosic fiber reinforced polymer composites. *Int. J. Biol. Macromol.* **2019**, *141*, 1–13. [[CrossRef](#)]
105. Neto, J.; Queiroz, H.; Aguiar, R.; Lima, R.; Cavalcanti, D.; Doina Banea, M. A Review of Recent Advances in Hybrid Natural Fiber Reinforced Polymer Composites. *J. Renew. Mater.* **2022**, *10*, 561–589. [[CrossRef](#)]
106. Price, D.; Horrocks, A.R.; Akalin, M.; Farooq, A.A. Influence of flame retardants on the mechanism of pyrolysis of cotton (cellulose) fabrics in air. *J. Anal. Appl. Pyrolysis* **1997**, *40–41*, 511–524. [[CrossRef](#)]
107. Alongi, J.; Colleoni, C.; Rosace, G.; Malucelli, G. Sol-gel derived architectures for enhancing cotton flame retardancy: Effect of pure and phosphorus-doped silica phases. *Polym. Degrad. Stab.* **2014**, *99*, 92–98. [[CrossRef](#)]
108. Alongi, J.; Carosio, F.; Malucelli, G. Influence of ammonium polyphosphate-/poly(acrylic acid)-based layer by layer architectures on the char formation in cotton, polyester and their blends. *Polym. Degrad. Stab.* **2012**, *97*, 1644–1653. [[CrossRef](#)]
109. Montava-Jordà, S.; Torres-Giner, S.; Ferrandiz-Bou, S.; Quiles-Carrillo, L.; Montanes, N. Development of Sustainable and Cost-Competitive Injection-Molded Pieces of Partially Bio-Based Polyethylene Terephthalate through the Valorization of Cotton Textile Waste. *Int. J. Mol. Sci.* **2019**, *20*, 1378. [[CrossRef](#)] [[PubMed](#)]
110. Wang, S.; Liu, J.; Sun, L.; Wang, H.; Zhu, P.; Dong, C. Preparation of flame-retardant/dyed cotton fabrics: Flame retardancy, dyeing performance and flame retardant/dyed mechanism. *Cellulose* **2020**, *27*, 10425–10440. [[CrossRef](#)]
111. Sánchez-Jiménez, P.E.; Pérez-Maqueda, L.A.; Crespo-Amorós, J.E.; López, J.; Perejón, A.; Criado, J.M. Quantitative Characterization of Multicomponent Polymers by Sample-Controlled Thermal Analysis. *Anal. Chem.* **2010**, *82*, 8875–8880. [[CrossRef](#)]
112. Šimkovic, I. TG/DTG/DTA evaluation of flame retarded cotton fabrics and comparison to cone calorimeter data. *Carbohydr. Polym.* **2012**, *90*, 976–981. [[CrossRef](#)]
113. Davies, D.; Horrocks, A.R.; Greenhalgh, M. Ignition studies on cotton cellulose by DTA. *Thermochim. Acta* **1983**, *63*, 351–362. [[CrossRef](#)]
114. Shafizadeh, F.; Bradbury, A.G.W.; DeGroot, W.F.; Aanerud, T.W. Role of inorganic additives in the smoldering combustion of cotton cellulose. *Ind. Eng. Chem. Prod. Res. Dev.* **1982**, *21*, 97–101. [[CrossRef](#)]
115. Ghanadpour, M.; Carosio, F.; Wågberg, L. Ultrastrong and flame-resistant freestanding films from nanocelluloses, self-assembled using a layer-by-layer approach. *Appl. Mater. Today* **2017**, *9*, 229–239. [[CrossRef](#)]
116. Li, J.; Jiang, W. Synthesis of a novel P-N flame retardant for preparing flame retardant and durable cotton fabric. *Ind. Crops Prod.* **2021**, *174*, 114205. [[CrossRef](#)]
117. Li, Q.-L.; Huang, F.-Q.; Wei, Y.-J.; Wu, J.-Z.; Zhou, Z.; Liu, G. A Phosphorus-Nitrogen Flame-retardant: Synthesis and Application in Cotton Fabrics. *Mater. Sci.* **2018**, *24*, 448–452. [[CrossRef](#)]
118. Gaan, S.; Sun, G. Effect of phosphorus and nitrogen on flame retardant cellulose: A study of phosphorus compounds. *J. Anal. Appl. Pyrolysis* **2007**, *78*, 371–377. [[CrossRef](#)]
119. Lawler, T.E.; Drews, M.J.; Barker, R.H. Pyrolysis and combustion of cellulose. VIII. Thermally initiated reactions of phosphonomethyl amide flame retardants. *J. Appl. Polym. Sci.* **1985**, *30*, 2263–2277. [[CrossRef](#)]
120. Teli, M.; Pandit, P. Development of thermally stable and hygienic colored cotton fabric made by treatment with natural coconut shell extract. *J. Ind. Text.* **2018**, *48*, 87–118. [[CrossRef](#)]
121. El Messoudi, M.; Boukhriss, A.; Bentis, A.; El Bouchti, M.; Ait Chaoui, M.; El Kouali, M.; Gmouh, S. Flame retardant finishing of cotton fabric based on ionic liquid compounds containing boron prepared with the sol-gel method. *J. Coat. Technol. Res.* **2022**, *19*, 1609–1619. [[CrossRef](#)]
122. Zhu, P.; Sui, S.; Wang, B.; Sun, K.; Sun, G. A study of pyrolysis and pyrolysis products of flame-retardant cotton fabrics by DSC, TGA, and PY-GC-MS. *J. Anal. Appl. Pyrolysis* **2004**, *71*, 645–655. [[CrossRef](#)]

123. Bourbigot, S.; Chlebicki, S.; Mamleev, V. Thermal degradation of cotton under linear heating. *Polym. Degrad. Stab.* **2002**, *78*, 57–62. [[CrossRef](#)]
124. Tian, C.M.; Shi, Z.H.; Zhang, H.Y.; Xu, J.Z.; Shi, J.R.; Guo, H.Z. Thermal degradation of cotton cellulose. *J. Therm. Anal. Calorim.* **1999**, *55*, 93–98. [[CrossRef](#)]
125. Nakanishi, S.; Masuko, F.; Hori, K.; Hashimoto, T. Pyrolytic Gas Generation of Cotton Cellulose With and Without Flame Retardants at Different Stages of Thermal Degradation: Effects of Nitrogen, Phosphorus, and Halogens. *Text. Res. J.* **2000**, *70*, 574–583. [[CrossRef](#)]
126. Gaan, S.; Sun, G. Effect of nitrogen additives on thermal decomposition of cotton. *J. Anal. Appl. Pyrolysis* **2009**, *84*, 108–115. [[CrossRef](#)]
127. Kang, M.; Chen, S.; Yang, R.; Li, D.; Zhang, W. Fabrication of an Eco-Friendly Clay-Based Coating for Enhancing Flame Retardant and Mechanical Properties of Cotton Fabrics via LbL Assembly. *Polymers* **2022**, *14*, 4994. [[CrossRef](#)] [[PubMed](#)]
128. Weil, E.D.; Levchik, S. Current Practice and Recent Commercial Developments in Flame Retardancy of Polyamides. *J. Fire Sci.* **2004**, *22*, 251–264. [[CrossRef](#)]
129. Granzow, A. Flame retardation by phosphorus compounds. *Acc. Chem. Res.* **1978**, *11*, 177–183. [[CrossRef](#)]
130. MOSTASHARI, S.M.; FAYYAZ, F. A Thermogravimetric Study of Cotton Fabric Flame-Retardancy by Means of Impregnation with Red Phosphorus. *Chin. J. Chem.* **2008**, *26*, 1030–1034. [[CrossRef](#)]
131. Mostashari, S.M.; Baie, S. TG studies of synergism between red phosphorus (RP)–calcium chloride used in flame-retardancy for a cotton fabric favorable to green chemistry. *J. Therm. Anal. Calorim.* **2010**, *99*, 431–436. [[CrossRef](#)]
132. Mostashari, S.M.; Fayyaz, F. A Combination of Red Phosphorus-Zinc Chloride for Flame-Retardancy of a Cotton Fabric. *Int. J. Polym. Mater.* **2007**, *57*, 125–131. [[CrossRef](#)]
133. Mngomezulu, M.E.; John, M.J.; Jacobs, V.; Luyt, A.S. Review on flammability of biofibres and biocomposites. *Carbohydr. Polym.* **2014**, *111*, 149–182. [[CrossRef](#)]
134. Lee, H.C.; Lee, S. Flame retardancy for cotton cellulose treated with  $H_3PO_3$ . *J. Appl. Polym. Sci.* **2018**, *135*, 46497. [[CrossRef](#)]
135. Lin, D.; Zeng, X.; Li, H.; Lai, X.; Wu, T. One-pot fabrication of superhydrophobic and flame-retardant coatings on cotton fabrics via sol-gel reaction. *J. Colloid Interface Sci.* **2019**, *533*, 198–206. [[CrossRef](#)]
136. Wang, D.; Ma, J.; Liu, J.; Tian, A.; Fu, S. Intumescent flame-retardant and ultraviolet-blocking coating screen-printed on cotton fabric. *Cellulose* **2021**, *28*, 2495–2504. [[CrossRef](#)]
137. Lu, S.-Y.; Hamerton, I. Recent developments in the chemistry of halogen-free flame retardant polymers. *Prog. Polym. Sci.* **2002**, *27*, 1661–1712. [[CrossRef](#)]
138. Zhang, Q.-H.; Zhang, W.; Chen, G.-Q.; Xing, T.-L. Combustion properties of cotton fabric treated by boron doped silica sol. *Therm. Sci.* **2015**, *19*, 1345–1348. [[CrossRef](#)]
139. Zhu, W.; Yang, M.; Huang, H.; Dai, Z.; Cheng, B.; Hao, S. A phytic acid-based chelating coordination embedding structure of phosphorus–boron–nitride synergistic flame retardant to enhance durability and flame retardancy of cotton. *Cellulose* **2020**, *27*, 4817–4829. [[CrossRef](#)]
140. Nine, M.J.; Tran, D.N.H.; Tung, T.T.; Kabiri, S.; Losic, D. Graphene-Borate as an Efficient Fire Retardant for Cellulosic Materials with Multiple and Synergetic Modes of Action. *ACS Appl. Mater. Interfaces* **2017**, *9*, 10160–10168. [[CrossRef](#)]
141. Mostashari, S.M.; Fayyaz, F. TG of a cotton fabric impregnated by sodium borate decahydrate ( $Na_2B_4O_7 \cdot 10H_2O$ ) as a flame-retardant. *J. Therm. Anal. Calorim.* **2008**, *93*, 933–936. [[CrossRef](#)]
142. Tawiah, B.; Yu, B.; Yang, W.; Yuen, R.K.K.; Fei, B. Facile flame retardant finishing of cotton fabric with hydrated sodium metaborate. *Cellulose* **2019**, *26*, 4629–4640. [[CrossRef](#)]
143. Akarslan, F. Investigation on Fire Retardancy Properties of Boric Acid Doped Textile Materials. *Acta Phys. Pol. A* **2015**, *128*, B-403–B-405. [[CrossRef](#)]
144. Liu, H.; Du, Y.; Lei, S.; Liu, Z. Flame-retardant activity of modified boron nitride nanosheets to cotton. *Text. Res. J.* **2020**, *90*, 512–522. [[CrossRef](#)]
145. Bentis, A.; Boukhriss, A.; Gmouh, S. Flame-retardant and water-repellent coating on cotton fabric by titania–boron sol–gel method. *J. Sol-Gel Sci. Technol.* **2020**, *94*, 719–730. [[CrossRef](#)]
146. Shen, K.K. Review of Recent Advances on the Use of Boron-based Flame Retardants. In *Polymer Green Flame Retardants*; Elsevier: Amsterdam, The Netherlands, 2014; pp. 367–388.
147. Global Organic Textile Standard (GOTS) 2020. Version 6.0. Available online: <https://www.global-standard.org> (accessed on 25 May 2023).
148. Dislich, H. Glassy and crystalline systems from gels, chemical basis and technical application. *J. Non. Cryst. Solids* **1984**, *63*, 237–241. [[CrossRef](#)]
149. Segal, D.L. Sol-gel processing: Routes to oxide ceramics using colloidal dispersions of hydrous oxides and alkoxide intermediates. *J. Non. Cryst. Solids* **1984**, *63*, 183–191. [[CrossRef](#)]
150. Brinker, C.J.; Scherer, G.W. *The Physics and Chemistry of Sol–Gel Processing*; Academic Press: New York, NY, USA, 1990.
151. Sfameni, S.; Hadhri, M.; Rando, G.; Drommi, D.; Rosace, G.; Trovato, V.; Plutino, M.R. Inorganic Finishing for Textile Fabrics: Recent Advances in Wear-Resistant, UV Protection and Antimicrobial Treatments. *Inorganics* **2023**, *11*, 19. [[CrossRef](#)]
152. Sfameni, S.; Del Tedesco, A.; Rando, G.; Truant, F.; Visco, A.; Plutino, M.R. Waterborne Eco-Sustainable Sol–Gel Coatings Based on Phytic Acid Intercalated Graphene Oxide for Corrosion Protection of Metallic Surfaces. *Int. J. Mol. Sci.* **2022**, *23*, 12021.

153. Innocenzi, P. The Precursors of the Sol-Gel Process. In *The Sol-to-Gel Transition. SpringerBriefs in Materials*; Springer: Cham, Switzerland, 2019; pp. 7–19.
154. Ielo, I.; Giacobello, F.; Castellano, A.; Sfameni, S.; Rando, G.; Plutino, M.R. Development of Antibacterial and Antifouling Innovative and Eco-Sustainable Sol–Gel Based Materials: From Marine Areas Protection to Healthcare Applications. *Gels* **2022**, *8*, 26.
155. Giacobello, F.; Ielo, I.; Belhamdi, H.; Plutino, M.R. Geopolymers and Functionalization Strategies for the Development of Sustainable Materials in Construction Industry and Cultural Heritage Applications: A Review. *Materials* **2022**, *15*, 1725. [[CrossRef](#)]
156. Sfameni, S.; Rando, G.; Marchetta, A.; Scolaro, C.; Cappello, S.; Urzi, C.; Visco, A.; Plutino, M.R. Development of Eco-Friendly Hydrophobic and Fouling-Release Coatings for Blue-Growth Environmental Applications: Synthesis, Mechanical Characterization and Biological Activity. *Gels* **2022**, *8*, 528. [[CrossRef](#)]
157. Figueira, R.B.; Silva, C.J.R.; Pereira, E.V. Organic–inorganic hybrid sol–gel coatings for metal corrosion protection: A review of recent progress. *J. Coat. Technol. Res.* **2014**, *12*, 1–35. [[CrossRef](#)]
158. Mahltig, B.; Textor, T. *Nanosols and Textiles*; World Scientific Publishing Co. Pte. Ltd.: Singapore, 2008.
159. Sfameni, S.; Rando, G.; Plutino, M.R. Sustainable Secondary-Raw Materials, Natural Substances and Eco-Friendly Nanomaterial-Based Approaches for Improved Surface Performances: An Overview of What They Are and How They Work. *Int. J. Mol. Sci.* **2023**, *24*, 5472. [[CrossRef](#)]
160. Sakka, S. (Ed.) *Sol-Gel Science and Technology: Topics and Fundamental Research and Applications*; Kluwer Academic Publishers: Norwell, Australia, 2003; ISBN 978-1402072918.
161. Colleoni, C.; Guido, E.; Migani, V.; Rosace, G. Hydrophobic behaviour of non-fluorinated sol-gel based cotton and polyester fabric coatings. *J. Ind. Text.* **2015**, *44*, 815–834. [[CrossRef](#)]
162. Sfameni, S.; Lawnick, T.; Rando, G.; Visco, A.; Textor, T.; Plutino, M.R. Super-Hydrophobicity of Polyester Fabrics Driven by Functional Sustainable Fluorine-Free Silane-Based Coatings. *Gels* **2023**, *9*, 109. [[CrossRef](#)] [[PubMed](#)]
163. Guido, E.; Colleoni, C.; De Clerck, K.; Plutino, M.R.; Rosace, G. Influence of catalyst in the synthesis of a cellulose-based sensor: Kinetic study of 3-glycidoxypropyltrimethoxysilane epoxy ring opening by Lewis acid. *Sens. Actuators B Chem.* **2014**, *203*, 213–222. [[CrossRef](#)]
164. Min, L.; Xiaoli, Z.; Shuilin, C. Enhancing the wash fastness of dyeings by a sol-gel process. Part 1; Direct dyes on cotton. *Color. Technol.* **2003**, *119*, 297–300. [[CrossRef](#)]
165. Schramm, C.; Binder, W.H.; Tessadri, R. Durable Press Finishing of Cotton Fabric with 1,2,3,4-Butanetetracarboxylic Acid and TEOS/GPTMS. *J. Sol-Gel Sci. Technol.* **2004**, *29*, 155–165. [[CrossRef](#)]
166. Haufe, H.; Muschter, K.; Siegert, J.; Böttcher, H. Bioactive textiles by sol–gel immobilised natural active agents. *J. Sol-Gel Sci. Technol.* **2008**, *45*, 97–101. [[CrossRef](#)]
167. El-Hady, M.M.A.; Farouk, A.; Sharaf, S. Flame retardancy and UV protection of cotton based fabrics using nano ZnO and polycarboxylic acids. *Carbohydr. Polym.* **2013**, *92*, 400–406. [[CrossRef](#)]
168. Colleoni, C.; Massafra, M.R.; Rosace, G. Photocatalytic properties and optical characterization of cotton fabric coated via sol–gel with non-crystalline TiO<sub>2</sub> modified with poly(ethylene glycol). *Surf. Coat. Technol.* **2012**, *207*, 79–88. [[CrossRef](#)]
169. Sfameni, S.; Lawnick, T.; Rando, G.; Visco, A.; Textor, T.; Plutino, M.R. Functional Silane-Based Nanohybrid Materials for the Development of Hydrophobic and Water-Based Stain Resistant Cotton Fabrics Coatings. *Nanomaterials* **2022**, *12*, 3404. [[CrossRef](#)] [[PubMed](#)]
170. Sfameni, S.; Rando, G.; Plutino, M.R. *Perspective Chapter: Functional Sol–Gel Based Coatings for Innovative and Sustainable Applications*; Singh, D.J.P., Acharya, D.S.S., Kumar, D.S., Dixit, D.S.K., Eds.; IntechOpen: Rijeka, Croatia, 2023; p. Ch. 3. ISBN 978-1-80355-415-0.
171. Poli, R.; Colleoni, C.; Calvimontes, A.; Polášková, H.; Dutschk, V.; Rosace, G. Innovative sol–gel route in neutral hydroalcoholic condition to obtain antibacterial cotton finishing by zinc precursor. *J. Sol-Gel Sci. Technol.* **2015**, *74*, 151–160. [[CrossRef](#)]
172. Alongi, J.; Malucelli, G. Cotton flame retardancy: State of the art and future perspectives. *RSC Adv.* **2015**, *5*, 24239–24263. [[CrossRef](#)]
173. Hench, L.L.; West, J.K. The sol-gel process. *Chem. Rev.* **1990**, *90*, 33–72. [[CrossRef](#)]
174. Pierre, A. *Introduction to Sol-Gel Processing*; The Kluwer International Series in Sol-Gel Processing: Technology and Applications; Springer: Boston, MA, USA, 1998; ISBN 978-0-7923-8121-1.
175. Malucelli, G.; Carosio, F.; Alongi, J.; Fina, A.; Frache, A.; Camino, G. Materials engineering for surface-confined flame retardancy. *Mater. Sci. Eng. R Rep.* **2014**, *84*, 1–20. [[CrossRef](#)]
176. Alongi, J.; Ciobanu, M.; Malucelli, G. Thermal stability, flame retardancy and mechanical properties of cotton fabrics treated with inorganic coatings synthesized through sol–gel processes. *Carbohydr. Polym.* **2012**, *87*, 2093–2099. [[CrossRef](#)]
177. Cireli, A.; Onar, N.; Ebeoglugil, M.F.; Kayatekin, I.; Kutlu, B.; Culha, O.; Celik, E. Development of flame retardancy properties of new halogen-free phosphorous doped SiO<sub>2</sub> thin films on fabrics. *J. Appl. Polym. Sci.* **2007**, *105*, 3748–3756. [[CrossRef](#)]
178. Alongi, J.; Ciobanu, M.; Tata, J.; Carosio, F.; Malucelli, G. Thermal stability and flame retardancy of polyester, cotton, and relative blend textile fabrics subjected to sol-gel treatments. *J. Appl. Polym. Sci.* **2011**, *119*, 1961–1969. [[CrossRef](#)]
179. Colleoni, C.; Donelli, I.; Freddi, G.; Guido, E.; Migani, V.; Rosace, G. A novel sol-gel multi-layer approach for cotton fabric finishing by tetraethoxysilane precursor. *Surf. Coat. Technol.* **2013**, *235*, 192–203. [[CrossRef](#)]
180. Zhang, X.; Wang, Z.; Zhou, S.; You, F.; Li, D.; Zhou, C.; Pan, Y.; Wang, J. Enhanced flame retardancy level of a cotton fabric treated by an ammonium pentaborate doped silica-KH570 sol. *J. Ind. Text.* **2022**, *52*, 152808372211165. [[CrossRef](#)]

181. Alongi, J.; Ciobanu, M.; Malucelli, G. Sol–gel treatments for enhancing flame retardancy and thermal stability of cotton fabrics: Optimisation of the process and evaluation of the durability. *Cellulose* **2011**, *18*, 167–177. [[CrossRef](#)]
182. Alongi, J.; Malucelli, G. *Thermal Degradation of Cellulose and Cellulosic Substrates*; Wiley: Hoboken, NJ, USA, 2015.
183. Alongi, J.; Ciobanu, M.; Malucelli, G. Sol–gel treatments on cotton fabrics for improving thermal and flame stability: Effect of the structure of the alkoxy silane precursor. *Carbohydr. Polym.* **2012**, *87*, 627–635. [[CrossRef](#)] [[PubMed](#)]
184. Birnbaum, L.S.; Staskal, D.F. Brominated flame retardants: Cause for concern? *Environ. Health Perspect.* **2004**, *112*, 9–17. [[CrossRef](#)] [[PubMed](#)]
185. Barcelo, D.; Kostianoy, A.G. Handbook environmental chemistry. In *Brominated Flame Retardants*; Heidelberg, S.-V.B., Ed.; Springer: New York, NY, USA, 2011; Volume 16.
186. Alongi, J.; Carosio, F. All-inorganic intumescent nanocoating containing montmorillonite nanoplatelets in ammonium polyphosphate matrix capable of preventing cotton ignition. *Polymers* **2016**, *8*, 430. [[CrossRef](#)]
187. Kiliaris, P.; Papaspyrides, C.D. Polymer/layered silicate (clay) nanocomposites: An overview of flame retardancy. *Prog. Polym. Sci.* **2010**, *35*, 902–958. [[CrossRef](#)]
188. Alongi, J.; Carosio, F.; Kiekens, P. Recent Advances in the Design of Water Based-Flame Retardant Coatings for Polyester and Polyester–Cotton Blends. *Polymers* **2016**, *8*, 357. [[CrossRef](#)]
189. Carosio, F.; Alongi, J. Ultra-Fast Layer-by-Layer Approach for Depositing Flame Retardant Coatings on Flexible PU Foams within Seconds. *ACS Appl. Mater. Interfaces* **2016**, *8*, 6315–6319. [[CrossRef](#)]
190. Carosio, F.; Alongi, J.; Malucelli, G. Flammability and combustion properties of ammonium polyphosphate-/poly(acrylic acid)-based layer by layer architectures deposited on cotton, polyester and their blends. *Polym. Degrad. Stab.* **2013**, *98*, 1626–1637. [[CrossRef](#)]
191. Alongi, J.; Han, Z.; Bourbigot, S. Intumescence: Tradition versus novelty. A comprehensive review. *Prog. Polym. Sci.* **2015**, *51*, 28–73. [[CrossRef](#)]
192. Hall, P.L. The application of electron spin resonance spectroscopy to studies of clay minerals: I. Isomorphous substitutions and external surface properties. *Clay Miner.* **1980**, *15*, 321–335. [[CrossRef](#)]
193. Murray, H.H. Chapter 2 Structure and Composition of the Clay Minerals and their Physical and Chemical Properties. In *Developments in Clay Science*; Elsevier: Amsterdam, The Netherlands, 2006; pp. 7–31.
194. Bergaya, F.; Lagaly, G. Chapter 1 General Introduction: Clays, Clay Minerals, and Clay Science. In *Developments in Clay Science*; Elsevier: Amsterdam, The Netherlands, 2006; pp. 1–18.
195. Rando, G.; Sfameni, S.; Galletta, M.; Drommi, D.; Cappello, S.; Plutino, M.R. Functional Nanohybrids and Nanocomposites Development for the Removal of Environmental Pollutants and Bioremediation. *Molecules* **2022**, *27*, 4856. [[CrossRef](#)]
196. Kotal, M.; Bhowmick, A.K. Polymer nanocomposites from modified clays: Recent advances and challenges. *Prog. Polym. Sci.* **2015**, *51*, 127–187. [[CrossRef](#)]
197. Murray, H.H. Overview—Clay mineral applications. *Appl. Clay Sci.* **1991**, *5*, 379–395. [[CrossRef](#)]
198. Klopogge, J.T. Synthesis of Smectites and Porous Pillared Clay Catalysts: A Review. *J. Porous Mater.* **1998**, *5*, 5–41. [[CrossRef](#)]
199. Ielo, I.; Galletta, M.; Rando, G.; Sfameni, S.; Cardiano, P.; Sabatino, G.; Drommi, D.; Rosace, G.; Plutino, M.R. Design, synthesis and characterization of hybrid coatings suitable for geopolymeric-based supports for the restoration of cultural heritage. *IOP Conf. Ser. Mater. Sci. Eng.* **2020**, *777*, 012003. [[CrossRef](#)]
200. Masini, J.C.; Abate, G. Guidelines to Study the Adsorption of Pesticides onto Clay Minerals Aiming at a Straightforward Evaluation of Their Removal Performance. *Minerals* **2021**, *11*, 1282. [[CrossRef](#)]
201. Perelomov, L.; Mandzhieva, S.; Minkina, T.; Atroshchenko, Y.; Perelomova, I.; Bauer, T.; Pinsky, D.; Barakhov, A. The Synthesis of Organoclays Based on Clay Minerals with Different Structural Expansion Capacities. *Minerals* **2021**, *11*, 707. [[CrossRef](#)]
202. Undabeytia, T.; Shuali, U.; Nir, S.; Rubin, B. Applications of Chemically Modified Clay Minerals and Clays to Water Purification and Slow Release Formulations of Herbicides. *Minerals* **2020**, *11*, 9. [[CrossRef](#)]
203. Jacquet, A.; Geatches, D.; Clark, S.; Greenwell, H. Understanding Cationic Polymer Adsorption on Mineral Surfaces: Kaolinite in Cement Aggregates. *Minerals* **2018**, *8*, 130. [[CrossRef](#)]
204. Lazorenko, G.; Kasprzhitskii, A.; Yavna, V. Comparative Study of the Hydrophobicity of Organo-Montmorillonite Modified with Cationic, Amphoteric and Nonionic Surfactants. *Minerals* **2020**, *10*, 732. [[CrossRef](#)]
205. Li, A.; Wang, A.-Q.; Chen, J.-M. Preparation and Properties of Poly (acrylic acid-potassium acrylate)/Attapulgite Superabsorbent Composite. *J. Funct. Polym.* **2004**, *17*, 200–206.
206. Taylor, R.K.; Smith, T.J. The engineering geology of clay minerals: Swelling, shrinking and mudrock breakdown. *Clay Miner.* **1986**, *21*, 235–260. [[CrossRef](#)]
207. Chi, M. Cation Exchange Capacity of Kaolinite. *Clays Clay Miner.* **1999**, *47*, 174–180. [[CrossRef](#)]
208. Theng, B.K.G. *Formation and Properties of Clay-Polymer Complexes*; Elsevier: Amsterdam, The Netherlands, 2012; ISBN 9780080885278.
209. Rezaei, A.; Daeihamed, M.; Capanoglu, E.; Tomas, M.; Akbari-Alavijeh, S.; Shaddel, R.; Khoshnoudi-Nia, S.; Boostani, S.; Rostamabadi, H.; Falsafi, S.R.; et al. Possible health risks associated with nanostructures in food. In *Safety and Regulatory Issues of Nanoencapsulated Food Ingredients*; Elsevier: Amsterdam, The Netherlands, 2021; pp. 31–118.
210. Churchman, G.J.; Lowe, D.J. Alteration, formation, and occurrence of minerals in soils. In *Handbook of Soil Sciences: Properties and Processes*; CRC Press: Boca Raton, FL, USA, 2012.

211. Chalasani, R.; Gupta, A.; Vasudevan, S. Engineering New Layered Solids from Exfoliated Inorganics: A Periodically Alternating Hydrotalcite—Montmorillonite Layered Hybrid. *Sci. Rep.* **2013**, *3*, 3498. [CrossRef]
212. Kausar, A.; Ahmad, I.; Maaza, M.; Eisa, M.H. State-of-the-Art Nanoclay Reinforcement in Green Polymeric Nanocomposite: From Design to New Opportunities. *Minerals* **2022**, *12*, 1495. [CrossRef]
213. Shan, G.; Jin, W.; Chen, H.; Zhao, M.; Surampalli, R.; Ramakrishnan, A.; Zhang, T.; Tyagi, R.D. Flame-Retardant Polymer Nanocomposites and Their Heat-Release Rates. *J. Hazard. Toxic Radioact. Waste* **2015**, *19*, 04015006. [CrossRef]
214. Kang, D.J.; Park, G.U.; Park, H.Y.; Park, J.-U.; Im, H.-G. A high-performance transparent moisture barrier using surface-modified nanoclay composite for OLED encapsulation. *Prog. Org. Coat.* **2018**, *118*, 66–71. [CrossRef]
215. Król-Morkisz, K.; Pielichowska, K. Thermal Decomposition of Polymer Nanocomposites With Functionalized Nanoparticles. In *Polymer Composites with Functionalized Nanoparticles*; Elsevier: Amsterdam, The Netherlands, 2019; pp. 405–435.
216. Jayrajsinh, S.; Shankar, G.; Agrawal, Y.K.; Bakre, L. Montmorillonite nanoclay as a multifaceted drug-delivery carrier: A review. *J. Drug Deliv. Sci. Technol.* **2017**, *39*, 200–209. [CrossRef]
217. Shunmugasamy, V.C.; Xiang, C.; Gupta, N. Clay/Polymer Nanocomposites: Processing, Properties, and Applications. In *Hybrid and Hierarchical Composite Materials*; Springer International Publishing: Cham, Switzerland, 2015; pp. 161–200.
218. Khalid, M.; Walvekar, R.; Ketabchi, M.R.; Siddiqui, H.; Hoque, M.E. Rubber/Nanoclay Composites: Towards Advanced Functional Materials. In *Nanoclay Reinforced Polymer Composites*; Springer: Berlin/Heidelberg, Germany, 2016; pp. 209–224.
219. Zare, Y.; Garmabi, H.; Sharif, F. Optimization of mechanical properties of PP/Nanoclay/CaCO<sub>3</sub> ternary nanocomposite using response surface methodology. *J. Appl. Polym. Sci.* **2011**, *122*, 3188–3200. [CrossRef]
220. Zare, Y.; Garmabi, H. Modeling of interfacial bonding between two nanofillers (montmorillonite and CaCO<sub>3</sub>) and a polymer matrix (PP) in a ternary polymer nanocomposite. *Appl. Surf. Sci.* **2014**, *321*, 219–225. [CrossRef]
221. de Oliveira, C.R.S.; Batistella, M.A.; Lourenço, L.A.; de Souza, S.M.d.A.G.U.; de Souza, A.A.U. Cotton fabric finishing based on phosphate/clay mineral by direct-coating technique and its influence on the thermal stability of the fibers. *Prog. Org. Coat.* **2021**, *150*, 105949. [CrossRef]
222. Furtana, S.; Mutlu, A.; Dogan, M. Thermal stability and flame retardant properties of calcium- and magnesium-hypophosphite-finished cotton fabrics and the evaluation of interaction with clay and POSS nanoparticles. *J. Therm. Anal. Calorim.* **2020**, *139*, 3415–3425. [CrossRef]
223. He, H.; Tao, Q.; Zhu, J.; Yuan, P.; Shen, W.; Yang, S. Silylation of clay mineral surfaces. *Appl. Clay Sci.* **2013**, *71*, 15–20. [CrossRef]
224. Romanzini, D.; Piroli, V.; Frache, A.; Zattera, A.J.; Amico, S.C. Sodium montmorillonite modified with methacryloxy and vinylsilanes: Influence of silylation on the morphology of clay/unsaturated polyester nanocomposites. *Appl. Clay Sci.* **2015**, *114*, 550–557. [CrossRef]
225. Illy, N.; Fache, M.; Ménard, R.; Negrell, C.; Caillol, S.; David, G. Phosphorylation of bio-based compounds: The state of the art. *Polym. Chem.* **2015**, *6*, 6257–6291. [CrossRef]
226. Tang, G.; Huang, X.; Ding, H.; Wang, X.; Jiang, S.; Zhou, K.; Wang, B.; Yang, W.; Hu, Y. Combustion properties and thermal degradation behaviors of biobased polylactide composites filled with calcium hypophosphite. *RSC Adv.* **2014**, *4*, 8985. [CrossRef]
227. Costantino, U.; Nocchetti, M.; Sisani, M.; Vivani, R. Recent progress in the synthesis and application of organically modified hydrotalcites. *Z. Für Krist.* **2009**, *224*, 273–281. [CrossRef]
228. Forano, C.; Hibino, T.; Leroux, F.; Taviot-Guého, C. Chapter 13.1 Layered Double Hydroxides. In *Developments in Clay Science*; Elsevier: Amsterdam, The Netherlands, 2006; pp. 1021–1095.
229. Alongi, J.; Tata, J.; Frache, A. Hydrotalcite and nanometric silica as finishing additives to enhance the thermal stability and flame retardancy of cotton. *Cellulose* **2011**, *18*, 179–190. [CrossRef]
230. Ishihara, S.; Sahoo, P.; Deguchi, K.; Ohki, S.; Tansho, M.; Shimizu, T.; Labuta, J.; Hill, J.P.; Ariga, K.; Watanabe, K.; et al. Dynamic Breathing of CO<sub>2</sub> by Hydrotalcite. *J. Am. Chem. Soc.* **2013**, *135*, 18040–18043. [CrossRef]
231. Wang, S.; Gainey, L.; Mackinnon, I.D.R.; Allen, C.; Gu, Y.; Xi, Y. Thermal behaviors of clay minerals as key components and additives for fired brick properties: A review. *J. Build. Eng.* **2023**, *66*, 105802. [CrossRef]
232. Shmuradko, V.T.; Panteleenko, F.I.; Reut, O.P.; Panteleenko, E.F.; Kirshina, N.V. Composition, structure, and property formation of heat insulation fire- and heat-reflecting materials based on vermiculite for industrial power generation. *Refract. Ind. Ceram.* **2012**, *53*, 254–258. [CrossRef]
233. Addison, J. Vermiculite: A Review of the Mineralogy and Health Effects of Vermiculite Exploitation. *Regul. Toxicol. Pharmacol.* **1995**, *21*, 397–405. [CrossRef] [PubMed]
234. Cain, A.A.; Plummer, M.G.B.; Murray, S.E.; Bolling, L.; Regev, O.; Grunlan, J.C. Iron-containing, high aspect ratio clay as nanoarmor that imparts substantial thermal/flame protection to polyurethane with a single electrostatically-deposited bilayer. *J. Mater. Chem. A* **2014**, *2*, 17609–17617. [CrossRef]
235. Suvorov, S.A.; Skurikhin, V.V. Vermiculite—A promising material for high-temperature heat insulators. *Refract. Ind. Ceram.* **2003**, *44*, 186–193. [CrossRef]
236. Ortelli, S.; Malucelli, G.; Cuttica, F.; Blosi, M.; Zanoni, I.; Costa, A.L. Coatings made of proteins adsorbed on TiO<sub>2</sub> nanoparticles: A new flame retardant approach for cotton fabrics. *Cellulose* **2018**, *25*, 2755–2765. [CrossRef]
237. Ortelli, S.; Malucelli, G.; Blosi, M.; Zanoni, I.; Costa, A.L. NanoTiO<sub>2</sub>@DNA complex: A novel eco, durable, fire retardant design strategy for cotton textiles. *J. Colloid Interface Sci.* **2019**, *546*, 174–183. [CrossRef] [PubMed]

238. Apaydin, K.; Laachachi, A.; Ball, V.; Jimenez, M.; Bourbigot, S.; Ruch, D. Layer-by-layer deposition of a TiO<sub>2</sub>-filled intumescent coating and its effect on the flame retardancy of polyamide and polyester fabrics. *Colloids Surfaces A Physicochem. Eng. Asp.* **2015**, *469*, 1–10. [[CrossRef](#)]
239. Qin, S.; Pour, M.G.; Lazar, S.; Köklükaya, O.; Gerringer, J.; Song, Y.; Wågberg, L.; Grunlan, J.C. Super Gas Barrier and Fire Resistance of Nanoplatelet/Nanofibril Multilayer Thin Films. *Adv. Mater. Interfaces* **2019**, *6*, 1801424. [[CrossRef](#)]
240. Ali, Z.A. A Seq to Seq Machine Translation from Urdu to Chinese. *J. Auton. Intell.* **2021**, *4*, 1. [[CrossRef](#)]
241. Beyer, G. Short communication: Carbon nanotubes as flame retardants for polymers. *Fire Mater.* **2002**, *26*, 291–293. [[CrossRef](#)]
242. Coleman, J.N.; Khan, U.; Blau, W.J.; Gun'ko, Y.K. Small but strong: A review of the mechanical properties of carbon nanotube-polymer composites. *Carbon* **2006**, *44*, 1624–1652. [[CrossRef](#)]
243. Moniruzzaman, M.; Winey, K.I. Polymer Nanocomposites Containing Carbon Nanotubes. *Macromolecules* **2006**, *39*, 5194–5205. [[CrossRef](#)]
244. Zare, Y.; Garmabi, H. Attempts to Simulate the Modulus of Polymer/Carbon Nanotube Nanocomposites and Future Trends. *Polym. Rev.* **2014**, *54*, 377–400. [[CrossRef](#)]
245. Liu, Y.; Wang, X.; Qi, K.; Xin, J.H. Functionalization of cotton with carbon nanotubes. *J. Mater. Chem.* **2008**, *18*, 3454. [[CrossRef](#)]
246. Kashiwagi, T.; Du, F.; Douglas, J.F.; Winey, K.I.; Harris, R.H.; Shields, J.R. Nanoparticle networks reduce the flammability of polymer nanocomposites. *Nat. Mater.* **2005**, *4*, 928–933. [[CrossRef](#)]
247. Ye, L.; Wu, Q.; Qu, B. Synergistic effects and mechanism of multiwalled carbon nanotubes with magnesium hydroxide in halogen-free flame retardant EVA/MH/MWNT nanocomposites. *Polym. Degrad. Stab.* **2009**, *94*, 751–756. [[CrossRef](#)]
248. Janas, D.; Rdest, M.; Koziol, K.K.K. Flame-retardant carbon nanotube films. *Appl. Surf. Sci.* **2017**, *411*, 177–181. [[CrossRef](#)]
249. Araby, S.; Philips, B.; Meng, Q.; Ma, J.; Laoui, T.; Wang, C.H. Recent advances in carbon-based nanomaterials for flame retardant polymers and composites. *Compos. Part B Eng.* **2021**, *212*, 108675. [[CrossRef](#)]
250. Cho, C.; Song, Y.; Allen, R.; Wallace, K.L.; Grunlan, J.C. Stretchable electrically conductive and high gas barrier nanocomposites. *J. Mater. Chem. C* **2018**, *6*, 2095–2104. [[CrossRef](#)]
251. Rizkalla, S.; Dawood, M.; Schnerch, D. Development of a carbon fiber reinforced polymer system for strengthening steel structures. *Compos. Part A Appl. Sci. Manuf.* **2008**, *39*, 388–397. [[CrossRef](#)]
252. He, W.; Gao, J.; Liao, S.; Wang, X.; Qin, S.; Song, P. A facile method to improve thermal stability and flame retardancy of polyamide 6. *Compos. Commun.* **2019**, *13*, 143–150. [[CrossRef](#)]
253. Lazar, S.T.; Kolibaba, T.J.; Grunlan, J.C. Flame-retardant surface treatments. *Nat. Rev. Mater.* **2020**, *5*, 259–275. [[CrossRef](#)]
254. Montazer, M.; Harifi, T. Flame-retardant textile nanofinishes. In *Nanofinishing of Textile Materials*; Elsevier: Amsterdam, The Netherlands, 2018; pp. 163–181.
255. Gonçalves, A.G.; Jarrais, B.; Pereira, C.; Morgado, J.; Freire, C.; Pereira, M.F.R. Functionalization of textiles with multi-walled carbon nanotubes by a novel dyeing-like process. *J. Mater. Sci.* **2012**, *47*, 5263–5275. [[CrossRef](#)]
256. Motaghi, Z.; Shahidi, S. Improvement of the Conductivity and Flame Retardant Properties of Carboxylated Single-Walled Carbon Nanotube/Cotton Fabrics Using Citric Acid and Sodium Hypophosphite. *J. Nat. Fibers* **2018**, *15*, 353–362. [[CrossRef](#)]
257. Xu, J.; Niu, Y.; Xie, Z.; Liang, F.; Guo, F.; Wu, J. Synergistic flame retardant effect of carbon nanohorns and ammonium polyphosphate as a novel flame retardant system for cotton fabrics. *Chem. Eng. J.* **2023**, *451*, 138566. [[CrossRef](#)]
258. Liu, H.; Du, Y.; Yang, G.; Zhu, G.; Gao, Y.; Ding, W. Flame retardance of modified graphene to pure cotton fabric. *J. Fire Sci.* **2018**, *36*, 111–128. [[CrossRef](#)]
259. Norouzi, M.; Zare, Y.; Kiany, P. Nanoparticles as Effective Flame Retardants for Natural and Synthetic Textile Polymers: Application, Mechanism, and Optimization. *Polym. Rev.* **2015**, *55*, 531–560. [[CrossRef](#)]
260. Cinausero, N.; Azema, N.; Lopez-Cuesta, J.-M.; Cochez, M.; Ferriol, M. Synergistic effect between hydrophobic oxide nanoparticles and ammonium polyphosphate on fire properties of poly(methyl methacrylate) and polystyrene. *Polym. Degrad. Stab.* **2011**, *96*, 1445–1454. [[CrossRef](#)]
261. Rault, F.; Pleyber, E.; Campagne, C.; Rochery, M.; Giraud, S.; Bourbigot, S.; Devaux, E. Effect of manganese nanoparticles on the mechanical, thermal and fire properties of polypropylene multifilament yarn. *Polym. Degrad. Stab.* **2009**, *94*, 955–964. [[CrossRef](#)]
262. Coyle, S.; Wu, Y.; Lau, K.-T.; De Rossi, D.; Wallace, G.; Diamond, D. Smart Nanotextiles: A Review of Materials and Applications. *MRS Bull.* **2007**, *32*, 434–442. [[CrossRef](#)]
263. Sundarajan, S.; Chandrasekaran, A.R.; Ramakrishna, S. An Update on Nanomaterials-Based Textiles for Protection and Decontamination. *J. Am. Ceram. Soc.* **2010**, *93*, 3955–3975. [[CrossRef](#)]
264. Yadav, A.; Prasad, V.; Kathe, A.A.; Raj, S.; Yadav, D. Functional finishing in cotton fabrics using zinc oxide nanoparticles. *Bull. Mater. Sci.* **2006**, *29*, 641–645. [[CrossRef](#)]
265. Xue, C.-H.; Yin, W.; Jia, S.-T.; Ma, J.-Z. UV-durable superhydrophobic textiles with UV-shielding properties by coating fibers with ZnO/SiO<sub>2</sub> core/shell particles. *Nanotechnology* **2011**, *22*, 415603. [[CrossRef](#)] [[PubMed](#)]
266. Dastjerdi, R.; Montazer, M. A review on the application of inorganic nano-structured materials in the modification of textiles: Focus on anti-microbial properties. *Colloids Surf. B Biointerfaces* **2010**, *79*, 5–18. [[CrossRef](#)]
267. El-Nahhal, I.M.; Zourab, S.M.; Kodeh, F.S.; Selmane, M.; Genois, I.; Babonneau, F. Nanostructured copper oxide-cotton fibers: Synthesis, characterization, and applications. *Int. Nano Lett.* **2012**, *2*, 14. [[CrossRef](#)]

268. Selvam, S.; Rajiv Gandhi, R.; Suresh, J.; Gowri, S.; Ravikumar, S.; Sundrarajan, M. Antibacterial effect of novel synthesized sulfated  $\beta$ -cyclodextrin crosslinked cotton fabric and its improved antibacterial activities with ZnO, TiO<sub>2</sub> and Ag nanoparticles coating. *Int. J. Pharm.* **2012**, *434*, 366–374. [[CrossRef](#)] [[PubMed](#)]
269. Esmail, W.A.; Darwish, A.M.Y.; Ibrahim, O.A.; Abadir, M.F. The effect of magnesium chloride hydrates on the fire retardation of cellulosic fibers. *J. Therm. Anal. Calorim.* **2001**, *63*, 831–838. [[CrossRef](#)]
270. Gulrajani, M.L.; Deepti, G. Emerging techniques for functional finishing of textile. *Indian J. Fibre Text. Res.* **2011**, *36*, 388–397.
271. Moafi, H.F.; Shojaie, A.F.; Zanjanchi, M.A. Flame-retardancy and photocatalytic properties of cellulosic fabric coated by nano-sized titanium dioxide. *J. Therm. Anal. Calorim.* **2011**, *104*, 717–724. [[CrossRef](#)]
272. Jolles, Z.E.; Jolles, G.I. Some notes on flame-retardant mechanisms in polymers. *Plast Polym.* **1972**, *40*, 319.
273. Shen, R.; Fan, T.; Quan, Y.; Ma, R.; Zhang, Z.; Li, Y.; Wang, Q. Thermal stability and flammability of cotton fabric with TiO<sub>2</sub> coatings based on biomineralization. *Mater. Chem. Phys.* **2022**, *282*, 125986. [[CrossRef](#)]
274. Fallah, M.H.; Fallah, S.A.; Zanjanchi, M.A. Synthesis and Characterization of Nano-sized Zinc Oxide Coating on Cellulosic Fibers: Photoactivity and Flame-retardancy Study. *Chin. J. Chem.* **2011**, *29*, 1239–1245. [[CrossRef](#)]
275. Prilla, K.A.V.; Jacinto, J.M.; Ricardo, L.J.O.; Box, J.T.S.; Lim, A.B.C.; Francisco, E.F.; De Vera, G.I.N.; Yaya, J.A.T.; Natividad, V.V.M.; Awi, E.N.; et al. Flame Retardant and Uv-Protective Cotton Fabrics Functionalized with Copper (II) Oxide Nanoparticles. *Antorcha* **2020**, *7*, 11–16.
276. Saleemi, S.; Naveed, T.; Riaz, T.; Memon, H.; Awan, J.A.; Siyal, M.I.; Xu, F.; Bae, J. Surface Functionalization of Cotton and PC Fabrics Using SiO<sub>2</sub> and ZnO Nanoparticles for Durable Flame Retardant Properties. *Coatings* **2020**, *10*, 124. [[CrossRef](#)]
277. Dhineshbabu, N.R.; Manivasakan, P.; Yuvakkumar, R.; Prabu, P.; Rajendran, V. Enhanced Functional Properties of ZrO<sub>2</sub>/SiO<sub>2</sub> Hybrid Nanosol Coated Cotton Fabrics. *J. Nanosci. Nanotechnol.* **2013**, *13*, 4017–4024. [[CrossRef](#)] [[PubMed](#)]
278. Rajendran, V.; Dhineshbabu, N.R.; Kanna, R.R.; Kaler, K.V.I.S. Enhancement of Thermal Stability, Flame Retardancy, and Antimicrobial Properties of Cotton Fabrics Functionalized by Inorganic Nanocomposites. *Ind. Eng. Chem. Res.* **2014**, *53*, 19512–19524. [[CrossRef](#)]
279. Frąckowiak, A.; Skibiński, P.; Gaweł, W.; Zaczyńska, E.; Czarny, A.; Gancarz, R. Synthesis of glycoside derivatives of hydroxyanthraquinone with ability to dissolve and inhibit formation of crystals of calcium oxalate. Potential compounds in kidney stone therapy. *Eur. J. Med. Chem.* **2010**, *45*, 1001–1007. [[CrossRef](#)] [[PubMed](#)]
280. Małecka, B.; Drożdż-Cieśla, E.; Małecki, A. Mechanism and kinetics of thermal decomposition of zinc oxalate. *Thermochim. Acta* **2004**, *423*, 13–18. [[CrossRef](#)]
281. Echigo, T.; Kimata, M.; Kyono, A.; Shimizu, M.; Hatta, T. Re-investigation of the crystal structure of whewellite [Ca(C<sub>2</sub>O<sub>4</sub>)·H<sub>2</sub>O] and the dehydration mechanism of caoxite [Ca(C<sub>2</sub>O<sub>4</sub>)·3H<sub>2</sub>O]. *Mineral. Mag.* **2005**, *69*, 77–88. [[CrossRef](#)]
282. Majumdar, R.; Sarkar, P.; Ray, U.; Roy Mukhopadhyay, M. Secondary catalytic reactions during thermal decomposition of oxalates of zinc, nickel and iron(II). *Thermochim. Acta* **1999**, *335*, 43–53. [[CrossRef](#)]
283. Gabal, M.; El-Bellihi, A.; El-Bahnasawy, H. Non-isothermal decomposition of zinc oxalate–iron(II) oxalate mixture. *Mater. Chem. Phys.* **2003**, *81*, 174–182. [[CrossRef](#)]
284. Mohamed, M.A.; Galwey, A.K.; Halawy, S.A. A comparative study of the thermal reactivities of some transition metal oxalates in selected atmospheres. *Thermochim. Acta* **2005**, *429*, 57–72. [[CrossRef](#)]
285. Vlaev, L.; Nedelchev, N.; Gyurova, K.; Zagorcheva, M. A comparative study of non-isothermal kinetics of decomposition of calcium oxalate monohydrate. *J. Anal. Appl. Pyrolysis* **2008**, *81*, 253–262. [[CrossRef](#)]
286. Donkova, B.; Mehandjiev, D. Mechanism of decomposition of manganese(II) oxalate dihydrate and manganese(II) oxalate trihydrate. *Thermochim. Acta* **2004**, *421*, 141–149. [[CrossRef](#)]
287. Weil, E.D.; Levchik, S.; Moy, P. Flame and Smoke Retardants in Vinyl Chloride Polymers—Commercial Usage and Current Developments. *J. Fire Sci.* **2006**, *24*, 211–236. [[CrossRef](#)]
288. Holdsworth, A.F.; Horrocks, A.R.; Kandola, B.K.; Price, D. The potential of metal oxalates as novel flame retardants and synergists for engineering polymers. *Polym. Degrad. Stab.* **2014**, *110*, 290–297. [[CrossRef](#)]
289. Ji, W.; Wang, H.; Yao, Y.; Wang, R. Mg(OH)<sub>2</sub> and PDMS-coated cotton fabrics for excellent oil/water separation and flame retardancy. *Cellulose* **2019**, *26*, 6879–6890. [[CrossRef](#)]
290. Plentz, R.S.; Miotto, M.; Schneider, E.E.; Forte, M.M.C.; Mauler, R.S.; Nachtigall, S.M.B. Effect of a macromolecular coupling agent on the properties of aluminum hydroxide/PP composites. *J. Appl. Polym. Sci.* **2006**, *101*, 1799–1805. [[CrossRef](#)]
291. Sabet, M.; Hassan, A.; Ratnam, C.T. Flammability and Thermal Characterization of Aluminum Hydroxide Filled with LDPE. *Int. Polym. Process.* **2013**, *28*, 393–397. [[CrossRef](#)]
292. Lee, M.-Y.; Yen, F.-S.; Hsiang, H.-I. Generating Self-Shaped 2D Aluminum Oxide Nanopowders. *Nanomaterials* **2022**, *12*, 2955. [[CrossRef](#)]
293. Esposito Corcione, C.; Frigione, M.; Maffezzoli, A.; Malucelli, G. Photo—DSC and real time—FT-IR kinetic study of a UV curable epoxy resin containing o-Boehmites. *Eur. Polym. J.* **2008**, *44*, 2010–2023. [[CrossRef](#)]
294. Grand, A.F.; Wilkie, C.A. (Eds.) *Fire Retardancy of Polymeric Materials*; Marcel Dekker: New York, NY, USA, 2000; Chapter 9.
295. Alongi, J.; Brancatelli, G.; Rosace, G. Thermal properties and combustion behavior of POSS- and bohemite-finished cotton fabrics. *J. Appl. Polym. Sci.* **2012**, *123*, 426–436. [[CrossRef](#)]

- 
296. Sharma, V.; Basak, S.; Rishabh, K.; Umariya, H.; Ali, S.W. Synthesis of zinc carbonate nanoneedles, a potential flame retardant for cotton textiles. *Cellulose* **2018**, *25*, 6191–6205. [[CrossRef](#)]
297. de Paiva Teixeira, M.H.; Lourenço, L.A.; Artifon, W.; de Castro Vieira, C.J.; Gómez González, S.Y.; Hotza, D. Eco-Friendly Manufacturing of Nano-TiO<sub>2</sub> Coated Cotton Textile with Multifunctional Properties. *Fibers Polym.* **2020**, *21*, 90–102. [[CrossRef](#)]

**Disclaimer/Publisher's Note:** The statements, opinions and data contained in all publications are solely those of the individual author(s) and contributor(s) and not of MDPI and/or the editor(s). MDPI and/or the editor(s) disclaim responsibility for any injury to people or property resulting from any ideas, methods, instructions or products referred to in the content.